REMARKS

Reconsideration of this application is respectfully requested. Claims 1, 4, 5 and 8-12 have been amended. These changes do not introduce new matter, and their entry is respectfully requested.

In the Office Action of July 28, 2006, the Examiner set forth a number of grounds for rejection. These grounds are addressed individually and in detail below.

Claim objections

Claims 1 and 8-12 stand objected to as containing to non-elected subject matter. Claims 1 and 8-12 have been amended to delete non-elected subject matter from the claims.

Claim 5 stands objected to because the recitation "a vector of expression." Claim 5 has been amended to recite "an expression vector," as recommended by the Examiner.

Applicants respectfully submit that the grounds of the objection have been obviated. Withdrawal of the objections are respectively requested.

Claim Rejections Under 35 U.S.C. §112, second paragraph

Claims 1, 2 and 4-12 stand rejected under 35 U.S.C. §112, second paragraph, as being indefinite for the reasons set forth on pages 2-3 of the Office Action. Specifically, the Examiner alleges that the metes and bounds of the term "derivative" are unclear, and that it is unclear to what the word "thereof" refers.

Regarding the word "thereof," claims 1 and 8-12 have been amended to indicated that the recited polynucleotide sequence codes all or part of the disintegrin domain of an adamalysin or a derivative the disintegrin domain of an adamalysin.

Regarding the word "derivatives" in claims 1 and 8-12, the Applicants submit that one of ordinary skill in the art would immediately understand the metes and bounds of this term, based on the teachings of the specification. Paragraph [0039] of the specification defines "derivative" of the claimed polypeptides as

> functional equivalents having antiangiogenic, anti-invasive and/or antimetastatic properties that one skilled in the art can determine from the teaching of this invention and, more particularly, from the models and tests presented in the experimental part below. The derivatives can be fragments of truncated form, sequences modified by deletion, addition, suppression or replacement of one or more amino acids. The derivatives can also be fragments corresponding to said derivatives constituted by chemically modified amino acids, these modifications making the derivatives more stable. The invention also pertains to polynucleotide sequences coding for said derivatives.

As amended, claims 1 and 8-12 specify that the encoded polypeptide contains an RGD sequence, and also can inhibit migration and proliferation of endothelial cells, adhesion of endothelial cells to matrix substrates and formation of capillary structures (corresponding to the antiangiogenic properties discussed in paragraph [0039]). Thus, "derivatives" of the polypeptide as recited in these claims has both structural features (a disintegrin domain with an RGD sequence) and functional qualities that can be readily ascertained by one of ordinary skill in the art. Indeed, tests to determine the recited functional qualities are extensively disclosed in the specification. Thus, it would have been clear to one of ordinary skill in the art, as of the filing date of this application, what constituted a "derivative" of an adamalysin as recited in claims 1 and 8-12.

The Office action also alleges that claim 1 is vague and indefinite because the metes and bounds of the phrase "inhibiting angiogenesis or invasion or formation of metastases" are unclear. The Applicants have amended claim 1 to recite "inhibiting angiogenesis, tumor invasion, or formation of metastases."

The Office action further alleges that claim 5 is vague and indefinite because the metes and bounds of the phrase "wherein the nucleic acid molecule comprises a vector or is joined to a vector of expression" are unclear. Claim 5 has been amended to recite "wherein the nucleic acid molecule is inserted into an expression vector."

Applicants respectfully submit that the amendments obviate the indefiniteness rejections of claims 1, 2 and 4-12. Withdrawal of the rejection under 35 U.S.C. §112, second paragraph, is respectfully requested.

Claim Rejections Under 35 U.S.C. §112, first paragraph

Claims 1, 2 and 4-12 stand rejected under 35 U.S.C. §112, first paragraph for the reasons set forth on pages 3-9 of the outstand Office Action. The Examiner states that the specification, while enabling for a method of administering and expressing the disintegrin domain from SEQ ID NO: 1 Met 420 to Gly 511 of SEQ ID NO: 1 at a site to be targeted for diminution of the number of intratumoral vessels for inhibition of growth of melanoma and for inhibition of pulmonary metastases, does not reasonably provide enablement for any other embodiment. The Examiner further states the specification does not enable any person skilled in the art to which it pertains, or with which it is most nearly connected, to make or use the invention commensurate in scope with these claims. Applicants respectfully traverse the rejection.

The test of enablement is whether one skilled in the art could make and use the claimed invention from the disclosures in the patent coupled with information known in the art without undue experimentation. *United States v. Teletronics, Inc.*, 8 USPQ2d 1217 (Fed. Cir. 1988). Whether undue experimentation is required is not based on a single factor but is rather a conclusion reach by

weighing many factors. According to the Federal Circuit in *In re Wands*, 8 USPQ2d 1400 (Fed. Cir. 1988), these factors include, but are not limited to:

(A) The breadth of the claims;

(B) The nature of the invention;

(C) The state if the prior art;

(D) The level of one of ordinary skill;

(E) The level of predictability in the art;

(F) The amount of direction provided by the inventor;

(G) The existence of working examples; and

(H) The quantity of experimentation needed to make or use the invention based on the content of the disclosure.

The present invention relates to the fields of molecular biology, oncology and cell biology. In this application, the claims are drawn to methods for inhibiting angiogenesis, tumor invasion, or formation of metastases in a mammal (claim 1), or for treating cancer (claim 8), inflammatory disease (claim 9), atherosclerosis (claim 10), macular degeneration (claim 11) and psoriasis (claim 12). The methods comprise the step of administering a therapeutically effective amount of a nucleic acid molecule comprising a polynucleotide sequence coding a polypeptide coding all or part of the disintegrin domain of an adamalysin to the mammal. The recited disintegrin domain of the polypeptide contains an RGD sequence, and the polypeptide can also inhibit migration and proliferation of endothelial cells, adhesion of endothelial cells to matrix substrates and formation of capillary structures.

With respect to the state of the prior art ("Wands" factor C), it is known that the adamylase proteins, particularly ADAM-9, ADAM-12 and ADAM-23 have the capacity to bind to integrins *via*

their disintegrin domain. [See e.g., Zhou, M., et al., "MDC-9 (ADAM-9/Meltrin gamma) functions as an adhesion molecule by binding the α(v) β(5) integrin". *Biochem Biophys. Res.* Commun., 19:280(2):574-80 (2001); Eto, K., et al., "RGD-independent binding of integrin α9 β1 to the ADAM-12 and -15 disintegrin domains mediates cell-cell interaction. *J. Biol. Chem.* 10:275(45):34922-30 (2000); and Cal, S., et al., ADAM 23/MDC3, a human disintegrin that promotes cell adhesion via interaction with the α(v) β(3) integrin through an RGD-independent mechanism, *Mol Biol Cell*, 11:1457-69 (2000)]. Here, the Applicants have demonstrated that an RGD-containing disintegrin domain of an adamalysin (such as metargidin) has antiangiogenic and antimetastatic activities, and that these activities are related to the binding of the disintegrin domain to integrins. This disintegrin domain, and derivatives of this domain, "simultaneously inhibits all of the stages of angiogenesis: migration and proliferation of endothelial cells, their adhesion to different matrix substrates and formation of capillary structures (paragraph [0017] of the specification. *See also* the working examples and Trochon et al., *Cancer Research*, 64: 2062-2069 (2004), a post-filing publication of the inventors'.

With respect to Wands factor (D), the level of one of ordinary skill in this field is high. A person skilled in the art typically has a Ph.D. or M.D. degree and several years of research experience.

With respect to Wands factors (E)-(H), the present specification clearly describes a method of treating cancer or inhibiting angiogenesis, tumor invasion, and formation of metastases in a mammal comprising: administering a therapeutically effective amount of the claimed polynucleotide. See, for example, paragraphs 0003 and 0004 on pages 1-2; paragraph 0026 on page 5; paragraphs 0028-0035 on pages 6-8. The present specification further teaches how to construct a vector carrying the polynucleotide sequence coding the disintegrin domain of adamalysin and how to introduce the

vector into cells in both *in vitro* and *in vivo* settings. As admitted by the Examiner, it was known at the time the invention was made that: "within the ADAMS, the disintegrin domain functions to prevent integrin-mediated cell to cell and cell to matrix interactions such as plate aggregation, adhesion, migration of tumor cells or neutrophils or angiogenesis." (The Office Action, page 5).

Furthermore, Applicants have provided examples showing that the disintegrin domain of metargidin, called "AMEP," inhibits adhesion, migration and proliferation of endothelial cells, induces apoptosis in endothelial cells and inhibits the formation of capillary structures, and that AMEP inhibits tumor growth in nude mice and syngenic mice (see figures and working examples of the present application and Trochon et al., *supra*).

The Office Action alleges that the method of delivery of polynucleotides is highly unpredictable and cited Verma et al. as support. Applicants respectfully submit that Verma's comments were made in 1997, seven years before the filing date of the instant application. In fact, gene transfer technologies had developed rapidly since 1997 and reliable gene transfer have been achieved with a variety of vectors in many animal models. Indeed, the Applicants show in paragraphs [0087]-[0090], Table 3 and Figure 8 that a polynucleotide coding a polypeptide as claimed can be successfully transfected into mouse muscle cells and expressed, where it generated a therapeutic effect. Similar results were published in Trochon et al., *supra*. One skilled in the art would therefore understand that the techniques used to transfer and express the claimed polynucleotide are readily applicable to other mammals, and can be used with other polynucleotides falling within the claims.

As discussed above, claims 1 and 8-12 have been amended to indicate that the recited polypeptides contain an RGD sequence, and also can inhibit migration and proliferation of endothelial cells, adhesion of endothelial cells to matrix substrates and formation of capillary

structures. The presence of the RGD sequence can readily be determined by routine sequencing of a polypeptide or polynucleotide. The ability of a polypeptide to inhibit the various stages of angiogenesis, as claimed, can also be readily determined by routine assays which are well within the level of ordinary skill in the art. The application discloses the performance and interpretation of these routine assays in detail.

In view of the foregoing, the Applicants respectfully submit that the specification, at the time this application was filed, clearly taught one skilled in the art how to make and/or use the full scope of the claimed invention without undue experimentation. The specification provides sufficient guidance for one skilled in the art to produce a nucleic acid molecule comprising a polynucleotide sequence coding a polypeptide comprising all or part of the disintegrin domain of an adamalysin, and how treat for the various conditions recited in the claims.

Regarding the treatment of inflammatory disease (claim 9), atherosclerosis (claim 10), macular degeneration (claim 11) and psoriasis (claim 12), one skilled in the art would understand that the integrin binding function of the claimed polypeptides would result in the recited therapeutic effect. In particular, one skilled in the art would understand that macular degeneration results from retinal neovascularization, and that inhibition of angiogenesis in the eye would necessarily treat this condition.

Accordingly, these grounds of the enablement rejection have been obviated, and withdrawal of the rejection 35 U.S.C. §112, first paragraph is respectfully requested.

Claim Rejections Under 35 U.S.C. §102

Claims 1, 2 and 4-12 stand rejected under 35 U.S.C. §102(e) as being anticipated by Ruben et al. (US 2002/0165377) (hereinafter "Ruben") for the reasons set forth on page 10 of the Office

Action. Claims 1 and 4-12 also stand rejected under 35 U.S.C. §102(a) as being anticipated by Young et al. (US 2003/0194797) (hereinafter "Young") for the reasons set forth on page 10 of the Office Action. Applicants respectfully traverse the rejection.

It is well established that a claim is anticipated only if each and every element as set forth in the claim is described in a single prior art reference.

Claims 1 and 8-12 have been amended to recite that the polypeptide coded by the recited polynucleotide contains an RGD sequence in the disintegrin domain. The claimed polypeptide can also inhibit migration and proliferation of endothelial cells, adhesion of endothelial cells to matrix substrates and formation of capillary structures.

The disintegrin domains of the ADAMs proteins disclosed in Rubens or Young do not contain an RGD sequence. Thus, these references do not disclose every feature of claims 1 and 8-12, and cannot anticipate these claims. As claims 2 and 4-7 depend directly or indirectly from claim 1, these claims are also not anticipated by Rubens or Young.

The Applicants note that the claimed polypeptides differ from known RGD-containing peptides, in that the previously known RGD-containing peptides do not inhibit all stages of angiogenesis (see paragraph [0099] of the specification). There is also no recognition in Rubens or Young that the disintegrin domains of ADAMS proteins which contain RGD sequences can produce the claimed effects. Indeed, neither Rubens nor Young even disclose an ADAMS protein which contain an RGD sequence in the disintegrin domain.

In view of the foregoing, Applicants respectfully submit that these grounds of the anticipation rejection have been obviated, and withdrawal of the rejection under 35 U.S.C. §102 is respectfully requested.

All of the stated grounds of rejection have been properly traversed, accommodated, or rendered moot. Applicants therefore respectfully request that the Examiner reconsider all presently outstanding rejections and that they be withdrawn. It is believed that a full and complete response has been made to the outstanding Office Action and, as such, the present application is now in condition for allowance.

If the Examiner believes, for any reason, that personal communication will expedite prosecution of this application, the Examiner is invited to contact attorneys listed below.

Respectfully submitted,

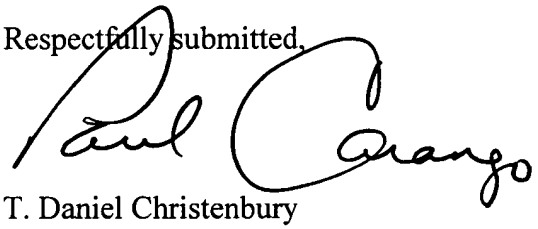

T. Daniel Christenbury
Reg. No. 31,750

Paul Carango
Reg. No. 42,386
Attorneys for Applicants

TDC/PC/sh
(215) 656-3381

[CANCER RESEARCH 64, 2062 2069, March 15, 2004]

Evidence of Antiangiogenic and Antimetastatic Activities of the Recombinant Disintegrin Domain of Metargidin

Véronique Trochon-Joseph,[1,2] Dominique Martel-Renoir,[3] Lluis M. Mir,[3] Annick Thomaïdis,[1] Paule Opolon,[3] Elisabeth Connault,[3] Hong Li,[3,4] Christophe Grenet,[1] Françoise Fauvel-Lafève,[1] Jeannette Soria,[5] Chantal Legrand,[1] Claudine Soria,[1,4] Michel Perricaudet,[3] and He Lu[1]

[1]Inserm U553, Hôpital Saint-Louis, Paris; [2]Bioalliance Pharma SA, Paris; [3]Unité Mixte de Recherche 8121, Centre National de la Recherche Scientifique, Institut Gustave-Roussy, Villejuif; [4]DIFEMA, Faculté de Médecine et Pharmacie de Rouen, Rouen; and [5]Laboratoires Sainte-Marie and EMI 353 INSERM, Hôtel-Dieu, Paris, France

ABSTRACT

Metargidin, a transmembrane protein of the adamalysin family, and integrins, *e.g.*, $\alpha5\beta1$ and αv, are preferentially expressed on endothelial cells on angiogenesis. Furthermore, metargidin interacts with these integrins via its disintegrin domain. In this study, recombinant human disintegrin domain (RDD) was produced in *Escherichia coli* by subcloning its cDNA into the pGEX-2T vector, and the effect of purified RDD on different steps of angiogenesis was evaluated. At concentrations of 2–10 μg/ml, RDD exhibited inhibitory activities in a variety of *in vitro* functional assays, including endothelial cell proliferation and adhesion on the integrin substrates fibronectin, vitronectin, and fibrinogen. RDD (10 μg/ml) totally abrogated endothelial cell migration and blocked most capillary formation in a three-dimensional fibrin gel. To test RDD efficacy *in vivo*, the *RDD* gene inserted into pBi vector containing a tetracycline-inducible promoter was electrotransferred into nude mouse muscle. RDD was successfully synthesized by muscle cells *in vivo* as shown by immunolabeling and Western blotting. In addition, 78% less MDA-MB-231 tumor growth, associated with strong inhibition of tumor angiogenesis, was observed in athymic mice bearing electrotransferred RDD. Moreover, in the presence of RDD, 74% fewer B16F10 melanoma lung metastases were found in C57BL/6 mice. Taken together, these results identified this RDD as a potent intrinsic inhibitor of angiogenesis, tumor growth, and metastasis, making it a promising tool for use in anticancer treatment.

INTRODUCTION

Angiogenesis, the development of new capillaries from preexisting blood vessels, is essential for the growth and progression of primary solid tumors. A strategy aimed at inhibiting such neovascularization within tumors has thus been proposed (1). To date, various proteolytic fragments of extracellular matrix (ECM) components, *e.g.*, angiostatin, endostatin, canstatin, and tumstatin, have been found to inhibit tumor angiogenesis and subsequent tumor growth (2–7). Antiangiogenic therapy presents at least two obvious advantages to contain cancer: (*a*), the vast variety of cancer phenotypes and genotypes becomes unimportant because angiogenesis is a phenomenon common to all malignancies; and (*b*), restriction and regression of tumor neovascularization should prevent the passage of tumor cells into the circulation and, therefore, lower the metastatic risk.

The family of adamalysin proteins, also referred to as A disintegrin and metalloproteinase proteins (ADAMs) or metalloproteinase-disintegrin cysteine-rich proteins (MDCs), has a particular primary structure containing disintegrin domain located on the COOH-terminal side of metalloproteinase domain. The disintegrin region contains an integrin-binding sequence in a disintegrin loop that interacts with integrins and may mediate cell–cell interactions (8). All family members potentially possess cell-adhesion and protease activities; however, only half of them have been reported to have an active metalloproteinase site to mediate proteolytic cleavage of ECM components (9). Adamalysins are implicated in diverse biological processes, such as fertilization, myogenesis, neurogenesis, and cytokine release (10).

Metargidin (metalloprotease-RGD-disintegrin protein), also called human MDC-15 or ADAM-15, is a transmembrane adamalysin expressed by smooth muscle cells, mesangial cells, and at a much higher level, activated endothelial cells. To date, its function has remained poorly understood (11–13). However, recently reported data implicated metargidin in mesangial cell migration associated with the gelatinase activity of its metalloproteinase domain (13). Metargidin has also been shown to colocalize with a cell-adhesion molecule, vascular endothelial cadherin, which mediates endothelial cell adherent junction formation (14). Furthermore, metargidin is the only known adamalysin that possesses a RGD motif at the tip of its disintegrin loop (CRPTRGDCD), which binds integrins $\alpha v\beta3$ and $\alpha5\beta1$ (11, 15, 16). More recently, mouse ADAM-15, a homolog of human metargidin, has been shown to bind integrin $\alpha9\beta1$ in an RGD-independent manner (17). Integrins are heterodimeric transmembrane cell-surface molecules that mediate adhesion to ECM and cell–cell interactions (18). In particular, αv integrins are involved in angiogenic processes; monoclonal antibodies, *e.g.*, vitaxin, and cyclic RGD peptides targeting these integrins inhibited angiogenesis, leading to tumor regression (18–22). However, the mechanisms of how αv integrins modulate angiogenesis remain unclear (23–30) because the deletion of $\beta3$, $\beta5$, or αv integrins in knockout mice failed to block angiogenesis but rather showed extensive angiogenesis (27, 28).

In a previous study using a synthetic adamalysin inhibitor (GL129471) to block the metalloproteinase domain, we provided evidence implicating adamalysin in angiogenesis *in vitro* (31). Because angiogenesis is thought to require the interaction between metargidin and integrin, we postulated that the disintegrin domain of metargidin, expressed as soluble recombinant protein, might prevent this interaction. To test this hypothesis, we produced this recombinant disintegrin domain (RDD) and evaluated its effect on angiogenesis *in vitro*. Moreover, the potential therapeutic efficacy of RDD against tumor angiogenesis, growth, and metastasis was evaluated after plasmid DNA electrotransfer using a previously described tetracycline-inducible system (32) in two experimental animal models: human MDA-MB-231 tumors grafted into nude mice, and the dissemination of B16F10 melanoma cells to the lungs of syngeneic mice.

MATERIALS AND METHODS

Materials. A peptide (KGWQCRPTRGDC) from the disintegrin domain of human metargidin (MDC-15) was synthesized by Neosystem (Strasbourg, France) and used to immunize rabbits as described by Herren *et al.* (12). The

Received 10/27/03; revised 12/12/03; accepted 1/9/04.

Grant support: Grant 8364 from Association Française contre la Myopathie (AFM); the Ligue National Contre le Cancer; Grants 7593 and 9061 from the Association pour la Recherche contre le Cancer (ARC); Grant 1999 001858 from Fondation de France and the Institut National de la Santé et de la Recherche Médicale (INSERM); le Centre National pour la Recherche Scientifique (CNRS); Institut Gustave Roussy; Institut Universitaire d'Hématologie of Paris VII; and Bioalliance Pharma SA.

The costs of publication of this article were defrayed in part by the payment of page charges. This article must therefore be hereby marked *advertisement* in accordance with 18 U.S.C. Section 1734 solely to indicate this fact.

Note: V. Trochon-Joseph and D. Martel-Renoir contributed equally to the manuscript.

Requests for reprints: He Lu, U553 INSERM, Hôpital Saint-Louis, 1, av. Claude Vellefaux, 75475 Paris Cedex 10, France. Phone: (33) 1 53 72 40 26; Fax: (33) 1 53 72 40 27; E-mail: helu@chu-stlouis.fr.

resulting antiserum was used to detect purified *Escherichia coli*-produced RDD by Western blotting.

RDD Production in *E. coli*. Glutathione *S*-transferase (GST)–RDD fusion protein was prepared by inserting cDNA that encodes the entire disintegrin domain of metargidin (MAAFCGNMFVEPGEQCDCGFLDDCVDPCCDSL-TCQLRPGAQCASDGPCCQNCQLRPSGWQCRPTRGDCDLPEFCPGDSSQCP-PDVSLGDGE) into the *Bam*HI site of the pGEX-2T vector, yielding pGEX-2T-RDD, a generous gift from Y. Takada (The Scripps Research Institute, La Jolla, CA). This fusion protein has a thrombin cleavage site between GST and RDD. *E. coli* DH5α synthesis of GST–RDD was induced by incubating the bacteria in 1 mM isopropyl-1-thio-β-D-galactopyranoside (Life Technologies, Inc., Paisley, United Kingdom) for 4 h. After addition of 1% Triton X-100, the bacterial suspension was sonicated, and the fusion protein was extracted. The fusion protein was purified by glutathione-agarose (Sigma-Aldrich, Saint Quentin Fallavier, France) affinity chromatography and eluted by competition with free glutathione (Sigma-Aldrich), as described by Smith and Johnson (33). RDD was cleaved from the fusion protein by use of bovine thrombin (Amersham Pharmacia; 1 unit/100 μg of fusion protein) for 16 h at room temperature. The GST fragment was then removed by glutathione-agarose affinity chromatography, and the final product was dialyzed against PBS for 3 h. Purified RDD (20 μl) was analyzed by use of a fast-performance liquid chromatography system (P-500 pump; Amersham Biosciences Europe, Orsay, France) with a Superdex 75 High Resolution 10/30 column (Amersham) connected to a Beckman Gold 168 spectrophotometer (detection at 230 nm; Beckman Instruments, Fullerton, CA) with PBS as the elution buffer at a flow rate of 0.5 ml/min and pressure of 0.7 MPa. The protein concentration was determined with the BCA assay (Pierce; Rockford, IL). Vehicle-control cultures (without RDD) for *in vitro* experiments contained a final bovine thrombin concentration never exceeding 1.6 units/ml (used for the highest RDD dose).

Plasmid Preparation for Electric Pulse Delivery to Muscle. The cDNA containing the disintegrin domain sequence from pGEX-2T–RDD was amplified by PCR with the forward primer 5′-ATC CGA GCT CTT ATG GCT GCT TTC TGC G-3′ and the reverse primer 5′-GCA TGC GGA TCC TTA CTC GCC A-3′ and subcloned into *Sac*I–*Bam*HI sites of the p1519 vector, which harbors the sequence of mouse urokinase signal peptide (34). The *Eco*RV–*Bam*HI restriction fragment encoding this signal peptide-fused RDD sequence was then subcloned into *Eco*RV–*Bgl*II sites of the pCO5 vector (Clontech, Palo Alto, CA). The *Nae*I–*Eco*RV restriction fragment was finally subcloned into the *Eco*RV site of the pBi vector (Clontech). This vector (pBi–RDD) carries the gene of interest from a tetracycline-responsive promoter in the Tet-On eukaryotic gene-expression system. The cDNA fragment of RDD fused to the urokinase signal peptide, with Flag-tag (DYKDDDDK) placed at the COOH terminus, was amplified by PCR from pBi–RDD by use of the forward primer 5′-AAT ACT AGC TAG CAT GAA AGT CTG GCT G-3′ and the reverse primer 5′-TTG ATA TCT CACTTG TCA TCG TCG TCC TTG TAG TCC TCG CCA TCC CCT AG-3′. The *Nhe*I–*Eco*RV restriction fragment was then subcloned into *Nhe*I/*Eco*RV sites of pBi to generate pBi–RDD–Flag. The tag enables detection of muscle cell-synthesized RDD by Western blotting and immunolabeling of muscle sections. The Tet-On vector expressing the transactivator rtTA (reverse tetracycline transcriptional activator) and the Tet-tTS vector expressing the silencer tTS (tetracycline transcriptional silencer) were purchased from Clontech. Plasmids were prepared by use of the Endo-Free Plasmid Maxi kit (Qiagen, Courtaboeuf, France). Purified plasmid DNA was solubilized in endotoxin-free 0.9% NaCl at the working concentration.

Intramuscular Electrotransfer of Plasmid DNA. Female nude (Janvier, Le Genest-sur-Isle, France) and C57BL/6 (Harlan, Gannat, France) mice, 8 weeks of age, were acclimated for 7 days and caged in groups of five or fewer. The hindlegs of C57BL/6 mice were shaved with an electric razor on the day before electrotransfer. Animals were anesthetized by intraperitoneal injection of ketamine (100 mg/kg of body weight; Ketalar; Panpharma, Fougères, France) and xylazine (40 mg/kg; Rompun; Bayer, Sens, France) before all procedures. Experiments were conducted in accordance with the recommendations of the NIH for animal experimentation. We injected 20 μg each of pBi (control), pBi–RDD (experimental treatment), or pBi–RDD–Flag (to visualize RDD secreted by muscle cells), together with 10 μg of the Tet-tTS and 20 μg of the Tet-On plasmids, in sterile 0.9% NaCl (final volume, 30 μl) into the tibialis cranialis muscle, and electrotransfer was conducted as described previously (32, 35). Briefly, eight transcutaneous square electric pulses (200 V/cm) were applied for 20 ms by use of two stainless steel plate electrodes placed ~5.7 mm apart on the leg at a frequency of 1 Hz by use of a PS-15 electropulsator (Jouan, St. Herblain, France) to obtain muscle cell electroporation that allowed passage of plasmids into the cells. The entire procedure was repeated for the second leg.

Cell Lines and Culture. Human microvascular endothelial cells (HMEC-1) were provided by Dr. E. W. Ades (CDC, Atlanta, GA), who established this line by transfecting human dermal endothelial cells with SV40 Large T antigen (36). HMEC-1 cells were grown as monolayers in MCDB 131 medium (Sigma-Aldrich) supplemented with 2 mM L-glutamine, 100 IU/ml penicillin, 100 μg/ml streptomycin, 10% FCS (Life Technologies, Inc.), 10 ng/ml epidermal growth factor (R&D Systems, Abingdon, United Kingdom), and 1 μg/ml hydrocortisone (Sigma-Aldrich). Human umbilical vein endothelial cells (HUVECs), obtained as described by Jaffe *et al.* (37), were grown in M199 culture medium supplemented with 20% FCS, 2 mM L-glutamine, 100 IU/ml penicillin, 100 μg/ml streptomycin, 75 mM HEPES, 3.7 mM sodium bicarbonate (pH 7.5), and 5 μg/ml fungizone (Life Technologies, Inc.). Human dermal microvascular endothelial cells (HMVEC-d; Biowhittaker Europe, Verviers, Belgium) were grown in EGM-2MV medium (Biowhittaker Europe) containing 10% FCS, 2 mM L-glutamine, 100 IU/ml penicillin, and 100 μg/ml streptomycin and used at passages 4–6. Calf pulmonary artery endothelial (CPAE) cells provided by Dr. J. Badet (Laboratoire de Biotechnologie des Cellules Eucaryotes, Université de Créteil, Créteil, France), were grown as monolayers in MEM supplemented with 20% FCS, 2 mM L-glutamine, 100 IU/ml penicillin, and 100 μg/ml streptomycin and used at passages 12–20. Human mammary adenocarcinoma cell line MDA-MB-231 and murine skeletal muscle cell line C2C12 (American Type Culture Collection, Rockville, MD) were maintained in DMEM supplemented with 10% FCS, 2 mM L-glutamine, 100 IU/ml penicillin, and 100 μg/ml streptomycin. Murine melanoma B16F10 (ATCC) was grown in DMEM supplemented with 10% FCS, 2 mM L-glutamine, 100 IU/ml penicillin, and 100 μg/ml streptomycin, adjusted to contain 1.5 g/L of sodium bicarbonate (Invitrogen, Cergy-Pontoise, France). The six media supplemented as stated above for the seven corresponding cell lines are hereafter referred to as the appropriate complete media.

Assessment of Capillary Formation by Use of Microcarrier Beads in a Fibrin Gel. HMEC-1-coated microcarrier beads were cultured according to the method of Nehls and Drenckhahn (38), and details of the experiment were described by Trochon *et al.* (31). Briefly, HMEC-1-covered beads were embedded in a fibrin matrix containing RDD (5 μg/ml) or bovine thrombin (0.8 units/ml) as the control. Sprouting of capillary-like tubes from the periphery of microcarrier beads was observed as of the fourth day of culture. This neovascularization was photographed with an Olympus OM-2 camera on an inverted microscope, and capillary lengths were measured on the photos.

Cell Proliferation Assay. Cells were cultured in 96-well plates in the appropriate complete medium (2000 cells/well). After 24 h, the serum concentration in the same culture medium was halved to induce the cells to accumulate at the G_0-G_1 phase during the next 24 h. The cells were then cultured for 30 h in fresh medium with the full concentration in the presence of RDD at the indicated concentrations or 1.6 units/ml bovine thrombin. [^{3}H]Thymidine (1 μCi/well) was then added to the cells and allowed to incorporate for 16 h. The incorporated [^{3}H]thymidine was adsorbed on a filter paper with a Skatron (Lier, Norway) harvester, and the radioactivity was counted in a liquid scintillation counter (Beckman).

Assessment of Apoptosis by Flow Cytometry Analysis. To detect and quantify apoptosis, we used the AnnexinV-FITC Kit (R&D Systems). Briefly, CPAE (1×10^6) cells were cultured for 24 h in the presence of RDD (5 μg/ml) or bovine thrombin (0.8 units/ml). Pellets of 1×10^6 cells were resuspended in 100 μl of the kit reaction buffer containing propidium iodide (5 μg/ml) and 1:100 AnnexinV-FITC, according the manufacturer's instructions. After mixing, cells were incubated for 15 min in the dark at room temperature. Flow cytometry was performed on a FACS flow cytometer (EPICS XL-MCL; Coulter, Hialeah, FL). Experiments were run in triplicate.

Cell Attachment Assay. We coated 96-well plates overnight at 4°C with 100 μl of fibrinogen (40 μg/ml; Sigma-Aldrich), vitronectin (10 μg/ml; Sigma-Aldrich), or fibronectin (30 μg/ml; Sigma-Aldrich) in PBS. Negative controls consisted of wells coated with 2% BSA. CPAE cells (1×10^6) were cultured with 10 μg/ml RDD or bovine thrombin (1.6 units/ml) for 48 h. Cells were then detached from culture flasks by incubation with 1.5 mM EDTA and resuspended to a final concentration of 5×10^5 cells/ml in adhesion buffer

[140 mM NaCl, 10 mM HEPES, 5.56 mM glucose, 5.4 mM KCl, 2 mM $CaCl_2$, 1 mM $MgCl_2$, 1 mM $MnCl_2$ (pH 7.4)]]. The cell suspension (100 μl) was incubated for 20 min at 37°C on coated plates. Nonadherent cells were removed by washing the wells three times with 200 μl of adhesion buffer containing 1% BSA. Adherent cells were quantified by measuring cell phosphatase activity. Briefly, 100 μl of *p*-nitrophenylphosphate (3 mg/ml; Sigma-Aldrich) in sodium acetate buffer (pH 5.5) containing 0.1% Triton X-100 were added to the wells and incubated for 2 h at 37°C. The reaction was then stopped by the addition of 65 μl of 1 N NaOH. Released *p*-nitrophenol, which indicates the number of adherent cells, was measured by reading the absorbance at 405 nm in an ELISA reader (Labsystem, Cergy Pontoise, France). Nonspecific binding on BSA-coated plates was subtracted from the raw data. All experiments were run in triplicate.

Endothelial Cell Migration Assay. The migration assay was performed in 24-well culture plates, as described previously (39). Briefly, the wells were filled with 1.2% agarose (Sigma-Aldrich) dissolved in the culture medium, and the gel was allowed to set. The agarose cylinders were removed and cutoff in half, and each half was placed in a separate well into which 6.0×10^4 CPAE cells were deposited on the empty side and allowed to grow to confluence. The demi-agarose gel was then removed, RDD at the indicated concentrations or bovine thrombin (1.6 units/ml) was added, and the cells were allowed to migrate toward and through the newly created free space. Cell migration into free space could be measured by use of transparent graph paper stuck to the bottom of the culture plates.

Transient Transfection of C2C12 Skeletal Muscle Cells. C2C12 murine muscle cells were routinely grown in the appropriate complete medium. C2C12 cells maintained in tetracycline-free serum (Clontech) for at least 1 week were transfected with equimolar amounts (3 μg of total DNA) of each plasmid (pBi, pBi–RDD-Flag and both Tet-On and Tet-tTS) at 50% saturation in 6-well plates with Lipofectamine plus reagent (Life Technologies, Inc.), according to the protocol recommended by the manufacturer. Doxycycline (1 μg/ml final concentration; Sigma-Aldrich) was added daily to the culture medium starting on the day of transfection, and supernatants were collected 48 h later.

Subcellular Fractionation and Western Blotting. The two tibialis cranialis muscles per mouse were washed in ice-cold PBS, minced with scissors, and homogenized in 800 μl of iced-cold PBS in a glass Potter Elvejem homogenizer (VWR International, Strasbourg, France). The homogenate was then centrifuged at 700 × *g* for 10 min at 4°C, and the supernatant was collected. To detect RDD–Flag synthesized after electrotransfer of plasmids, 100 μg of total protein, determined with the BCA assay, were loaded on 10–20% tricine gels from Novex (Invitrogen, Cergy-Pontoise, France). Proteins were separated electrophoretically and transferred to nitrocellulose membranes (Sartorius, Göttingen, Germany). Membranes were blocked for 1 h in 10% nonfat dry milk in Tris-buffered saline [10 mM Tris (pH 7.5), 200 mM NaCl] containing 0.05% Tween 20. Membranes were then either incubated with polyclonal rabbit anti-RDD serum (Neosystem, Strasbourg, France), diluted 1:1000, for 1 h to detect *E. coli*-produced RDD or rabbit anti-Flag antibody (5 μg/ml; Sigma) to visualize RDD–Flag synthesized by skeletal muscle cells. After five washes with Tris-buffered saline–Tween, filters were incubated with an appropriate horseradish peroxidase-linked secondary antibody (Dako, Trappes, France), diluted 1:2000, for 1 h. Membranes were washed five times in Tris-buffered saline–Tween, and immunolabeling was detected by the enhanced chemiluminescence protocol (Amersham Pharmacia Biotech, Orsay, France).

Tumor Growth in Nude Mice. The regulatory plasmids Tet-On and Tet-tTS, together with 20 μg of either pBi–RDD or pBi (control), were electrotransferred into female nude mice. Cultured log-phase MDA-MB-231 cells were harvested with EDTA (0.2 g/L), washed, and resuspended in sterile PBS to a final concentration of 2×10^7 cells/ml. Cell suspension (200 μl) was injected s.c. into the backs of mice. Tumor size was monitored by measuring two perpendicular diameters with a dial caliper, and tumor volume was calculated as: $(\text{length} \times \text{width}/2)^3 \times \pi/6$. When tumors reached ~18 mm^3 in volume, RDD synthesis was induced in plasmid-electrotransferred muscle by the addition of doxycycline (200 μg/ml) to drinking water supplemented with 5% sucrose. Tumor size was monitored until day 14 after initiation of doxycycline stimulation.

Melanoma Pulmonary Metastases in Syngeneic Mice. The regulatory plasmids Tet-On and Tet-tTS together with 20 μg of either pBi–RDD or pBi (control) were electrotransferred into female C57BL/6 mice, and doxycycline RDD induction (see above) was started 3 days before log-phase cultured B16F10 melanoma cells were detached with 0.02% EDTA and resuspended to the final concentration of 2×10^6/ml in sterile 0.9% NaCl. We injected 100 μl of the suspension i.v. into the retro-orbital sinus of the mice. Ten days later, the mice were sacrificed, the lungs were excised, and metastatic nodules were counted under a dissecting microscope.

Immunohistochemistry. Paraffin sections (5-μm thick) of MDA-MB-231 tumor and tibialis cranialis muscles were cut, treated with xylene, rehydrated, and stained with H&E–saffranin. For immunohistochemistry, endogenous peroxidase activity was quenched by incubation with 3% H_2O_2 for 10 min. The sections were then washed in distilled water, incubated with blocking serum in Optimax wash buffer 1/10 (BioGenex, San Ramon, CA) for 10 min, and incubated with monoclonal rat anti-CD31 antibody (volume/volume mixture of MEC13.1 and 390; Becton Dickinson Europe, Le Pont De Claix, France), diluted 1:50, or polyclonal rabbit anti-Flag antibodies (Sigma), diluted 1:400, for 1 h. After two washes with Optimax, slides were incubated with peroxidase-conjugated goat polyclonal antirat or peroxidase-conjugated goat polyclonal antirabbit antibodies diluted 1:50, followed by two washes with Optimax. Slides were exposed to diaminobenzidine chromogenic substrate (PowerVision Histostaining Kit; ImmunoVision Technologies, Dady City, CA) for 10 min, washed with distilled water, counterstained with Mayer's hematoxylin, and mounted in permanent medium (Pertex). All slides were immunolabeled the same day, thus assuring standardized intensities of immunochemical signals and counterstaining.

Image Analysis. For each nude mouse, a representative histological sample, CD31-immunolabeled, was subjected to image analysis with a Zeiss Axiophot microscope coupled with a Sony 3 charge-coupled device camera (resolution, 768 × 576 pixels). Only viable tumor tissue was considered, excluding necrotic and fibrotic areas. For each specimen, the whole surface or eight contiguous fields were digitized when specimens were too large. Images were then analyzed with a specifically developed Linux-based program, as described by Martel-Renoir *et al.* (32).

RESULTS

RDD Purification. Human RDD was synthesized in *E. coli* as a GST fusion protein. Soluble GST–RDD (36 kDa) was purified by glutathione-agarose affinity chromatography and detected by Western blotting with rabbit polyclonal antiserum directed against a RDD peptide (Fig. 1*A*, *Lane 1*). GST–RDD was cleaved by bovine thrombin and further purified by glutathione-agarose chromatography to remove the fused GST. Purified RDD (10 kDa) migrated as a single

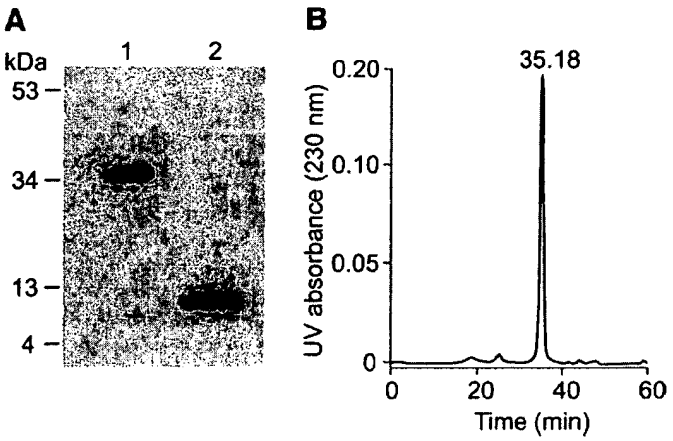

Fig. 1. Western blotting and fast-performance liquid chromatography analysis of purified recombinant human disintegrin domain (RDD). Recombinant glutathione *S*-transferase (GST)–RDD (36 kDa) was synthesized in *E. coli*. RDD (10 kDa) was obtained after thrombin cleavage of GST–RDD and further purified by glutathione-agarose affinity chromatography. GST–RDD (*Lane 1*) and RDD (*Lane 2*) were visualized by immunoblotting with rabbit antiserum (1:1000) to an RDD peptide (*A*). Purified RDD was analyzed by fast-performance liquid chromatography with Sephadex, and a single peak corresponding to RDD was observed (*B*).

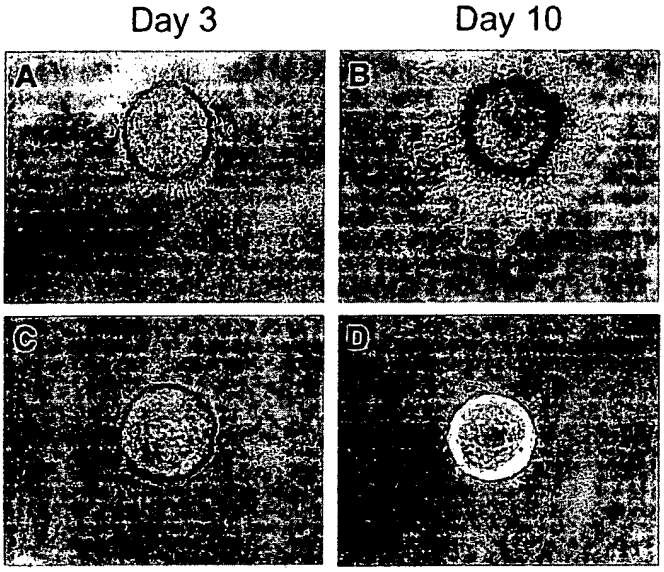

Fig. 2. Recombinant human disintegrin domain (RDD) inhibition of *in vitro* angiogenesis. The effect on capillary-like structure formation was investigated after 3 and 10 days of RDD treatment. Microcarrier beads entirely covered with confluent HMEC-1 cells were embedded in three-dimensional fibrin matrix in the absence (*A* and *B*) or the presence (*C* and *D*) of RDD (5 μg/ml). Aggregates were photographed under an inverted microscope.

band on tricine gel, and no residual GST–RDD was detected by immunoblotting (Fig. 1*A*, *Lane 2*). Size-exclusion fast-performance liquid chromatography gave a single RDD peak at the expected position, demonstrating a purity >95% (Fig. 1*B*).

RDD Inhibition of Capillary-Like Structure Formation. To study the effect of RDD on angiogenesis, we induced HMEC-1 cells, adapted for tube-like structure formation (38), to form anastomosing networks of capillary-like tubes in a fibrin gel, as described previously (40). Cells were cultured on microcarrier beads until confluence and were then embedded a in three-dimensional fibrin gel. As illustrated in Fig. 2, after 3 days of incubation, a capillary-like tube sprouting from HMEC-1 cells was visible (Fig. 2*A*), and RDD (5 μg/ml) inhibition of this proliferation could be observed (Fig. 2*C*). This inhibition was more obvious after 10 days of incubation (Fig. 2*D*). The mean length was reduced by 90.3 ± 1.5% after 10 days compared with control (Fig. 2*B*; $P < 0.05$, Mann–Whitney *U* test; data from 10 microcarrier beads for each condition).

Effect of RDD on Endothelial Cell Proliferation and Apoptosis. The ability of RDD (5 μg/ml) to inhibit proliferation of several endothelial cell lines (microvascular HMEC-1 and HMVEC-d cells, and macrovascular CPAE cells and HUVECs) was assessed in thymidine incorporation assays. The respective mean (±SE) percentages of inhibition were 33.1 ± 3.9, 53.6 ± 0.8, 57.2 ± 13.1 and 52.7 ± 3.0%. CPAE inhibition was dose-dependent with a maximum inhibition of 59.3% ($P < 0.01$, Student's *t* test; $n = 3$; Fig. 3*A*) at the RDD concentration of 10 μg/ml. We also studied the effect of RDD on CPAE apoptosis. The Annexin V method was used to determine the percentage of apoptotic cells after 24 h of treatment with RDD. Although cells entering apoptosis represented only a minor cell population (mean ± SE, 12.8 ± 2.5%), there were 3-fold more of them compared with the control (4.6 ± 0.9%; $n = 3$), suggesting that RDD did not intervene strongly in CPAE apoptosis.

RDD Inhibition of Endothelial Cell Migration. Because angiogenesis is highly dependent on endothelial cell motility, we examined the effect of RDD on CPAE migration in an *in vitro* assay, as we described previously (39). During this study, we observed morphological changes in the features of CPAE cells incubated with 5 μg/ml RDD: they formed long pseudopodia, and cell–cell interactions were altered (not shown). RDD inhibited CPAE migration in a concentration-dependent fashion between 2 and 10 μg/ml (Fig. 3*B*), with migration totally stopped at 10 μg/ml.

Effect of RDD on Endothelial Cell Adhesion. Endothelial cell adhesion to ECM essentially implicates integrins αvβ3 and α5β1, which have been reported to interact with metargidin (15, 16). We therefore analyzed the RDD effect on CPAE adhesion to immobilized fibrinogen, vitronectin, or fibronectin. Cells were cultured for 2 days in the presence of RDD (2, 5, or 10 μg/ml), and their adhesion to each substrate was evaluated. RDD at 10 μg/ml inhibited CPAE adhesion by ~30% (Fig. 3*C*), compared with the control, for the three adhesive proteins tested, indicating that RDD may interfere with cell adhesion but not block integrin-mediated cell adhesion. Lower concentrations showed no significant effect (results not shown).

RDD Synthesis by Skeletal Muscle Cells *in Vitro* and *in Vivo*. We evaluated RDD secretion by C2C12 muscle cells in culture, after transient transfection with the plasmids Tet-On and Tet-tTS together with pBi–RDD–Flag or control pBi. Starting the day of transfection, doxycycline (1 μg/ml) was added daily to the cell culture medium. RDD–Flag was detected in the supernatants of day 2 cultures by Western blotting with an anti-Flag antibody (Fig. 4*A*, *Lane 2*). A

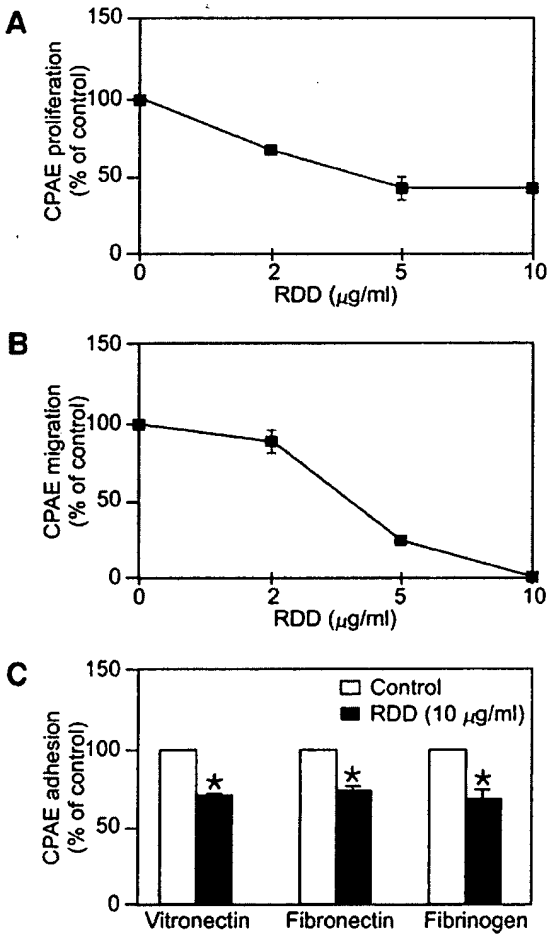

Fig. 3. Recombinant human disintegrin domain (RDD) inhibition of calf pulmonary artery endothelial (CPAE) cell proliferation, migration, and adhesion. CPAE proliferation (*A*) and migration (*B*) were estimated in the presence of the indicated RDD concentrations. To evaluate CPAE adhesion (*C*), cells preincubated for 48 h in the absence or presence of RDD (10 μg/ml) were detached and then incubated for 20 min in wells precoated with vitronectin (10 μg/ml), fibronectin (30 μg/ml), or fibrinogen (40 μg/ml). Nonadherent cells were removed by washing and adherent cells were quantified by measurement of cell phosphatase activity. Results are expressed as percentages of the controls. Results are the means ± SE (*error bars*) of three determinations. *, $P < 0.05$, Student's *t* test.

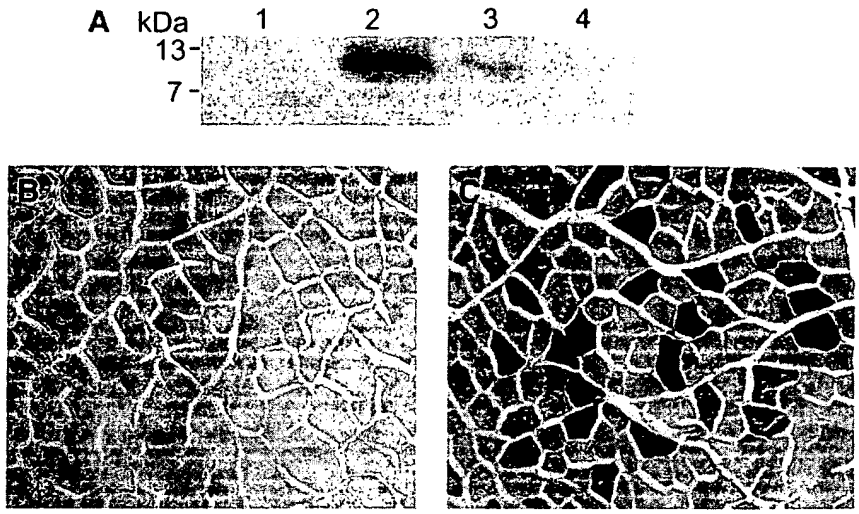

Fig. 4. Recombinant human disintegrin domain (RDD)–Flag secretion by skeletal muscle cells detected by Western blotting and immunolabeling on muscle sections. *A*, Western blot of RDD–Flag identified with anti-Flag antibody and visualized by chemiluminescence. Supernatants of muscle C2C12 cells transfected with the regulatory plasmids Tet-On and Tet-tTS plus empty pBi tetracycline-inducible plasmid (*Lane 1*) or plus pBi–RDD–Flag plasmid (*Lane 2*) were collected after 48 h of incubation in the presence of doxycycline (1 μg/ml). Nude mice were subjected to electrotransfer into muscle of the same plasmid system. Transgene expression was turned on for 1 week by the addition of doxycycline (200 μg/ml) to the drinking water. Muscle extracts were prepared, and 100 μg of total protein were loaded onto the gel. *Lane 3* contains the muscle extract from pBi–RDD–Flag-treated mice; *Lane 4* contains the pBi control plasmid. The molecular markers are indicated on the *left*. Sections of paraffin-embedded tibialis cranialis muscle from nude mice that had received the pBi control (*B*) or pBi–RDD–Flag plasmids (*C*) were immmunolabeled with anti-Flag antibodies then revealed by peroxidase-conjugated antibodies and diaminobenzidine chromogen.

10-kDa band was observed, corresponding to the RDD–Flag molecular mass, whereas no band appeared in control conditioned medium (Fig. 4*A*, *Lane 1*). *In vivo* RDD synthesis was evaluated after muscle-targeted gene electrotransfer of pBi–RDD–Flag or pBi together with Tet-On and Tet-tTS into nude mouse skeletal muscle (tibialis cranialis). After 1 week of doxycycline stimulation, the presence of RDD–Flag in muscle extracts was evaluated by Western blotting with anti-Flag antibodies. The expected 10-kDa band was detected (Fig. 4*A*, *Lane 3*) in RDD–Flag-treated animals. This band migrated just like the one produced *in vitro* by the pBi–RDD–Flag plasmid transfected into C2C12 muscle cells. No band was detected in the control animals (Fig. 4*A*, *Lane 4*). The presence of RDD–Flag in the muscle sections was visualized by immunochemical labeling (Fig. 4, *B* and *C*). This demonstration of transgene expression in the myofibers validated our use of this expression system in this animal model.

RDD Inhibition of MDA-MB-231 Tumor Growth in Nude Mice. We then examined the effect of skeletal muscle-synthesized and -secreted RDD on the growth of established MDA-MB-231 breast tumors. As above, mice received Tet-On, Tet-tTS, and pBi–RDD or pBi by electrotransfer before being inoculated s.c. with 4×10^6 MDA-MB-231 cells/animal. When tumors reached 18 mm^3, RDD expression was turned on by doxycycline. Tumor growth in the RDD-treated group was significantly inhibited compared with the controls (Fig. 5*A*). This inhibition became detectably by day 7 post-RDD induction. By day 14 postinduction, the mean tumor volume in RDD-treated mice was 98.1 mm^3, whereas in the control group, it had reached 451.2 mm^3, which corresponded to 78.2% inhibition of tumor growth. The tumors were removed on day 14, and intratumoral vascularization was visualized by immunolabeling of CD31 in tissue sections (Fig. 5, *B* and *C*) and quantified of the staining by digitized color imaging; there were 53.4 ± 0.2% ($P < 0.01$, Student's t test; $n = 10$) fewer vessels within RDD-treated tumors than in control tumors. This observation suggests that RDD inhibition of tumor growth corresponds to the inhibition of blood vessel development.

RDD Inhibition of Experimental Metastatic Spread. The same gene delivery system as that described above for MDA-MB-231 was used to investigate the effect of RDD on an experimental model of lung metastasis formation, using the melanoma cells line B16F10. The plasmids were electrotransferred into syngeneic C57BL/6 mice, and doxycycline induction was started immediately. Three days later, these mice received an i.v. injection of B16F10 cells. One week after inoculation, mice were sacrificed, their lungs were excised, and lung metastases were counted. In the presence of RDD, 74.2% fewer metastatic nodules were detected in the experimental group than the controls (Fig. 6). The experiment was repeat twice with similar results. This observation demonstrates that, in the presence of RDD, fewer metastatic nodules developed in the lungs.

DISCUSSION

During angiogenesis, activated endothelial cells undergo phenotypic changes and express a variety of functionally important molecules on their surfaces (41). Metargidin expression has been reported to be up-regulated on angiogenic endothelial cell surfaces (12). Because the soluble disintegrin domain of metargidin binds integrins, such as $\alpha5\beta1$, a proangiogenic adhesion integrin, and $\alpha v\beta3$, an integrin preferentially expressed on angiogenic blood vessel (15, 16), it can be suggested that the functions of these integrins and metargidin may be mutually dependent. This hypothesis led us to explore the action of the metargidin disintegrin domain, RDD, on angiogenesis. RDD synthesized and secreted by *E. coli* was tested *in vitro* on endothelial cells derived from large vessels (HUVECs and CPAE cells) or from microcapillaries (HMVEC-d and HMEC-1 cells). RDD antiangiogenic activity was clearly demonstrated in the three-dimensional fibrin gel model. RDD (5 μg/ml) potently inhibited capillary tube formation by 90%. Because capillary formation represents an end result of endothelial cell proliferation, adhesion, and migration, we further examined the effect of RDD on each of these processes. We noticed that RDD strongly affected endothelial cell migration. This assay, previously developed in our laboratory (39), enabled the accurate measurement of the CPAE cell front edge migration. RDD inhibited endothelial cell migration in a dose-dependent manner within the range of 2–10 μg/ml, with cell mobility being completely stopped at a RDD concentration of 10 μg/ml. In contrast, cell adhesion was only moderately affected, regardless of the integrin ligand substrate tested (vitronectin, fibronectin, or fibrinogen), suggesting that RDD action on cell migration is only partially dependent on inhibition of cell adhesion via integrin molecules.

RDD also inhibited endothelial cell proliferation in a concentration-dependent manner. An inhibition of ~50% at 5 μg/ml RDD was constantly observed in our experiments using HUVEC, CPAE, or HMVEC-d cell lines. Apparently RDD affects both endothelial cell migration and proliferation, and these dual actions have been reported for other antiangiogenic molecules, such as angiostatin and endostatin (2, 3, 42, 43). In addition, we found weak proapoptotic activity for RDD. RDD inhibition of angiogenesis therefore probably results from

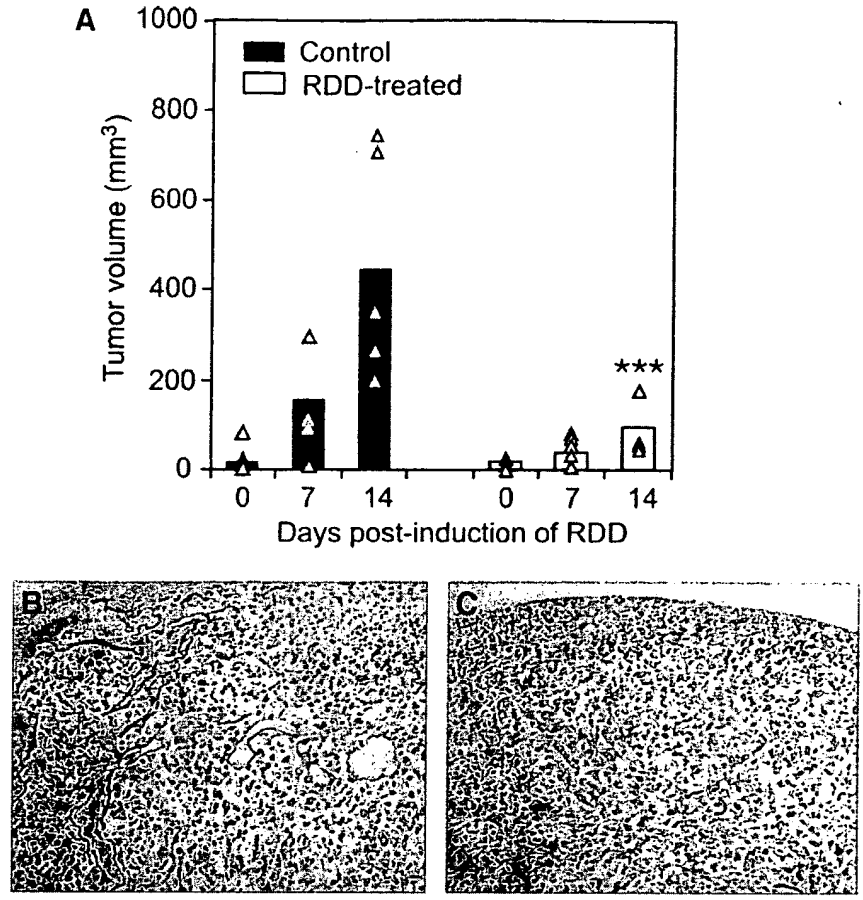

Fig. 5. Recombinant human disintegrin domain (RDD) inhibition of MDA-MB-231 tumor growth and angiogenesis. Equimolar concentrations of the Tet-On and Tet-tTS regulatory plasmids and pBi-RDD 20 μg or pBi (control) plasmids in 0.9% NaCl were injected into the tibialis cranialis of female nude mice and subjected to electrotransfer. MDA-MB-231 cells (4×10^6) were then injected s.c. into the flank. When tumor volumes reached 18 mm^3, muscle RDD production was turned on by the addition of doxycycline (200 μg/ml) to the drinking water. *A*, △ represent individual tumor volumes; the *histograms* are the mean values of each group of five mice. ***, $P < 0.01$, Mann–Whitney *U* test. The tumors were removed 14 days after transgene induction. Paraffin-embedded MDA-MB-231 sections were immunolabeled with an anti-CD31 antibody. *B* and *C*, photographs show control (*B*) and RDD-treated (*C*) tumors.

combined actions on endothelial cell migration, proliferation, and apoptosis.

One of the key mechanisms involved in RDD inhibition was first thought to be related to its integrin-binding domain. On the basis of the critical role of integrins in vascular development and cell survival (25, 44, 45), therapeutic agents blocking those integrins, expressed by angiogenic endothelial cells, have been tested in several laboratories. Specific reagents targeting αv integrins, such as vitaxin or RGD-based peptides, inhibited tumor-associated angiogenesis in various animal models (18–20) and induced endothelial cell apoptosis (25). At present, the exact roles of those integrins expressed on endothelial cells during angiogenesis is still unknown, because αv- and β3-integrin-null mice were found to exhibit enhanced neovascularization (28–30). Recently, Hynes (30) has suggested that these integrins are negative regulators of angiogenesis and that the antiangiogenic effect of drugs targeting them results from an agonistic rather than antagonistic action. In contrast to $\alpha v\beta 3$, $\alpha 5\beta 1$ integrin is unambiguously angiogenic, and an antagonist ligating this integrin was shown to successfully inhibit angiogenesis (46). Thus, RDD may exert its action by neutralizing integrin proangiogenic actions and/or increasing integrin inhibitory actions. Moreover, a recent observation showing the colocalization of metargidin with vascular endothelial cadherin (14) suggests that the antiangiogenic activity of RDD might also be associated with a defect in the formation of cell junctions between endothelial cells. This possibility could represent another mechanism involved in the RDD effect.

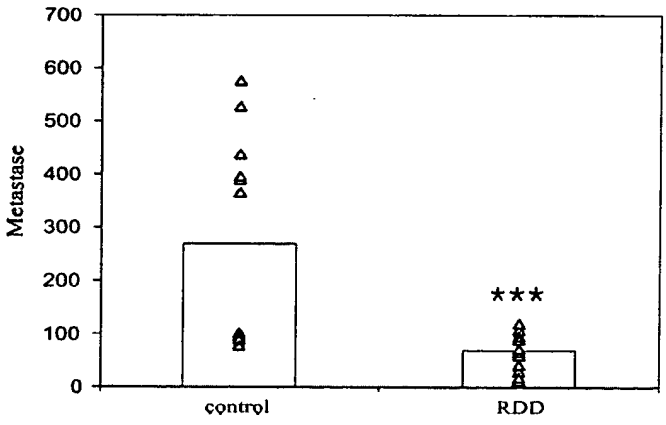

Fig. 6. Effect of recombinant human disintegrin domain (RDD) on B16F10 melanoma dissemination. C57BL/6 mice received pBi-RDD or pBi (control), Tet-tTS and Tet-On plasmids; doxycycline (200 μg/ml) was added to the drinking water from the day of electrotransfer. After 3 days, B16F10 cells (2×10^5) were injected into the retro-orbital sinuses of these animals. Lungs were removed from the mice 10 days after induction of RDD expression. △ represent the number of the pulmonary metastatic nodules from one mouse, and *histograms* are the mean values for each group of 15 mice. ***, $P < 0.01$, Mann–Whitney *U* test.

The observed multiple inhibitory activities of RDD were not surprising because metargidin is a multifunctional molecule, as suggested by its structure. Metargidin is composed of an active metalloproteinase domain and an intracellular signaling tail separated by a disintegrin domain (13, 47, 48). The interaction of metargidin with integrins expressed on cell membranes suggests that metargidin functions may be dictated by localization or distribution on the cell membrane. This situation would imply that its functions might be regulated by integrins or other, as yet unidentified, metargidin-binding proteins. On other hand, it has been postulated that RDD may most likely affect metargidin functions, *e.g.*, the proteolytic activity of its metalloproteinase domain, by preventing its association with binding proteins.

Thus, by blocking metargidin degradation of ECM components, RDD may prevent endothelial cell migration. This hypothesis is in good agreement with the potent inhibitory action of RDD on cell migration. Moreover, RDD may inhibit endothelial cell proliferation by interfering with metargidin intracellular signaling via binding partners of its cytoplasmic domain and/or a related integrin (23, 47–49).

We further evaluated the effect of RDD on angiogenesis-mediated tumor growth and metastasis. The *RDD* gene inserted in plasmids was electrotransferred into mouse skeletal muscles in a tetracycline-inducible system. This system has been used successfully in many *in vivo* studies (32, 35, 50–53). We recently demonstrated that the *in vivo* expression of the transgene in this model was rapid, stable, and tightly regulated (32). Moreover, protein was detected in the blood (~50 ng/ml) and could last more than 2 months (32). Our present results show that RDD production *in vivo* inhibited s.c. MDA-MB-231 tumor growth by 78% at day 14 after transgene induction and that this was associated with significantly less tumor vascularization. In addition, in the presence of RDD, 74% fewer B16F10 melanoma metastatic nodules formed in mouse lungs after 1 week of treatment.

Although the precise mechanisms involved in these effects require further investigation, the results of this study demonstrate the antiangiogenic and anticancer activities of RDD. These results are in good agreement with recent data showing the involvement of ADAM-15 in pathological neovascularization in knockout mice (54). It is reasonable to postulate that the human RDD used in this study might affect angiogenesis and tumor metastasis through $\alpha v\beta 3$ and $\alpha 5\beta 1$ *in vivo*. Nevertheless, the disintegrin domain of mouse metargidin differs from that of human metargidin because it has a TDD sequence instead of RGD (55). Thus, mouse metargidin interacts with $\alpha 9\beta 1$ instead of $\alpha v\beta 3$ and $\alpha 5\beta 1$ (17). Therefore, it will be very interesting to investigate the effect of mouse RDD *in vivo* in comparison with human RDD.

Disintegrins derived from snake venom, such as rhodostomin, accutin, and salmosin, have already been shown to have important inhibitory effects on angiogenesis (56–58) and on metastatic properties of melanoma cells (59, 60). Compared with those disintegrin, RDD has the singular advantage of being the first endogenous disintegrin molecule of human origin and, hence, might avoid immunogenic side effects from the point of the view of future clinical settings. We believe that further investigations will support the potential clinical use of RDD as a potent and promising anticancer agent.

ACKNOWLEDGMENTS

We are grateful to Monique Stanciu (Institut Gustave Roussy, Villejuif, France) for excellent technical contributions to this study. We thank Dr. E. W. Ades for the gift of the HMEC-1 cell line, Dr. J. Badet for the CPAE cell line, and Dr. Y. Takada for the pGEX-2T vector.

REFERENCES

1. Folkman J Angiogenesis in cancer, vascular, rheumatoid and other diseases. Nat Med 1995;1:27–31.
2. O'Reilly MS, Holmgren L, Shing Y, et al. Angiostatin, a novel angiogenesis inhibitor that mediates the suppression of metastases of Lewis lung carcinoma. Cell 1994;79: 315–28.
3. O'Reilly MS, Boehm T, Shing Y, et al. Endostatin: an endogenous inhibitor of angiogenesis and tumor growth. Cell 1997;88:277–85.
4. Kamphaus GD, Colorado PC, Panka DJ, et al. Canstatin, a novel matrix-derived inhibitor of angiogenesis and tumor growth. J Biol Chem 2000;275:1209–15.
5. Colorado PC, Torre A, Kamphaus G, et al. Anti-angiogenic cues from vascular basement membrane collagen. Cancer Res 2000;60:2520–6.
6. Han J, Ohno N, Pasco S, Monboisse JC, Borel JP, Kefalides NA. A cell binding domain from the α3 chain of type IV collagen inhibits proliferation of melanoma cells. J Biol Chem 1997;272:20395–401.
7. Maeshima Y, Colorado PC, Kalluri R. Two RGD-independent $\alpha v\beta 3$ integrin binding sites on tumstatin regulate distinct anti-tumor properties. J Biol Chem 2000;275: 23745–50.
8. Wolfsberg TG, Primakoff P, Myles DG, White JM. ADAM, a novel family of membrane proteins containing a disintegrin and metalloprotease domain: multipotential functions in cell–cell and cell–matrix interactions. J Cell Biol 1995;131:275–8.
9. Black RA, White JM. ADAMs: focus on the protease domain. Curr Opin Cell Biol 1998;10:654–9.
10. Duffy MJ, Lynn DJ, Lloyd AT, O'Shea CM. The ADAMs family of proteins: from basic studies to potential clinical applications. Thromb Haemost 2003;89: 622–31.
11. Krätzschmar J, Lum L Blobel C. Metargidin, a membrane-anchored metalloprotease–disintegrin protein with an RGD integrin binding sequence. J Biol Chem 1996;271: 4593–6.
12. Herren B, Raines EW, Ross R. Expression of a disintegrin-like protein in cultured human vascular cells and *in vivo*. FASEB J 1997;11:173–80.
13. Martin J, Eynstone LV, Davies M, Williams JD, Steadman R. The role of ADAM15 in glomerular mesangial cell migration. J Biol Chem 2002;277:33683–9.
14. Ham C, Levkau B, Raines EW, Herren B. ADAM15 is an adherens junction molecule whose surface expression can be driven by VE-cadherin. Exp Cell Res 2002;279: 239–47.
15. Zhang XP, Kamata T, Yokoyama K, Puzon-McLaughlin W, Takada Y. Specific interaction of the recombinant disintegrin-like domain of MDC-15 (metargidin, ADAM-15) with integrin $\alpha v\beta 3$. J Biol Chem 1998;273:7345–50.
16. Nath D, Slocombe PM, Stephens PE, et al. Interaction of metargidin (ADAM-15) with $\alpha v\beta 3$ and $\alpha 5\beta 1$ integrins on different haemopoietic cells. J Cell Sci 1999;112: 579–87.
17. Eto K, Puzon-McLaughlin W, Sheppard D, Sehara-Fujisawa A, Zhang X-P, Takada Y. RGD-independent binding of integrin $\alpha 9\beta 1$ to the ADAM-12 and -15 disintegrin domains mediates cell–cell interaction. J Biol Chem 2000;275:34922–30.
18. Brooks PC, Montgomery AM, Rosenfeld M, et al. Integrin $\alpha v\beta 3$ antagonists promote tumor regression by inducing apoptosis of angiogenic blood vessels. Cell 1994;79: 1157–64.
19. Drake CJ, Cheresh DA, Little CD. An antagonist of integrin $\alpha v\beta 3$ prevents maturation of blood vessels during embryonic neovascularization. J Cell Sci 1995;108:2655–61.
20. Hammes HP, Brownlee M, Jonczyk A, Sutter A Preissner KT. Subcutaneous injection of a cyclic peptide antagonist of vitronectin receptor-type integrins inhibits retinal neovascularization. Nat Med 1996;2:529–33.
21. Kerr JS, Wexler RS, Mousa SA, et al. Novel small molecule αv integrin antagonists: comparative anti-cancer efficacy with known angiogenesis inhibitors. Anticancer Res 1999;19:959–68.
22. Patel SR, Jenkins J, Papadopolous N, et al. Pilot study of vitaxin–an angiogenesis inhibitor–in patients with advanced leiomyosarcomas. Cancer 2001;92:1347–8.
23. Hynes RO. Integrins: versatility, modulation, and signaling in cell adhesion. Cell 1992;69:11–25.
24. Friedlander M, Brooks PC, Shaffer RW, Kincaid CM, Varner JA, Cheresh DA. Definition of two angiogenic pathways by distinct αv integrins. Science 1995;270: 1500–2.
25. Eliceiri BP, Cheresh DA. Role of αv integrins during angiogenesis. Cancer J 2000; 6:245–9.
26. Eliceiri BP, Cheresh DA. Adhesion events in angiogenesis. Curr Opin Cell Biol 2001;13:563–8.
27. Bader BL, Rayburn H, Crowley D, Hynes RO. Extensive vasculogenesis, angiogenesis, and organogenesis precede lethality in mice lacking all αv integrins. Cell 1998;95:507–19.
28. Reynolds LE, Wyder L, Lively JC, et al. Enhanced pathological angiogenesis in mice lacking β3 integrin or β3 and β5 integrins. Nat Med 2002;8:27–34.
29. Cheresh DA, Stupack, DG. Integrin-mediated death: an explanation of the integrin-knockout phenotype? Nat Med 2002;8:193–4.
30. Hynes RA reevaluation of integrins as regulators of angiogenesis. Nat Med 2002;8: 918–21.
31. Trochon V, Li H, Vasse M, et al. Endothelial metalloprotease–disintegrin protein (ADAM) is implicated in angiogenesis *in vitro*. Angiogenesis 1998;2:277–85.
32. Martel-Renoir D, Trochon-Joseph V, Galaup A, et al. Co-electrotransfer to skeletal muscle of three plasmids coding for anti-angiogenic factors and regulatory factors of the tetracycline-inducible system: tightly regulated expression, inhibition of transplanted tumor growth, and anti-metastatic effect. Mol Ther 2003;8:425–33.
33. Smith DB, Johnson KS. Single-step purification of polypeptides expressed in *Escherichia coli* as fusions with glutathione *S*-transferase. Gene 1988;67:31–40.
34. Li H, Lu H, Griscelli F, et al. Adenovirus-mediated delivery of a uPA/uPAR antagonist suppresses angiogenesis-dependent tumor growth and dissemination in mice. Gene Ther 1998;5:1105–13.
35. Mir LM, Bureau MF, Gehl J, et al. High-efficiency gene transfer into skeletal muscle mediated by electric pulses. Proc Natl Acad Sci USA 1999;96:4262–7.
36. Xu Y, Swerlick RA, Sepp N, Bosse D, Ades EW, Lawley TJ. Characterization of expression and modulation of cell adhesion molecules on an immortalized human dermal microvascular endothelial cell line (HMEC-1). J Investig Dermatol 1994;102: 833–7.
37. Jaffe EA, Hoyer LW, Nachman RL. Synthesis of von Willebrand factor by cultured human endothelial cells. Proc Natl Acad Sci USA 1974;71:1906–9.
38. Nehls V Drenckhahn D. A novel, microcarrier-based *in vitro* assay for rapid and reliable quantification of three-dimensional cell migration and angiogenesis. Microvasc Res 1995;50:311–22.
39. Trochon V, Mabilat C, Bertrand P, et al. Evidence of involvement of CD44 in endothelial cell proliferation, migration and angiogenesis *in vitro*. Int J Cancer 1996;66:664–8.

40. Trochon V, Mabilat-Pragnon C, Bertrand P, et al. Hyaluronectin blocks the stimulatory effect of hyaluronan-derived fragments on endothelial cells during angiogenesis *in vitro*. FEBS Lett 1997;418:6–10.
41. Jekunen A, Kairemo K. Inhibition of angiogenesis at endothelial cell level. Microsc Res Tech 2003;60:85–97.
42. Claesson-Welsh L, Welsh M, Ito N, et al. Angiostatin induces endothelial cell apoptosis and activation of focal adhesion kinase independently of the integrin-binding motif RGD. Proc Natl Acad Sci USA 1998;95:5579–83.
43. Yamaguchi N, Anand-Apte B, Lee M, et al. Endostatin inhibits VEGF-induced endothelial cell migration and tumor growth independently of zinc binding. EMBO J 1999;18:4414–23.
44. Meredith JE, Fazeli B Schwartz MA. The extracellular matrix as a cell survival factor. Mol Biol Cell 1993;4:953–61.
45. Re F, Zanetti A, Sironi M, et al. Inhibition of anchorage-dependent cell spreading triggers apoptosis in cultured human endothelial cells. J Cell Biol 1994;127:537–46.
46. Kim S, Bell K, Mousa SA, Varner JA. Regulation of angiogenesis *in vivo* by ligation of integrin $\alpha 5\beta 1$ with the central cell-binding domain of fibronectin. Am J Pathol 2000;156:1345–62.
47. Howard L, Nelson KK, Maciewicz RA, Blobel CP. Interaction of the metalloprotease disintegrins MDC9 and MDC15 with two SH3 domain-containing proteins, endophilin I and SH3PX1. J Biol Chem 1999;274:31693–9.
48. Poghosyan Z, Robbins SM, Houslay MD, Webster A, Murphy G Edwards DR. Phosphorylation-dependent interactions between ADAM15 cytoplasmic domain and Src family protein-tyrosine kinases. J Biol Chem 2002;277:4999–5007.
49. Aplin AE, Howe A, Alahari SK, Juliano RL. Signal transduction and signal modulation by cell adhesion receptors: the role of integrins, cadherins, immunoglobulin-cell adhesion molecules, and selectins. Pharmacol Rev 1998;50:197–263.
50. Athanasopoulo T, Owen JS, Hassall D, et al. Intramuscular injection of a plasmid vector expressing human apolipoprotein E limits progression of xanthoma and aortic atheroma in apoE-deficient mice. Hum Mol Genet 2000;9:2545–51.
51. Nakano A, Matsumori A, Kawamoto S, et al. Cytokine gene therapy for myocarditis by *in vivo* electroporation. Hum Gene Ther 2001;12:1289–97.
52. Lucas ML, Heller L, Coppola D Heller R. IL-12 plasmid delivery by *in vivo* electroporation for the successful treatment of established subcutaneous B16F10 melanoma. Mol Ther 2002;5:668–75.
53. Perez N, Plence P, Millet V, et al. Tetracycline transcriptional silencer tightly controls transgene expression after *in vivo* intramuscular electrotransfer: application to interleukin 10 therapy in experimental arthritis. Hum Gene Ther 2002;13:2161–72.
54. Horiuchi K, Weskamp G, Lum L, et al. Potential role for ADAM15 in pathological neovascularization in mice Mol Cell Biol 2003;23:5614–24.
55. Lum L, Reid MS, Blobel CP. Intracellular maturation of the mouse metalloprotease disintegrin MDC15. J Biol Chem 1998;273:26236–47.
56. Yeh CH, Peng HC, Yang RS, Huang, T-F. Rhodostomin, a snake venom disintegrin, inhibits angiogenesis elicited by basic fibroblast growth factor and suppresses tumor growth by a selective $\alpha v\beta 3$ blockade of endothelial cells. Mol Pharmacol 2001;59:1333–42.
57. Yeh CH, Peng HC, Huang TF. Accutin, a new disintegrin, inhibits angiogenesis *in vitro* and *in vivo* by acting as integrin $\alpha v\beta 3$ antagonist and inducing apoptosis. Blood 1998;92:3268–76.
58. Kang IC, Lee YD, Kim DS. A novel disintegrin salmosin inhibits tumor angiogenesis. Cancer Res 1999;59:3754–60.
59. Beviglia L, Stewart GJ, Niewiarowski S. Effect of four disintegrins on the adhesive and metastatic properties of B16F10 melanoma cells in a murine model. Oncol Res 1995;7:7–20.
60. Kang IC, Kim DS, Jang Y, Chung KH. Suppressive mechanism of salmosin, a novel disintegrin in B16 melanoma cell metastasis. Biochem Biophys Res Commun 2000;275:169–73.

Biochemical and Biophysical Research Communications 280, 574–580 (2001)
doi:10.1006/bbrc.2000.4155, available online at http://www.idealibrary.com on IDEAL®

MDC-9 (ADAM-9/Meltrin γ) Functions as an Adhesion Molecule by Binding the $\alpha_v\beta_5$ Integrin

Min Zhou, R. Graham, G. Russell, and Peter I. Croucher
Division of Genomic Medicine, University of Sheffield Medical School, Sheffield. United Kingdom

Received December 11, 2000

MDC-9 is a widely expressed member of the metalloproteinase/disintegrin/cysteine-rich protein family. The disintegrin domain of MDC-9 lacks an RGD motif but has recently been reported to bind the $\alpha_6\beta_1$ integrin; however, it is unclear whether MDC-9 can bind other integrins. In the present study myeloma cells, but not lymphoblastoid cells, were shown to bind to immobilised, recombinantly expressed MDC-9 disintegrin domain (A9dis). Binding was divalent cation-dependent, being supported by Mn^{2+} and Ca^{2+}. Adhesion of myeloma cells to A9dis was completely inhibited by an antibody to the $\alpha_v\beta_5$ integrin but not by antibodies to other subunits. RGD-containing peptides had no effect on binding, suggesting that MDC-9 interacts with $\alpha_v\beta_5$ in an RGD-independent manner. Flow cytometric analyses demonstrated that myeloma cells, but not lymphoblastoid cells, expressed $\alpha_v\beta_5$ on the cell membrane. These data indicated that the disintegrin domain of MDC-9 can function as an adhesion molecule by interacting with an $\alpha_v\beta_5$ integrin. © 2001 Academic Press

Key Words: **MDC-9; ADAM-9; meltrin γ; adhesion; integrin; $\alpha_v\beta_5$; disintegrin.**

The MDC (metalloproteinase/disintegrin/cysteine-rich) or ADAM (a disintegrin and metalloproteinase) family is a recently described group of proteins with a characteristic domain structure (1). This includes the presence of a pro-region, a metalloproteinase domain, a disintegrin-like region, a cysteine-rich domain, a transmembrane region and a short cytoplasmic tail (1). The functions of members of this family are unclear. However, their domain organisation suggest that they may play roles in a number of important biological processes, including proteolysis, cell/cell or cell/matrix interactions and cell signalling (2–4). Recent studies have focused on their role in proteolysis and have implicated members of the family in the processing of cytokines, the shedding of cytokine receptors and adhesion molecules(5–10), and the remodelling of extracellular matrix components (11–13). However, less is known of the function of other domains of MDC/ADAMs, including the disintegrin-like domain.

Studies have demonstrated that the disintegrin-like domain of the sperm protein fertilin β (ADAM-2), which mediates sperm–egg fusion (14–16), may recognise the $\alpha_6\beta_1$ integrin on the egg membrane (17–19). Human metargidin (ADAM-15), which is the only member of the MDC family to contain the RGD tripeptide motif in the disintegrin-like domain (20), has been demonstrated to mediate cell adhesion via interactions with either $\alpha_v\beta_3$ or $\alpha_5\beta_1$ integrins (21, 22). More recently, murine metargidin, which contains TDD in place of RGD and ADAM-12, which also lacks RGD, have been reported to bind the integrin $\alpha_9\beta_1$ (23). Furthermore, ADAM-23, another non-RGD containing member of the family has recently been shown to interact with the $\alpha_v\beta_3$ integrin (24). However, it is unclear whether the non-RGD containing members of the MDC/ADAM family interact with a single specific integrin or whether they have the capacity to bind to other integrin heterodimers, as is the case with human metargidin (22). MDC-9, a widely expressed, non-RGD containing, member of this family (25, 26), has recently been shown to bind to the $\alpha_6\beta_1$ integrin on fibroblasts, although it is not clear whether it can also bind to other integrins on different cells. Therefore in the present study we have expressed the disintegrin-like domain of MDC-9 as a GST fusion protein and demonstrate that this protein can also mediate binding to human myeloma cells. Furthermore, we provide evidence that the distingrin-like domain of MDC-9 mediates this adhesive interaction by binding to the $\alpha_v\beta_5$ integrin suggesting that this non-RGD containing MDC/ADAM family member has the capacity to interact with more than one integrin.

MATERIALS AND METHODS

Antibodies and cell lines. The mouse IgG_1 anti-human $\alpha_v\beta_5$ mAb ascites (P1F6), mouse IgG_1 anti-human α_2 mAb ascites (P1E6), RGD peptide (GRGDSP) and control peptide (GRGESP) were from GIBCO Life-Technologies (Paisley, UK) and the mouse IgG_1 anti-human β_3

0006-291X/01 $35.00

antibody (PM6/13) was purchased from Serotec (Oxford, UK). The rat anti-human β_1 (mAB 13) and rat anti-human α_5 (mAB 16) were a kind gift from Prof. K. Yamada (NIH, U.S.A.). Isotype control mouse IgG_1 and rat IgG were from Sigma (Poole, UK). Rabbit anti mouse $F(ab')_2$ IgG and HRP conjugated anti-rabbit IgG were obtained from DAKO (Ely, UK). The human myeloma cell lines NCI-H929 and RPMI-8226, and lymphoblastic cell line, ARH-77, were obtained from the European Collection of Animal Cell Cultures (Salisbury, UK). The human myeloma cell line, JJN-3, was provided by Professor I. Franklin (Glasgow, UK). Cells were maintained in RPMI 1640 supplemented with 10% fetal calf serum (FCS), 2 mM L-glutamine, 1 mM sodium pyruvate, 1× MEM non-essential amino acids and 5 μM 2-mercaptoethanol at 37°C in a humidified atmosphere of 95% air and 5% CO_2.

Generation of GST/MDC-9 disintegrin domain fusion protein. A cDNA encoding the entire disintegrin domain, and containing an equal number of cysteine residues, was generated by polymerase chain reaction (PCR) from a JJN-3 cDNA library using the following primers, 5'-primer, 5'-GGA-TCC-AGT-GCA-GAG-GAC-TTT-GAG-AA and 3'-primer, 5'-G-AAT-TCT-GCC-GTT-GTA-GCA-ATA-GGC. The 5'-primer contained a *Bam*HI restriction site introduced for subcloning and encodes the most C'-terminal 7 amino acids of the metalloproteinase domain. The 3' primer contained an *Eco*RI restriction site and was complementary to the cDNA sequence of MDC-9, predicted to encode the start (N-terminal region) of the cysteine-rich domain between residues 508–515. The cDNA fragment bearing full length MDC-9 disintegrin domain was subcloned into the *Bam*HI and *Eco*RI site of a pGEX-2T expression vector (Amersham Pharmacia Biotech, Little Chalfont, UK) and transformed into the XL-1 Blue strain of *E. coli* (Stratagene, Cambridge, UK). Plasmids containing the disintegrin domain of MDC-9 (pGEX-2T-A9dis) were sequenced and transformed into the BL21 strain of *E. coli* for production of recombinant protein (A9dis). Synthesis of the glutathione *S*-transferase (GST)/MDC-9 disintegrin domain fusion protein (GST/A9dis) was induced in BL21 cells by 0.1 mM isopropyl-1-thio-β-D-galactopyranoside (IPTG) (Amersham Pharmacia Biotech). The fusion protein was extracted by mild sonication in PBS and purified using glutathione Sepharose 4B (Pharmacia Biotech) affinity chromatography. A9dis was released from GST by cleavage with thrombin (Pharmacia Biotech). The concentration of A9dis was quantitated using the BCA protein assay. The quality of the purified GST/A9dis and A9dis was determined by SDS–PAGE with Coomassie brilliant blue staining.

Cell adhesion assays. 96-well microtiter plates were coated with the purified recombinant A9dis, diluted to the specified concentration in PBS (pH 7.2). As a control, protein was also prepared by subjecting the empty pGEX-2T vector to an identical expression, purification and coating protocol as the pGEX-2T-A9dis vector. The remaining protein binding sites were blocked by incubating wells with bovine serum albumin (10 mg/ml, BSA, Sigma) in PBS.

To assess whether A9dis could function as an adhesion molecule, human myeloma cells or human lymphoblastoid cells were harvested from tissue culture, washed and resuspended in RPMI 1640 medium containing 1 mg/ml BSA. 1×10^5 cells were added to each well of precoated 96-well plates and incubated at 37°C for 1.5 h. The non-adherent cells were removed by gentle washing with PBS and bound cells were then fixed with 4% formaldehyde. Wells were then washed once in 70% ethanol, once with PBS and air-dried. 100 μl of 5 μM propidium iodide were added to each well to stain the nuclei. The fluorescence associated with each well was measured on a fluorescence plate reader at an excitation wavelength of 530 nm and an emission wavelength of 620 nm.

In experiments to examine the effect of divalent cations on cell binding, human myeloma cells (1×10^5), containing one of the following divalent ions, Mg^{2+}, Mn^{2+}, Ca^{2+}, Zn^{2+} and Ni^{2+}, at a concentration of 1 mM in Hanks' balanced salt solution (HBSS) (KCl, 0.40 g/L, KH_2PO_4, 0.06 g/L, NaCl, 8.00 g/L, $NaHCO_3$, 0.35 g/L, Na_2HPO_4, 0.48 g/L, D-glucose, 1 g/L) containing 1 mg/ml BSA and 25 mM Hepes, pH 7.4, were added to A9dis-coated plates and incubated at 37°C for 1.5 h. To determine whether the concentration of Ca^{2+} affects cell adhesion to A9dis binding was performed in the presence of Ca^{2+} at a concentration of 0.05, 0.5, 1 and 2.5 mM. In blocking experiments, cells were preincubated with 1:5000 dilution of anti-$\alpha_v\beta_5$ mAb, 10 μg/ml anti-β_3, 1:150 dilution of anti-α_2 mAb, 10 μg/ml anti-β_1, 15 μg/ml anti-α_5, or appropriate control in RPMI 1640 medium containing 1 mg/ml BSA for 45 min. The RGD peptide and control peptide, at a concentration of 10 μg/ml, were also used to pre-incubate cells prior to introduction into the adhesion assay. The myeloma cells (1×10^5/well), containing blocking agents, were then added to the A9dis or control coated wells and allowed to adhere for 1.5 h. Adherent cells were stained with propidium iodide and the fluorescence associated with each well was assessed as described above. The fluorescence associated with wells coated with control protein was subtracted from that of those coated with A9dis to determine levels of specific binding.

Flow cytometric analysis. To assess the level of expression of the integrin $\alpha_v\beta_5$ on RPMI-8226, NCI-H929, JJN-3 and ARH-77 cells, flow cytometric analysis was performed using standard protocols. Briefly, 1×10^6 cells were removed from culture and washed. Cells were incubated with mouse anti-αvβ5 antibody or isotype control antibody, followed by FITC-conjugate $F(ab')_2$ rabbit anti-mouse secondary antibody. PI was added at a final concentration of 8 μg/ml before samples were analysed on a Becton–Dickinson FACSort benchtop cytometer.

Statistics. Data are presented at the mean ± SD of triplicate measurements. Experiments were repeated on a minimum of three separate occasions and a representative experiment is shown in each case. Comparisons between groups were performed by Student's *t* test.

RESULTS

Expression of the MDC-9 Disintegrin Domain Protein, A9dis

A cDNA encoding the MDC-9 disintegrin domain was amplified by PCR and introduced into the polylinker of pGEX-2T. Automated fluorescence DNA sequencing confirmed the MDC-9 disintegrin domain sequence was located 5' and immediately downstream from the thrombin cleavage site, and in the correct reading frame (Fig. 1A). The pGEX-A9dis construct, or pGEX-2T alone, were transformed into *E. coli* BL21 and expression induced using the lactose analogue IPTG. The GST-A9dis fusion protein was expressed at between 2.5 and 8 mg per litre of culture, under optimal induction conditions. Figure 1B shows the overexpression of the fusion protein, at the expected size of 45kDa, by the cells carrying the pGEX-2T-A9dis expression construct (Fig. 1B, lane 2) and of GST, at the expected size of 29 kDa, by the cells bearing the control vector pGEX-2T (Fig. 1B, lane 1). The fusion protein was purified by Glutathione-Sepharose 4B affinity chromatography and liberated from GST by cleavage with thrombin. SDS–polyacrylamide gel electrophoretic analysis showed that the fusion protein migrated at a position of 45 kDa (Fig. 1B, lane 3). Following cleavage with thrombin the MDC-9 disintegrin domain (A9dis) was shown to be approximately 16 kDa in size (Fig. 1B, lane 5), whereas the GST that was

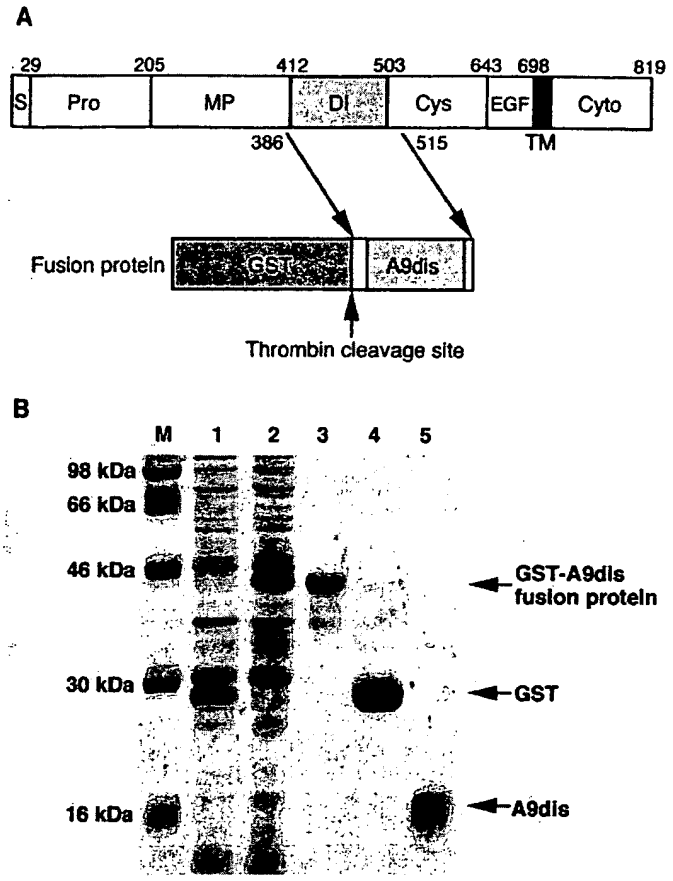

FIG. 1. Expression and purification of the MDC-9 disintegrin domain protein. (A) Schematic representation of the domain structure of MDC-9 and the GST-A9dis fusion protein. S, signal sequence; Pro, pro-region; MP, metalloproteinase domain; DI, disintegrin domain; Cys, cysteine-rich region; EGF, EGF-like domain; TM; transmembrane domain; and Cyto, cytoplasmic tail. The amino acid numbers are indicated. (B) Expression of the A9dis protein was analysed by 12.5% SDS–polyacrylamide gel and visualised by staining with 0.1% Coomassie brilliant blue R-250. Lane M, protein markers. Lane 1, supernatant of lyzed cells carrying the control GST vector. Lane 2, supernatant of lyzed cells carrying the GST-A9dis expression vector. Lane 3, GST-A9dis protein purified by Glutathione-Sepharose affinity chromatography. Lane 4, GST separated from A9dis following cleavage with thrombin. Lane 5, Purified MDC-9dis protein separated from GST following thrombin cleavage.

eluted from the affinity matrix was 29 kDa (Fig. 1B, lane 4).

The Disintegrin Domain of MDC-9 Functions as an Adhesion Molecule

To determine whether the disintegrin domain of MDC-9 could function as an adhesion molecule, RPMI-8226, JJN-3, NCI-H929 and ARH-77 cells were allowed to adhere to microtitre plates coated with A9dis, at either 5, 25 or 100 μg/ml, or an appropriate control protein. The myeloma cell lines RPMI-8226, JJN-3 and NCI-H929 were each able to bind to A9dis protein in a coating concentration dependent manner (Fig. 2). Significant binding of each of the myeloma cell lines to A9dis was seen at concentrations of protein as low as 5 μg/ml. In contrast, the lymphoblastic cell line, ARH-77, showed little ability to bind to A9dis.

Ca^{2+} (1 mM) increased binding of each of the myeloma cell lines examined to A9dis by 8- to 10-fold ($P < 0.005$ in each case) (Fig. 3). Mn^{2+} (1 mM) was also shown to promote an increase (4- to 8-fold) in A9dis-mediated myeloma cell adhesion, although the level of binding varied between cells lines (NCI-H929, $P < 0.05$; JJN-3, $P < 0.01$; and RPMI-8226, $P < 0.005$). In contrast, the presence of Zn^{2+} or Ni^{2+} had only modest effects on adhesion to A9dis. The presence of Zn^{2+} or Ni^{2+} were able to promote a small increase in adhesion of JJN-3 cells to A9dis ($P < 0.05$); however, Ni^{2+}, but not Zn^{2+}, was able to significantly increase the adhesion of RPMI-8226 cells ($P < 0.05$). Neither Zn^{2+} nor Ni^{2+} were able to promote adhesion of NCI-H929 cells to the A9dis protein. Mg^{2+}, which has been reported to support a number of integrin ligand interactions, was shown to have no effect on A9dis-mediated myeloma cell adhesion.

Although Ca^{2+} was shown to promote adhesion of myeloma cells to A9dis, previous studies have demonstrated that Ca^{2+} can both support and inhibit integrin ligand interactions depending on the specific ligand and the Ca^{2+} concentration. In the present study myeloma cells were shown to bind to A9dis in a Ca^{2+} concentration dependent manner (Fig. 3B). Al-

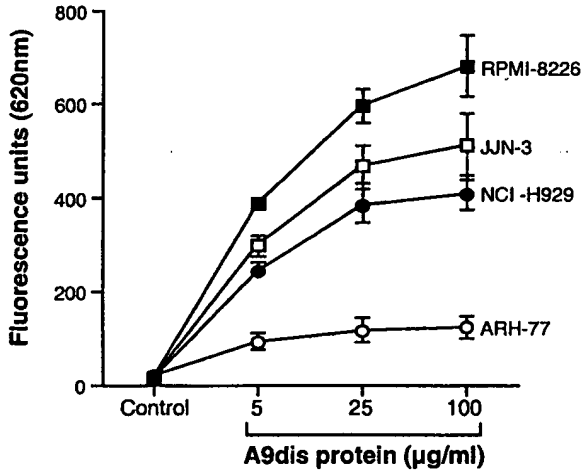

FIG. 2. Myeloma cells adhere to the A9dis protein. 96-well microtiter plates were coated with 5, 25, and 100 μg/ml of A9dis, or control protein. RPMI-8226, JJN-3, and NCI-H929 myeloma cells and ARH-77 lymphoblastoid cells were incubated in the coated 96-well plates for 1.5 h at 37°C. After washing to remove unbounded cells, the nuclei of cells adhered to plate were stained with propidium iodide and levels of fluorescence was measured with a fluorescence plate reader. Data are expressed in fluorescence units measured at 620 nm. The data shown represent one of four independent experiments. Each value represents the mean ± SD of triplicate measurements after the corresponding values of control protein had been subtracted.

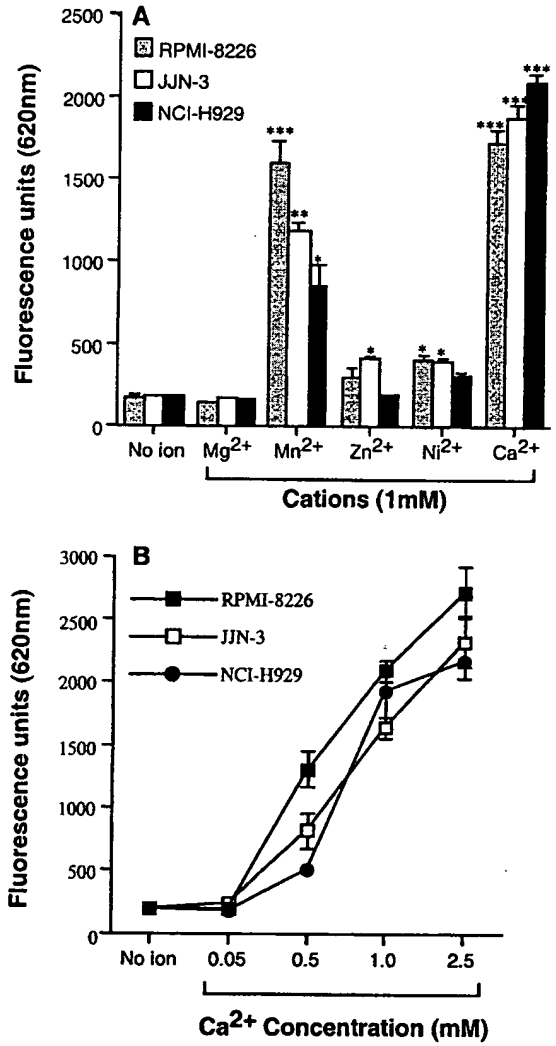

FIG. 3. Adhesion of myeloma cells to the MDC-9 disintegrin protein is cation dependent. 96-well microtiter plates were coated with 100 μg/ml of A9dis, or control protein. (A) RPMI-8226, JJN-3 or NCI-H929 myeloma cells (1×10^5), containing one of the following divalent ions: Mg^{2+}, Mn^{2+}, Ca^{2+}, Zn^{2+} or Ni^{2+}, at a concentration of 1 mM, in Hanks' balanced salt (HBSS) solution (KCl, 0.40 g/L, KH_2PO_4, 0.06 g/L, NaCl, 8.00 g/L, $NaHCO_3$, 0.35 g/L, Na_2HPO_4, 0.48g/L, D-glucose, 1 g/L) containing 1 mg/ml BSA and 25 mM Hepes, pH 7.4, were added and incubated for 1.5 h at 37°C. After washing, the cells were staining with PI and levels of fluorescence were determined. Data are expressed in fluorescence units measured at 620 nm. (B) RPMI-8226, JJN-3 or NCI-H929 myeloma cells (1×10^5), in HBSS containing increasing concentrations Ca^{2+}, were added to coated plates and incubated for 1.5 h at 37°C. Adhesion was measured as described previously. The data shown represent one of three independent experiments and each value represents the mean ± SD. of triplicate determination after the corresponding values of control protein had been subtracted. $^*P < 0.05$, $^{**}P < 0.01$, $^{***}P < 0.005$ compared to the no ion control.

though at low concentrations (0.05 mM) Ca^{2+} had no effect on cell adhesion, concentrations of 0.5 mM or higher promoted a significant increase in binding to A9dis.

The Integrin $\alpha_v\beta_5$ Mediates Adhesion of Myeloma Cells to A9dis

To define the molecules that may be involved in adhesion to the A9dis protein, myeloma cells were incubated with antibodies raised against specific integrins, or integrin subunits, including, β_1, β_3, α_2, α_5 and $\alpha_v\beta_5$, prior to binding to immobilised A9dis. The binding of myeloma cells to A9dis was almost completely inhibited by the anti-$\alpha_v\beta_5$ antibody, when compared to the effect of an isotype control antibody ($P < 0.001$) (Fig. 4A). The anti-β_1 antibody was also able to inhibit the adhesion of myeloma cells to A9dis ($P < 0.05$); however, the magnitude of the response was small when compared to the inhibition achieved by the antibody raised against $\alpha_v\beta_5$. Anti-α_2 and anti-α_5 antibodies had no effect on binding to A9dis. Interestingly, myeloma cell adhesion to A9dis was increased in the presence of the anti-β_3 antibody.

The integrin $\alpha_v\beta_5$ has been reported to be an adhesion receptor for vitronectin (27) and osteopontin (28) via binding to their RGD-binding sites. However, the disintegrin domain of MDC-9 does not possess an RGD motif in the predicted integrin-binding site but contains a TSE tripeptide sequence instead. Furthermore, a RGD containing peptide (GRGDSP) had no effect on the binding of myeloma cells to A9dis when compared to binding in the absence of peptide (control) or a control peptide (GRGESP) (Fig. 4B).

Myeloma Cells, but Not Lymphoblastoid Cells, Express the $\alpha_v\beta_5$ Integrin

Myeloma cell lines, but not the lymphoblastoid cell line, were shown to bind to A9dis. Furthermore binding could be almost completed inhibited by an antibody raised against the $\alpha_v\beta_5$ integrin; however, it was not clear whether this difference was a reflection of the ability of the different cell lines to express the $\alpha_v\beta_5$ integrin. Flow cytometric analysis confirmed that RPMI-8226, NCI-H929 and JJN-3 human myeloma cells stained strongly for the $\alpha_v\beta_5$ integrin (Fig. 5). In contrast, ARH-77 cells, showed little staining for $\alpha_v\beta_5$ (Fig. 5).

DISCUSSION

In the present study myeloma cells were shown to bind to the disintegrin-like domain of MDC-9 and this could be inhibited by an antibody raised against the $\alpha_v\beta_5$ integrin. An antibody to the β_1 subunit had a modest effect on adhesion. Although, this may suggest that binding could be mediated in part by a β_1 containing integrin, the level of inhibition was weak in comparison to that seen with anti-$\alpha_v\beta_5$ antibody. Antibodies to the β_3 and α_5 integrin subunits did not inhibit adhesion to the disintegrin domain of MDC-9 suggest-

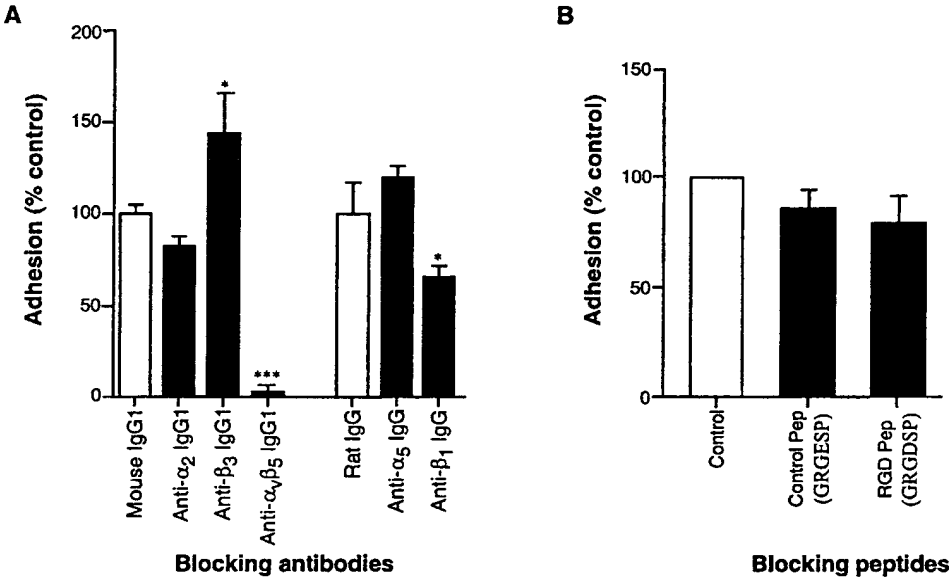

FIG. 4. The effects of blocking antibodies (A) and an RGD containing peptide (B) on the adhesion of myeloma cells to A9dis. 96-well plates were coated with A9dis. RPMI-8226 myeloma cells were preincubated with either (A) a 1:5000 dilution of anti-$\alpha_v\beta_5$ mAb, 10 μg/ml anti-β_3, a 1:150 dilution of anti-α_2 mAb, 10 μg/ml anti-β_1, 15 μg/ml anti-α_5, or an appropriate species specific control antibody, or (B) an RGD containing peptide or control peptide at a concentration of 10 μg/ml, in RPMI 1640 medium containing 1 mg/ml BSA, for 45 min. The myeloma cells (1×10^5/well), containing blocking agents, were then added to the A9dis-coated wells in triplicate and allowed to adhere for 1.5 h. Adhesion was measured as described in the legend to Fig. 2. The fluorescence associated with control protein coated wells was subtracted from that of the A9dis-coated wells. The data shown are a representative experiment from three independent experiments. Data (mean ± SD) represent adhesion as a percentage of control after the corresponding values from wells coated with control protein had been subtracted. $^*P < 0.05$, $^{**}P < 0.005$, $^{***}P < 0.001$ compared to the appropriate control.

ing that different members of the MDC/ADAM family may bind specifically to different integrins. Surprisingly, the antibody to the β_3 integrin promoted a small but significant increase in binding. Although the reason for this is unclear, this may suggest that the β_3 subunit is involved in an interaction with the disintegrin domain of MDC-9, possibly in conjunction with an α_v subunit, but that activation of this integrin is required before binding can take place. These data contrast with the data from Nath *et al.* that demonstrated that the extracellular region of MDC-9 could mediate binding of fibroblasts by binding to a $\alpha_6\beta_1$ integrin (29). Although binding of MDC-9 to the $\alpha_v\beta_5$ integrin was not examined in this study, binding was almost completely inhibited by antibodies to α_6 and β_1, suggesting that in fibroblasts, other integrins do not mediate MDC-9 adhesion(29). Taken together these data support the suggestion that MDC-9 may be able to mediate adhesion by binding to different integrins on different cells.

The $\alpha_v\beta_5$ integrin is thought to be able to bind to a number of extracellular matrix proteins including, vitronectin and osteopontin (27, 28). However, there are little data to demonstrate binding to an integral membrane protein. Binding to these extracellular matrix proteins appears to be RGD-dependent, as peptides containing this tripeptide motif inhibit binding to these proteins. In the present study RGD-containing pep-

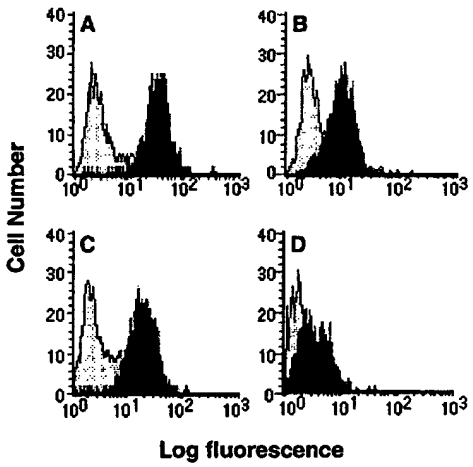

FIG. 5. Flow cytometric analysis of $\alpha_v\beta_5$ integrin expression by human myeloma cells and lymphoblastic cells. RPMI-8226 (A), NCI-H929 (B), JJN-3 (C) myeloma cells and ARH-77 (D) lymphoblastoid cells were stained with either a mouse anti-$\alpha_v\beta_5$ antibody (dark grey histograms) or an isotype control antibody (light grey histograms) and then with a FITC-conjugated goat anti-mouse antibody. The level of $\alpha_v\beta_5$ upon the cell surface was determined by flow cytometry, as described under Materials and Methods. The data are represented as histograms of FITC-fluorescence (x-axis) versus counts (y-axis). The mean channel fluorescence values for the isotype control-FITC-fluorescence data are RPMI-8226 = 3.17, NCI-H929 = 3.0, JJN-3 = 2.57 and ARH-77 = 2.47. The mean channel fluorescence values for the anti-$\alpha_v\beta_5$-FITC-fluorescence data are RPMI-8226 = 28.01, NCI-H929 = 9.82, JJN-3 = 23.11, and ARH-77 = 4.51.

tides had no effect on the adhesion of myeloma cells to the disintegrin domain of MDC-9. These data therefore suggest that the binding site in $\alpha_v\beta_5$, for the disintegrin domain of MDC-9 may be distinct from the RGD binding domain.

In the present study adhesion of myeloma cells to the disintegrin domain of MDC-9 was promoted by divalent cations. However, the profile of cation dependency was different than that reported previously for other $\alpha_v\beta_5$-substrate interactions. Ca^{2+} was able to promote a dose-dependent increase in binding to the disintegrin domain of MDC-9. This is consistent with previous studies that have demonstrated that binding of $\alpha_v\beta_5$ to vitronectin can also be supported by Ca^{2+} but contrast with the demonstration that $\alpha_v\beta_5$ mediated binding to osteopontin is insensitive to Ca^{2+} (28). Mn^{2+}, which promotes the ligand binding ability of a number of integrins, including $\alpha_v\beta_5$ dependent adhesion to vitronectin and osteopontin (28), was also able to promote the ability of myeloma cells to bind to the disintegrin domain of MDC-9. However, Mg^{2+}which supports $\alpha_v\beta_5$ mediated adhesion to both vitronectin and osteopontin (28) had no effect on myeloma cell adhesion to MDC-9. In support of this, Chen *et al.* have demonstrated that cation requirements for the binding of $\alpha_6\beta_1$ integrin to ADAM-2 differ from that required to bind laminin (30). Ca^{2+} promotes and Mn^{2+} inhibits $\alpha_6\beta_1$ binding to ADAM-2, whereas the converse is the case for binding to laminin, with Ca^{2+} inhibiting and Mn^{2+} promoting adhesion (30). These data support the suggestion that the binding sites, and/or activation states, required for $\alpha_v\beta_5$ binding to MDC-9, and $\alpha_6\beta_1$ binding of ADAM-2, are distinct from that previously reported for the binding of these integrins to specific extracellular matrix proteins, as the cation dependencies for these interactions are different. However, studies from Eto *et al.* have suggested that the cation dependency for ADAM-12 and murine ADAM-15 binding to the $\alpha_9\beta_1$ integrin do not differ from known integrin/extracellular matrix interactions (23). Thus, further studies will be required to determine the importance of specific cations in ADAM/integrin interactions and whether the specificity relates to different ADAMs or to different substrates.

In the present study we demonstrate that human myeloma cells bind to MDC-9 and they do so via the $\alpha_v\beta_5$ integrin. Lymphoblastoid cells, which do not express $\alpha_v\beta_5$ do not bind to MDC-9. These data suggest that at least in these cells MDC-9, interacts specifically with the $\alpha_v\beta_5$ integrin. However, Nath *et al.* were able to show that the adhesion of fibroblasts to MDC-9 was mediated by the $\alpha_6\beta_1$ integrin suggesting that different cell types may use different integrins to mediate binding to MDC-9. In support of this Nath *et al.* have also demonstrated that haemopoietic cells can bind to human metargidin using two different integrins, either $\alpha_v\beta_3$ or $\alpha_5\beta_1$, with different cell types utilising different integrins. However, since the entire extracellular domain was used to investigate binding in each of these studies, the possibility that different integrins maybe interacting with the different extracellular domains must be considered. In support of this, recent studies have suggested that peptides from the metalloproteinase domain of jararhagin, a snake venom metalloproteinase that also contains a disintegrin domain, may be able to bind to the α_2 integrin subunit (31). Furthermore, the cysteine-rich region of ADAM-12 has been shown to support cell adhesion via interactions with syndecans and the β_1 integrin subunit (32). Thus, although in the present study the $\alpha_v\beta_5$ integrin bound to the disintegrin-like domain of MDC-9 only, members of the MDC/ADAM family, or related molecules, may also be able to mediate cell adhesion via interactions with other domains. This could account for the different integrin requirements observed between the different studies.

In conclusion, the data presented in this study provide evidence to suggest that the non-RGD containing cellular disintegrin, MDC-9, mediates cell/cell adhesion. Adhesion to immobilised MDC-9 was mediated, in a non-RGD dependent manner, via an interaction with the $\alpha_v\beta_5$ integrin supporting the suggestion that this member of the MDC/ADAM family can bind to more than one integrin. These data also suggest that the $\alpha_v\beta_5$ integrin may be able to mediate cell to cell interactions in addition to being able to bind to extracellular matrix proteins. Thus, MDC-9 must now be considered to be a potential receptor for the $\alpha_v\beta_5$ integrin.

ACKNOWLEGMENTS

This work was supported in part by grants from the Leukaemia Research Fund and Yorkshire Cancer Research. P.I.C. is a Leukaemia Research Fund Bennett Senior Fellow. We are grateful to Professor K. Yamada for provision of antibodies mAB 13 and mAB 16, and to Professor M. Humphries for expert advice during the course of these studies.

REFERENCES

1. Wolfsberg, T. G., Primakoff, P., Myles, D. G., and White, J. M. (1995) *J. Cell Biol.* **131**, 275–278.
2. Huovial, A.-P. J., Almeida, E. A. C., and White, J. M. (1996) *Curr. Opin. Cell Biol.* **8**, 692–699.
3. Blobel, C. P. (1997) *Cell* **90**, 589–592.
4. Black, R. A., and White, J. M. (1998) *Curr. Opin. Cell Biol.* **10**, 654–659.
5. Black, R. A., Rauch, C. T., Kozlosky, C. J., Peschon, J. J., Slack, J. L., Wolfson, M. F., Castner, B. J., Stocking, K. L., Reddy, P., Srinivasan, S., Nelson, N., Boiani, N., Schooley, K. A., Gerhart, M., Davis, R., Fitzner, J. N., Johnson, R. S., Paxton, R. J., March, C. J., and Cerretti, D. P. (1997) *Nature* **385**, 729–733.
6. Moss, M. L., Jin, S.-L. C., Milla, M. E., Burkhart, W., Carter, H. L., Chen, W.-J., Clay, W. C., Didsbury, J. R., Hassler, D., Hoffman, C. R., Kost, T. A., Lambert, M. H., Leesnitzer, M. A., McCauley, P., McGeehan, G., Mitchell, J., Moyer, M., Pahel, G., Rocque, W., Overton, L. K., Schoenen, F., Seaton, T., Su, J.-L.,

Warner, J., Willard, D., and Becherer, J. D. (1997) *Nature* **385**, 733–736.

7. Izumi, Y., Hirata, M., Hasuwa, H., Iwamoto, R., Umata, T., Miyado, K., Tamai, Y., Kurisaki, T., Sehara-Fujisawa, A., Ohno, S., and Mekada, E. (1998) *EMBO J.* **17**, 7260–7272.
8. Peschon, J. J., Slack, J. L., Reddy, P., Stocking, K. L., Sunnarborg, S. W., Lee, D. C., Russell, W. E., Castner, B. J., Johnson, R. S., Fitzner, J. N., Boyce, R. W., Nelson, N., Kozlosky, C. J., Wolfson, M. F., Rauch, C. T., Cerretti, D. P., Paxton, R. J., March, C. J., and Black, R. A. (1998) *Science* **282**, 1281–1284.
9. Lum, L., Wong, B. R., Josien, R., Becherer, J. D., Erdjument-Bromage, H., Schlondorff, J., Tempst, P., Choi, Y., and Blobel, C. P. (1999) *J. Biol. Chem.* **274**, 13613–13618.
10. Qi, H. L., Rand, M. D., Wu, X. H., Sestan, N., Wang, W., Rakic, P., Xu, T., and Artavanis-Tsakonas, S. (1999) *Science* **283**, 91–94.
11. Millichip, M., Dallas, D., Wu, E., Dale, S., and McKie, N. (1998) *Biochem. Biophys. Res. Commun.* **245**, 594–598.
12. Abbaszade, I., Liu, R. Q., Yang, F., Rosenfeld, S. A., Ross, O. H., Link, J. R., Ellis, D. M., Tortorella, M. D., Pratta, M. A., Hollis, J. M., Wynn, R., Duke, J. L., George, H. J., Hillman, M. C., Murphy, K., Wiswall, B. H., Copeland, R. A., Decicco, C. P., Bruckner, R., Nagase, H., Itoh, Y., Newton, R. C., Magolda, R. L., Trzasko, J. M., Hollis, G. F., Arner, E. C., and Burn, T. C. (1999) *J. Biol. Chem.* **274**, 23443–23450.
13. Tortorella, M. D., Burn, T. C., Pratta, M. A., Abbaszade, I., Hollis, J. M., Liu, R., Rosenfeld, S. A., Copeland, R. A., Decicco, C. P., Wynn, R., Rockwell, A., Yang, F., Duke, J. L., Solomon, K., George, H., Bruckner, R., Nagase, H., Itoh, Y., Ellis, D. M., Ross, H., Wiswall, B. H., Murphy, K., Hillman, M. C., Hollis, G. F., Newton, R. C., Magolda, R. L., Trzaskos, J. M., and Arner, E. C. (1999) *Science* **284**, 1664–1666.
14. Blobel, C. P., Wolfsberg, T. G., Turck, C. W., Myles, D. G., Primakoff, P., and White, J. M. (1992) *Nature* **356**, 248–252.
15. Evans, J. P., Schultz, R. M., and Kopf, G. S. (1995) *J. Cell Sci.* **108**, 3267–3278.
16. Cho, C., O'Dell Bunch, D., Faure, J.-E., Goulding, E. H., Eddy, E. M., Primakoff, P., and Myles, D. G. (1998) *Science* **281**, 1857–1859.
17. Almeida, E. A. C., Huovila, A.-P. J., Sutherland, A. E., Stephens, L. E., Calarco, P. G., Shaw, L. M., Mercurio, A. M., Sonnenberg, A., Primakoff, P., Myles, D. G., and White, J. M. (1995) *Cell* **81**, 1095–1104.
18. Chen, H., and Sampson, N. S. (1999) *Chem. Biol.* **6**, 1–10.
19. Bigler, D., Takahashi, Y., Chen, M. S., Almeida, E. A. C., Osbourne, L., and White, J. M. (2000) *J. Biol. Chem.* **275**, 11576–111584.
20. Kratzschmar, J., Lum, L., and Blobel, C. P. (1996) *J. Biol. Chem.* **271**, 4593–4596.
21. Zhang, X.-P., Kamata, T., Yokoyama, K., Puzon-McLaughlin, W., and Takada, Y. (1998) *J. Biol. Chem.* **273**, 7345–7350.
22. Nath, D., Slocombe, P. M., Stephens, P. E., Warn, A., Hutchinson, G. R., Yamada, K. M., Docherty, A. J. P., and Murphy, G. (1999) *J. Cell. Sci* **112**, 579–587.
23. Eto, K., Puzon-McLaughlin, W., Sheppard, D., Sehara-Fujisawa, A., and Takada, Y. (2000) *J. Biol. Chem.*, in press.
24. Cal, S., Freije, M. P., Lopez, J. M., Takada, Y., and Lopenz-Otin, C. (2000) *Mol. Biol. Cell* **11**, 1457–1469.
25. Weskamp, G., Kratzschmar, J., Reid, M. S., and Blobel, C. P. (1996) *J. Cell Biol.* **132**, 717–726.
26. McKie, N., Dallas, D. J., Edwards, T., Apperley, J. F., Russell, R. G. G., and Croucher, P. I. (1996) *Biochem. J.* **318**, 459–462.
27. Smith, J. W., Vestal, D. J., Irwin, S. V., Burke, T. A., and Cheresh, D. A. (1990) *J. Biol. Chem.* **265**, 11008–11013.
28. Hu, D. D., Lin, E. C. K., Kovach, N. L., Hoyer, J. R., and Smith, J. W. (1995) *J. Biol. Chem.* **270**, 26232–26238.
29. Nath, D., Slocombe, P. M., Webster, A., Stephens, P. E., Docherty, A. J. P., and Murphy, G. (2000) *J. Cell Sci.* **113**, 2319–2328.
30. Chen, M. S., Almeida, E. A. C., Huovila, A.-P. J., Takahashi, Y., Shaw, L. M., Mercurio, A. M., and White, J. M. (1999) *J. Cell Biol.* **144**, 549–561.
31. Pentikainen, O., Hoffren, A.-M., Ivaska, J., Kapyla, J., Nyronen, T., Heino, J., and Johnson, M. S. (1999) *J. Biol. Chem.* **274**, 31493–31505.
32. Iba, K., Albrechtsen, R., Gilpin, B., Frohlich, C., Loechel, F., Zolkiewska, A., Ishiguro, K., Koyima, T., Liu, W., Langford, J. K., Sanderson, R. D., Brakebusch, R., Fassler, R., and Wewer, U. M. (2000) *J. Cell Biol.* **149**, 1143–1155.

THE JOURNAL OF BIOLOGICAL CHEMISTRY
Vol. 275, No. 45, Issue of November 10, pp. 34922–34930, 2000
Printed in U.S.A.

RGD-independent Binding of Integrin $\alpha_9\beta_1$ to the ADAM-12 and -15 Disintegrin Domains Mediates Cell-Cell Interaction*

Received for publication, March 9, 2000, and in revised form, August 10, 2000
Published, JBC Papers in Press, August 15, 2000, DOI 10.1074/jbc.M001953200

Koji Eto‡, Wilma Puzon-McLaughlin‡, Dean Sheppard§, Atsuko Sehara-Fujisawa¶, Xi-Ping Zhang‡, and Yoshikazu Takada‡‖

From the ‡Department of Vascular Biology, Scripps Research Institute, La Jolla, California 92037, the §Lung Biology Center, Center for Occupational and Environmental Health, Cardiovascular Research Institute, Department of Medicine, University of California, San Francisco, California 94143, and the ¶Department of Cell Biology, Tokyo Metropolitan Institute of Medical Science, 3-18-22 Honkomagome, Bunkyo-ku, Tokyo 113-8613, Japan

ADAMs (a disintegrin and metalloproteases) mediate several important processes (*e.g.* tumor necrosis factor-α release, fertilization, and myoblast fusion). The ADAM disintegrin domains generally lack RGD motifs, and their receptors are virtually unknown. Here we show that integrin $\alpha_9\beta_1$ specifically interacts with the recombinant ADAMs-12 and -15 disintegrin domains in an RGD-independent manner. We also show that interaction between ADAM-12 or -15 and $\alpha_9\beta_1$ supports cell-cell interaction. Interestingly, the cation requirement and integrin activation status required for $\alpha_9\beta_1$/ADAM-mediated cell adhesion and cell-cell interaction is similar to those required for known integrin-extracellular matrix interaction. These results are quite different from recent reports that ADAM-2/$\alpha_6\beta_1$ interaction during sperm/egg fusion requires an integrin activation status distinct from that for extracellular matrix interaction. These results suggest that $\alpha_9\beta_1$ may be a major receptor for ADAMs that lack RGD motifs, and that, considering a wide distribution of ADAMs and $\alpha_9\beta_1$, this interaction may be of potential biological and pathological significance.

ADAM[1] (for a disintegrin and metalloprotease), or MDC (metalloprotease/disintegrin/cysteine-rich), proteins are a family of membrane-anchored glycoproteins. More than 30 ADAMs have been identified. ADAMs are involved in fertilization (ADAMs-1, -2, and -3) (1–4), muscle fusion (meltrin-α, ADAM-12) (5, 6), release of tumor necrosis factor-α from the plasma membrane (TACE, ADAM-17) (see Refs. 7 and 8 for review), and modulating the neurogenic function of Notch (Kuzbanian, ADAM-10) (8, 9) and Delta (10). ADAMs have a pro-domain, a metalloprotease domain, a disintegrin domain, a cysteine-rich region, an epidermal growth factor-like domain, a transmembrane domain, and a cytoplasmic tail (11–13). The catalytically active metalloprotease domain of several ADAMs has been reported to mediate proteolytic cleavage of cell-surface proteins in some of these critical biological processes.

The disintegrin domain of ADAMs is a potential integrin ligand, but generally lacks the RGD motif (unlike RGD-containing snake venom disintegrins): Human ADAM-15 is the only ADAM that has an RGD motif in its disintegrin-like domain (14). Integrin $\alpha_6\beta_1$ has been reported to interact with the disintegrin domains of fertilin α and β (ADAM-1 and -2) complex that has no RGD motif during fertilization (2). Integrin $\alpha_v\beta_3$ has been reported to specifically bind to the disintegrin domain of human ADAM-15 in an RGD-dependent manner (15, 16). Interestingly, mouse ADAM-15 (mADAM-15) has a TDD sequence instead of RGD (17). This raised doubts about the role of ADAM-15 as a genuine integrin ligand. ADAM-15 (metargidin) is widely expressed in various tissues and cell types (14, 17) and is implicated in atherosclerogenesis, since ADAM-15 is over-expressed in atherosclerotic legions (18). ADAM-12 has been implicated in myoblast fusion during myogenesis (5, 6), and has a catalytically active metalloprotease domain and a non-RGD disintegrin domain. The cysteine-rich domain of ADAM-12 has a putative fusion peptide and a short hydrophobic stretch (19, 20). The truncated mouse ADAM-12, which lacks the metalloprotease domain, enhances fusion of C2C12 myoblastic cells *in vitro* (5). These findings suggest that the disintegrin and/or cysteine-rich domains of ADAM-12 should be involved in cell-cell interaction during myoblast fusion. Since the ADAM-12 gene is activated in condensed mesenchymal cells that give rise to skeletal muscle, bones, and visceral organs (21), ADAM-12 may be involved in development of other organs as well.

A major question is whether the non-RGD disintegrin domains of ADAMs interact with integrins. In the present study, we designed experiments to address this question using recombinant disintegrin domain fragment and cells expressing recombinant ADAMs. We demonstrated a novel interaction between integrins and ADAMs that is RGD-independent and may play crucial roles in cell-cell interaction during development and in pathological conditions.

MATERIALS AND METHODS

Monoclonal Antibodies and Cell Lines—Hybridomas for antibodies TS2/16 (anti-β_1, activating) and AIIB2 (anti-β_1, function-blocking) were obtained from American Type Culture Collection. Chinese hamster ovary (CHO) cells expressing different integrins have been described (15). Ntera-2 human embryonal carcinoma cells were provided by Amos Baruch (Scripps Research Institute, La Jolla, CA). G361 human melanoma cells were obtained from American Type Culture Collection.

Preparation of K562 Cells Expressing Recombinant $\alpha_9\beta_1$—α_9 cDNA

* This work was supported by National Institutes of Health Grants GM47175 and GM49899 (to Y. T) and in part by a Uehara Memorial Foundation fellowship in Japan (to K. E.) and American Heart Association Western States Affiliate Fellowship 0020119Y (to K. E.). This is publication 12975-VB from the Scripps Research Institute. The costs of publication of this article were defrayed in part by the payment of page charges. This article must therefore be hereby marked "*advertisement*" in accordance with 18 U.S.C. Section 1734 solely to indicate this fact.

‖ To whom correspondence should be addressed: Dept. of Vascular Biology, CAL-10, Scripps Research Inst., 10550 N. Torrey Pines Rd., La Jolla, CA 92037. Tel.: 858-784-7636; Fax: 858-784-7645; E-mail: takada@scripps.edu.

[1] The abbreviations used are: ADAM, a disintegrin and metalloprotease; CHO, Chinese hamster ovary; EGFP, enhanced green fluorescent protein; GST, glutathione *S*-transferase; PBS, phosphate-buffered saline; PCR, polymerase chain reaction; mAb, monoclonal antibody; wt, wild type; BSA, bovine serum albumin.

in expression vector (22) was transfected into K562 cells. After selection with G-418 (1 mg/ml of medium), cells stably expressing human integrins were cloned by limited dilution and designated α_9-K562. α_9-K562 cells express α_9 (as $\alpha_9\beta_1$) as detected by flow cytometry in FACScan (Becton Dickinson, San Jose, CA) with the anti-α_9 antibody Y9A2 (23) (Fig. 4).

Preparation of the GST Fusion Protein of the Disintegrin-like Domain of Mouse ADAM-15, and Human and Mouse ADAM-12—A cDNA fragment of about 270 nucleotides that encodes the disintegrin-like domain of mouse ADAM-15 (Met-420 to Glu-510) (17) was amplified by polymerase chain reaction (PCR) with a mouse expressed sequence tag clone (AI317315) as a template using 5′-CGGGATCCATGGCTGCTTTCTGCGG and 5′-CGGGATCCTTACTCGCCATCCCCTAGGCTG as primers. A cDNA fragment of 264 nucleotides that encodes the disintegrin-like domain of human ADAM-12 (Gly-423 to His-513) was amplified by PCR with a human placenta cDNA library (Invitrogen) as a template using 5′-CGGGATCCGGGGGCCAGAAGTGTGGAAACAG and 5′-CGGAATTCTTAGTGCCCATCGTGCAGGTACACG as primers. A cDNA fragment of 270 nucleotides that encodes the disintegrin-like domain of mouse ADAM-12 (Gly-420 to His-510) was amplified by PCR with a full-length mouse ADAM-12 cDNA (5) as a template using 5′-CGGGATCCGGGGGCCGGAAGTGTGGAAATG and 5′-CGGAATTCTTAGTGGCCATCATGTAGGTACAC as primers. These cDNA fragments were subcloned into the *Bam*HI site of the modified pGEX-2T vector (Amersham Pharmacia Biotech), in which a 6-His sequence was inserted between the thrombin cleavage site and the *Bam*HI site. Synthesis of the GST fusion protein of the ADAM-15 disintegrin-like domain was induced in *Escherichia coli* DH5α by adding 0.1 mM isopropyl-1-thio-β-D-galactopyranoside in culture medium as described previously (24). Protein was extracted from the bacterial suspension by sonication and purified using glutathione-agarose (Sigma) affinity chromatography. The recombinant wild type fusion proteins used in this study are shown in Fig. 1*A*.

Protein concentration was calculated from absorbance at 280 nm. We calculated the extinction coefficients based on the amino acid sequence using the ExPASy Protparam tool available from the ExPASy web site (25).

Removal of GST from GST Fusion Protein—The GST fusion protein has a 6-His sequence inserted between its thrombin cleavage site and disintegrin domain. The GST fusion protein was digested with thrombin (Sigma; 1 unit/1 mg of GST fusion protein) at room temperature for 6 h. The GST portion was removed by passing the digested materials through a GSH-agarose column. The disintegrin fragment was further purified by nickel-nitriloacetic acid affinity chromatography. The disintegrin domain was eluted with 250 mM imidazole. Imidazole was removed using a G10 column (Amersham Pharmacia Biotech).

Adhesion Assays—Adhesion assays were performed as described previously (15). Briefly, 96-well Immulon-2 microtiter plates (Dynatech Laboratories, Chantilly, VA) were coated with 100 μl of PBS (10 mM phosphate buffer, 0.15 M NaCl, pH 7.4) containing substrates at a concentration of 20 μg/ml and were incubated overnight at 4 °C. Remaining protein binding sites were blocked by incubating with 1% bovine serum albumin (BSA; Calbiochem) for 1 h at room temperature. After washing with PBS, CHO cells (10^5 cells/well) in 100 μl of Dulbecco's modified Eagle medium supplemented with 1% BSA were added to the wells and incubated at 37 °C for 1 h. After unbound cells were removed by rinsing the wells with PBS, bound cells were quantified by measuring endogenous phosphatase activity (26). GST fusion protein of the 8–11th type III repeats of fibronectin (GST-FN) (15) was used as a positive control, since untransfected CHO cells express endogenous hamster $\alpha_5\beta_1$ (27, 28). Wild type GST (wt-GST) was used as a negative control. A function-blocking anti-human α_9 monoclonal antibody, Y9A2, was used at a concentration of 10 μg/ml. Hepes-Tyrode buffer (10 mM HEPES, 150 mM NaCl, 12 mM $NaHCO_3$, 0.4 mM NaH_2PO_4, 2.5 mM KCl, 0.1% glucose, 0.02% BSA) supplemented with 1 mM EDTA, 2 mM Ca^{2+}, 2 mM Mg^{2+}, or 1 mM Mn^{2+} was used instead of Dulbecco's modified Eagle medium for experiments to determine cation dependence.

Transient Expression of ADAMs Using the Bicistronic Expression System—We used the bicistronic expression system with an internal ribosome entry sequence (29, 30), pIRES2-EGFP (CLONTECH, Palo Alto, CA) to express human ADAM-15 or mouse ADAM-12 on the cell surface. The expression of enhanced green fluorescent protein (EGFP) was used as a marker for ADAM protein expression. Full-length human ADAM-15 cDNA, and a truncated human ADAM-15 cDNA fragment encoding residues 420–814 lacking pro- and metalloprotease domains (ADAM-15/PM−), were obtained by PCR amplification with a placenta cDNA library (Invitrogen, Carlsbad, CA) as a template. These cDNA contain a signal sequence (of ADAM-15) and a Myc tag sequence just after the signal sequence. These cDNAs were verified by DNA sequencing, and subcloned into the *Nhe*I site of the pIRES2-EGFP vector. Full-length mouse ADAM-12 cDNA (5) was also subcloned into the *Sal*I/*Bam*HI site of this vector.

Cell-Cell Binding Assay—The pIRES-EGFP vector constructs with or without ADAM cDNA (full-length or PM−) were transfected into CHO cells by electroporation as described (15). After 48 h, EGFP expression was determined by flow cytometry. 96-well plastic culture plates (Corning) were plated with CHO cells transiently expressing EGFP and ADAM protein (5×10^4/well), and cultured overnight. K562 or α_9-K562 cells were labeled with 2′,7′-bis-(2-carboxyethyl)-5-(and-6)-carboxyfluorescein, acetoxymethyl ester (Molecular Probes, Eugene, OR) according to the manufacturer's instructions. The labeled K562 cells (10^4/well) were added to the CHO cell monolayer expressing EGFP and ADAM protein and incubated for 90 min at 37 °C in RPMI 1640. After rinsing the wells with RPMI 1640 three times to remove unbound cells, bound cells were quantified by assaying fluorescence (excitation 485 nm, emission 530 nm) using a FL500 microplate fluorescence reader (Bio Tek Instruments, Winooski, VT). In soluble disintegrin competition experiments, soluble bacterial disintegrin domains were first added to labeled α_9-K562 cells in RPMI 1640 medium and incubated for 1 h at 37 °C (the volume of the soluble disintegrin was 10% of total). α_9-K562 cells were then incubated with a monolayer of CHO cells expressing ADAM-12 or -15 for 90 min at 37 °C. In some experiments, Hepes-Tyrode buffer containing 2 mM Ca^{2+}, 2 mM Mg^{2+}, or 1 mM Mn^{2+} was used instead of RPMI 1640 to determine the ion dependence of the cell to cell interaction.

Other Methods—Site-directed mutagenesis was carried out using the unique site elimination method (31). The presence of mutations was verified by DNA sequencing. Flow cytometry was performed as described previously (27).

RESULTS

Adhesion of Integrin $\alpha_9\beta_1$ to the Mouse ADAM-15 Disintegrin Domain in an RGD-independent Manner—We have previously shown that the recombinant disintegrin-like domain of human ADAM-15 binds to $\alpha_v\beta_3$ in an RGD-dependent manner (15). However, a mouse ADAM-15 homologue has recently been reported to have a TDD sequence instead of an RGD sequence in the putative integrin-binding site of its disintegrin domain (17). We generated a recombinant mouse ADAM-15 disintegrin fragment (Fig. 1*A*) and studied whether it supports $\alpha_v\beta_3$-mediated cell adhesion. We did not detect significant adhesion of β_3-CHO cells that express hamster α_v/human β_3 hybrid to the mouse ADAM-15 disintegrin domain (Fig. 1*B*).

We studied whether other integrin receptors bind to the mouse ADAM-15 disintegrin domain using CHO cells expressing different recombinant integrins. Parent CHO cells express $\alpha_5\beta_1$ and $\alpha_v\beta_1$, but do not express β_2 or β_3 (27). wt-GST (GST alone, a negative control) does not support adhesion to any integrins tested. GST-FN (a positive control: the rat fibronectin 8–11th type III repeats) supported adhesion to all of the cell lines tested. We found that the mouse ADAM-15 disintegrin domain supported adhesion of α_9-CHO cells (which express human α_9/hamster β_1 hybrid), but did not support adhesion of parent CHO cells and CHO cells expressing other integrins, including $\alpha_2\beta_1$, $\alpha_3\beta_1$, $\alpha_5\beta_1$, $\alpha_6\beta_1$, and $\alpha_v\beta_3$, except for $\alpha_4\beta_1$, which weakly bound to mouse ADAM-15 (Fig. 1*B*). These results indicate that $\alpha_9\beta_1$ recognizes the mouse ADAM-15 disintegrin domain.

Adhesion to the human and mouse ADAM-15 disintegrin domains was determined as a function of substrate concentration (Fig. 1*C*). α_9-CHO cells showed maximum adhesion to both human and mouse ADAM-15 disintegrin domains at the coating concentration of 20 μg/ml protein. β_3-CHO cells showed maximal adhesion to human ADAM-15 disintegrin domain at 5 μg/ml coating concentration, but never showed significant adhesion to mouse ADAM-15 disintegrin domain at the highest coating concentration used (50 μg/ml). These results are consistent with the previous results that $\alpha_v\beta_3$ recognizes ADAM-15 in an RGD-dependent manner (15). We studied

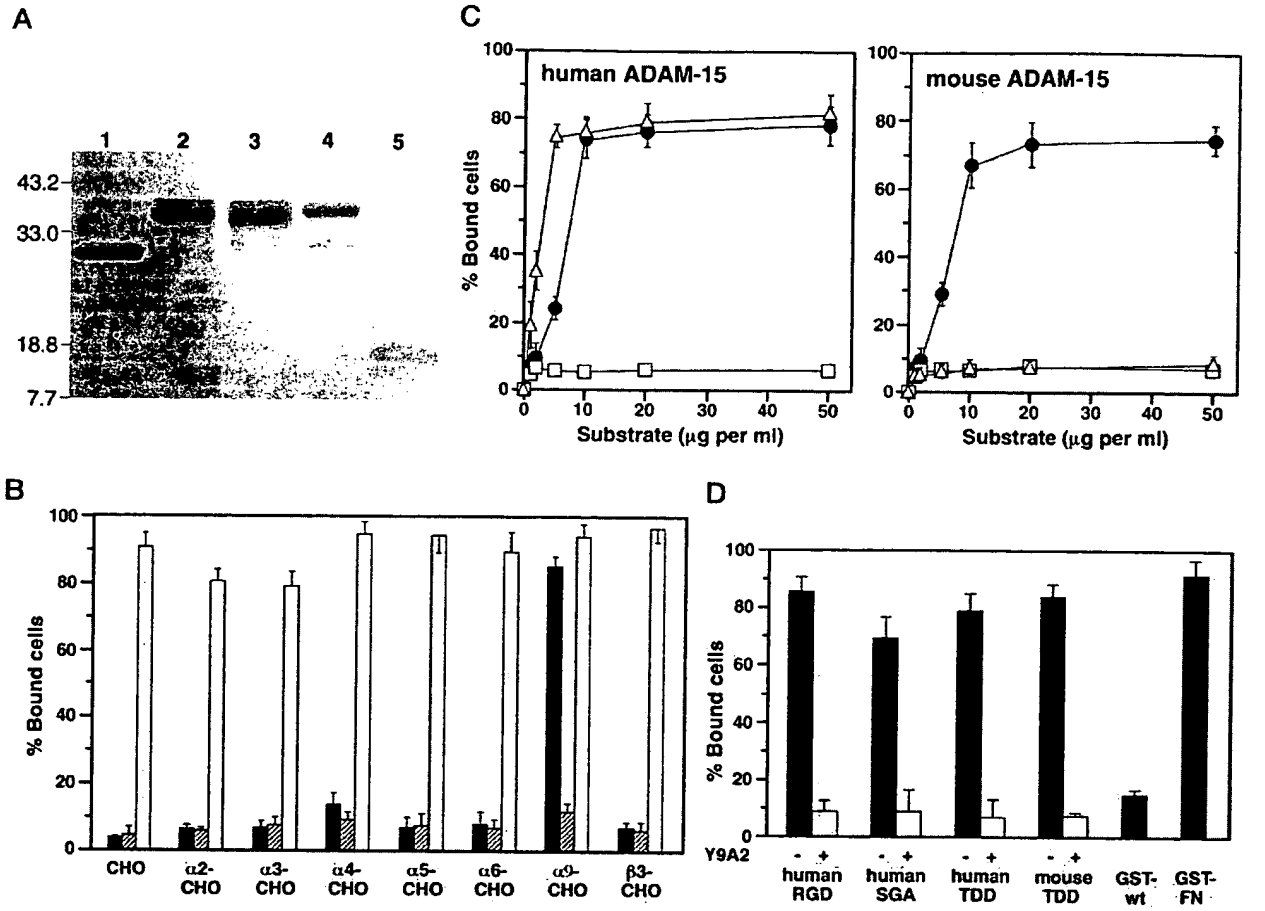

FIG. 1. **Specific binding of ADAM-15 to integrin $\alpha_9\beta_1$ in an RGD-independent manner.** *A*, SDS-PAGE of the recombinant wild-type disintegrin domains used in this study under non-reduced conditions. *Lane 1*, wild-type GST; *lanes 2–4*, disintegrin domain GST fusion protein of, mouse ADAM-15 (*lane 2*), human ADAM-12 (*lane 3*), and human ADAM-15 (*lane 4*); *lane 5*, the cleaved and purified disintegrin domain of human ADAM-15. *B*, adhesion of cells expressing different integrins to the recombinant disintegrin domain of mouse ADAM-15. Wells of 96-well microtiter plates were coated with GST-mouse ADAM-15 disintegrin domain (20 μg/ml in PBS) (*closed column*), GST-FN (*open column*), or wt GST (*shaded column*). Cells homogeneously expressing different human integrins were added to wells and incubated at 37 °C for 1 h. After rinsing the wells to remove unbound cells, bound cells were quantified using endogenous phosphatase activity. Data are shown as means ± S.D. of triplicate experiments. The data suggest that $\alpha_9\beta_1$ adheres to the mouse ADAM-15 disintegrin domain, but the other integrins tested do not. *C*, adhesion of β_3-CHO and α_9-CHO cells to human and mouse ADAM-15 disintegrin domain as a function of substrate concentrations. Adhesion of β_3-CHO and α_9-CHO cells to human and mouse ADAM-15 disintegrin domains was determined as a function of the substrate concentrations. Data are shown as means ± S.D. of triplicate experiments. The data suggest that the affinity of human ADAM-15 for $\alpha_9\beta_1$ (*closed circle*) is comparable to that of mouse ADAM-15, and that the affinity of the human ADAM-15 disintegrin domain for $\alpha_v\beta_3$ (*open triangle*) is comparable to or slightly higher than that for $\alpha_9\beta_1$. Parent CHO cells (*open square*). *D*, effect of mutating the RGD motif of the ADAM-15 disintegrin domain on the adhesion of α_9-CHO cells. The RGD motif of the human ADAM-15 disintegrin domain was mutated to SGA or TDD by site-directed mutagenesis. GST fusion proteins of these mutants were used for adhesion assays with α_9-CHO cells. Wells of a 96-well titer plate were coated with proteins at 20 μg/ml. An anti-α_9 function-blocking antibody (Y9A2) was used at 10 μg/ml. Data are shown as means ± S.D. of triplicate experiments. The data suggest that $\alpha_9\beta_1$ binding to ADAM-15 is not dependent on the RGD motif at the putative integrin-binding site.

whether mutation of the RGD motif in the putative integrin-binding site of the ADAM-15 disintegrin domain affects adhesion to $\alpha_9\beta_1$. α_9-CHO cells adhered to the two human ADAM-15 disintegrin domain mutants, human/SGA (in which the RGD sequence is mutated to SGA (Ref. 15)) and human/TDD (in which the RGD sequence is mutated to TDD), as well as to wild-type human and mouse ADAM-15 disintegrin domains. These results suggest that $\alpha_9\beta_1$ recognizes ADAM-15 in an RGD-independent manner. Adhesion of α_9-CHO cells to these recombinant proteins was completely blocked by Y9A2, an anti-human α_9 integrin monoclonal antibody (23) (Fig. 1*D*), suggesting that this adhesion is specific to $\alpha_9\beta_1$.

These results suggest that $\alpha_9\beta_1$ may bind to other non-RGD ADAMs. We studied whether another non-RGD ADAM, human and mouse ADAM-12, or meltrin-α, which lacks the RGD motif, binds to $\alpha_9\beta_1$ using CHO cells expressing different recombinant integrins. We found that the human and mouse ADAM-12 disintegrin domains supported adhesion of α_9-CHO cells, but not of parent CHO cells or cells expressing the other integrins we tested, except for $\alpha_4\beta_1$ and $\alpha_v\beta_3$, which weakly bound to this protein (Fig. 2*A*). The α_9-CHO cells showed maximum adhesion to both the human and mouse ADAM-12 disintegrin domains at a coating concentration of 20 μg of protein/ml (Fig. 2*B*). This interaction is also blocked by the anti-α_9 mAb Y9A2 (Fig. 2*C*), suggesting that ADAM-12 also specifically interacts with $\alpha_9\beta_1$.

We studied whether non-recombinant $\alpha_9\beta_1$ binds to ADAM-12 and -15 using Ntera-2 human embryonic carcinoma cells that express α_9 and β_1 on the surface (Fig. 3*A*). Ntera-2 cells adhered to ADAM-12 and -15 in an $\alpha_9\beta_1$-dependent manner, but required activation by activating anti-β_1 mAb TS2/16 (Fig. 3*B*). We obtained very similar results with G361 human melanoma cells that also express $\alpha_9\beta_1$ (32); G361 cells adhere to ADAM-12 and -15 in an α_9-dependent and activation-dependent manner (data not shown). These results suggest that

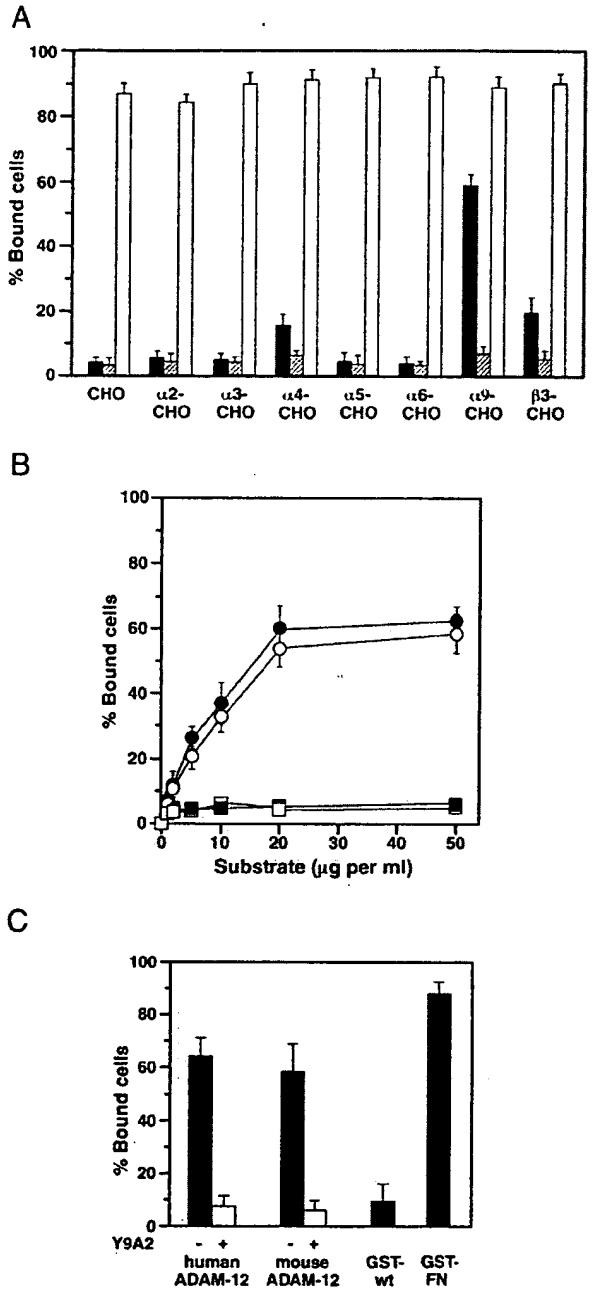

FIG. 2. **Adhesion of cells expressing different integrins to the recombinant disintegrin-like domain of human ADAM-12.** *A*, wells of 96-well microtiter plates were coated with 20 μg/ml (in PBS) GST-human ADAM-12 disintegrin domain (*closed column*), wt GST (*shaded column*), or GST-FN (*open column*). Adhesion assays with CHO cells homogeneously expressing different human integrins were performed as describe in the legend to Fig. 1. Data are shown as means ± S.D. of triplicate experiments. The data suggest that the ADAM-12 disintegrin domain specifically interacts with $\alpha_9\beta_1$. *B*, adhesion of α_9-CHO cells (*circle*) or CHO cells (*square*) to GST fusion protein of human MDC-12 disintegrin domain (*closed*) or mouse MDC-12 disintegrin domain (*open*) was determined as a function of the substrate concentration. Data are shown as means ± S.D. of triplicate experiments. The data suggest that adhesion of α_9-CHO cells to GST fusion protein of both human and mouse ADAM-12 disintegrin domain saturates at 20 μg/ml coating concentration. *C*, GST fusion proteins of human and mouse ADAM-12 disintegrin domain were used for adhesion assays with α_9-CHO cells. Wells of a 96-well titer plate were coated with proteins at 20 μg/ml. An anti-α_9 function-blocking antibody (Y9A2) was used at 10 μg/ml. Data are shown as means ± S.D. of triplicate experiments. The data suggest that adhesion to human and mouse ADAM-12 is specific to $\alpha_9\beta_1$.

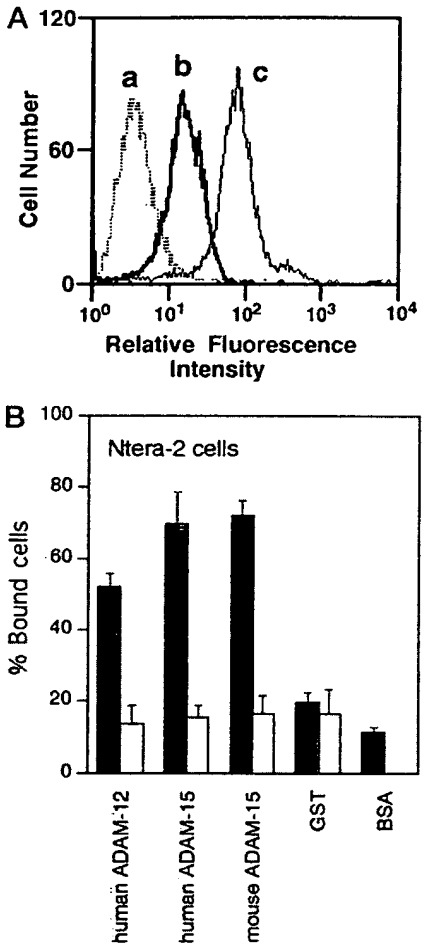

FIG. 3. **Expression of $\alpha_9\beta_1$ in Ntera-2 cells and their adhesion to ADAM-12 and -15.** *A*, flow cytometric profile of Ntera-2 cells. *a*, control mouse IgG; *b*, Y9A2 (anti-human α_9); *c*, TS2/16 (anti-human β_1). Y9A2 and TS2/16 were used at 10 and 2.5 μg/ml, respectively. *B*, adhesion of Ntera-2 cells to ADAM-12 and -15. Proteins were used at 20 μg/ml coating concentrations. Assays were performed with (*open bar*) and without (*closed bar*) function-blocking anti-human α_9 mAb Y9A2 (10 μg/ml). Activating anti-human β_1 mAb TS2/16 (2.5 μg/ml) is included in the assay medium (Dulbecco's modified Eagle's medium supplemented with 1% BSA) to fully activate $\alpha_9\beta_1$. Without activation, we do not detect significant adhesion to ADAM-12 and -15.

non-recombinant $\alpha_9\beta_1$ also mediates specific adhesion to ADAM-12 and -15.

$\alpha_9\beta_1$ and ADAM-15 or ADAM-12 Mediate Cell-Cell Interaction—ADAMs have been implicated in cell-cell interaction during fertilization and myoblast fusion. We studied whether $\alpha_9\beta_1$ interaction with ADAM-15 or ADAM-12 actually supports cell-cell interaction *in vitro*. We used CHO cells transiently expressing ADAM-15, ADAM-12 (full-length), and truncated ADAM-15 (ADAM-15/PM−), and K562 cells homogeneously expressing $\alpha_9\beta_1$ (α_9-K562 cells) (Fig. 4*A*) to detect $\alpha_9\beta_1$-ADAM protein interaction. Since monoclonal antibodies against ADAM-15 or ADAM-12 are not readily available, we used the IRES2-EGFP bicistronic vector (29, 30), in which both EGFP and ADAMs are encoded in a single mRNA with two separate translation starting sites. Transient EGFP expression was used as a marker of ADAM expression (Fig. 4*B*), and typically more than 30% of transfected cells are EGFP-positive.

Binding of fluorescence-labeled α_9-K562 and parent K562 cells to CHO cells transiently expressing ADAM-15, ADAM-15/PM−, or ADAM-12 was determined. α_9-K562 and parent K562 cells bound at low levels (typically 5% of added cells) to control

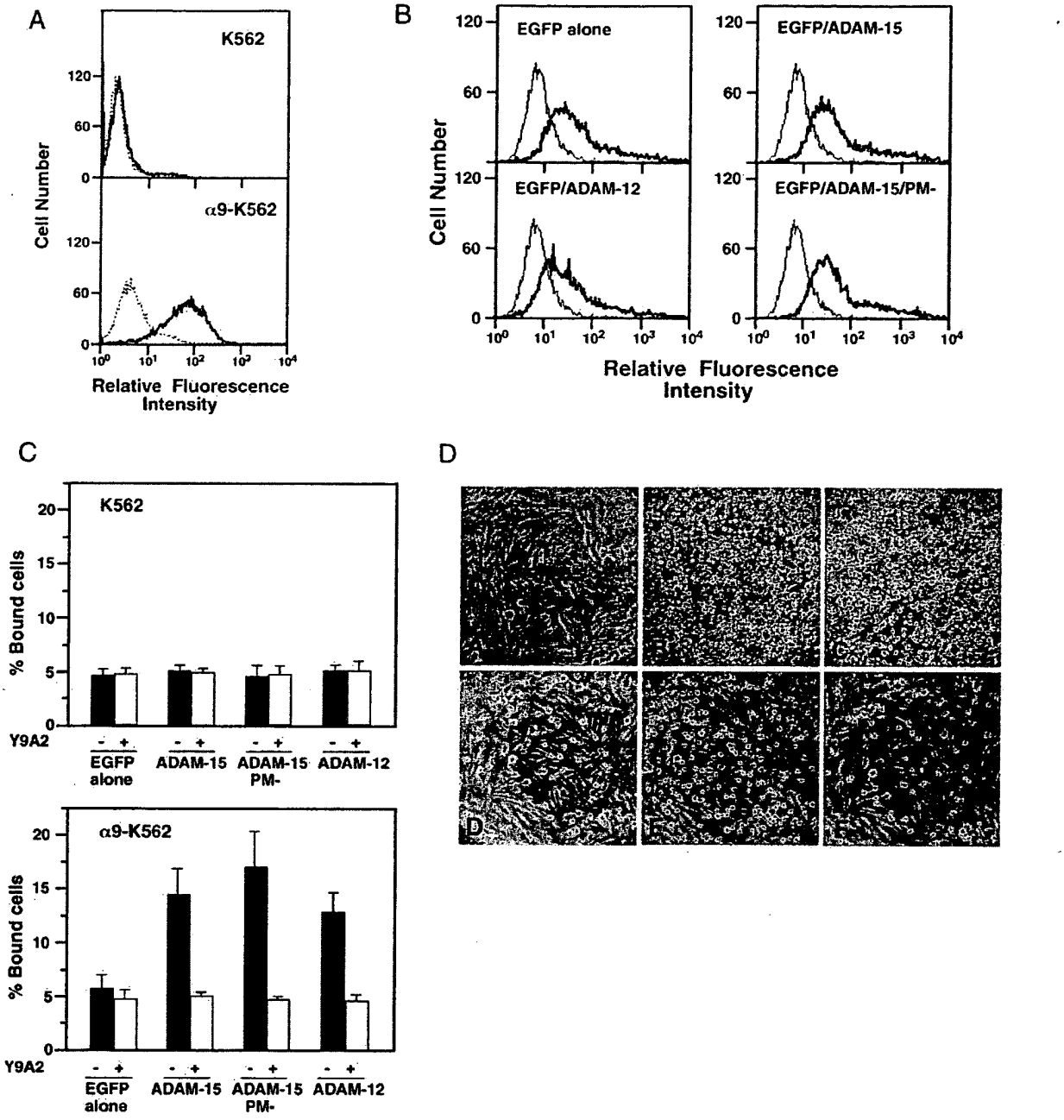

FIG. 4. **$\alpha_9\beta_1$ and ADAMs mediate cell-cell interaction.** *A*, expression of $\alpha_9\beta_1$ on K562 cells. Parent K562 cells or α_9-K562 cells were stained with control mouse IgG (*dotted line*) or Y9A2 (anti-α_9 mAb) (*solid line*), followed by fluorescein isothiocyanate-labeled goat anti-mouse IgG. Stained cells were analyzed by flow cytometry. The data suggest that α_9-K562 cells homogeneously express $\alpha_9\beta_1$. *B*, expression of EGFP or EGFP containing ADAMs on CHO cells. The IRES2-EGFP bicistronic vector, in which both EGFP and ADAMs are encoded in a single mRNA with two separate translation starting sites, was used. EGFP vector alone, EGFP vector containing the full-length human ADAM-15 cDNA, the truncated human ADAM-15 cDNA fragment encoding residues 420–814 lacking pro- and metalloprotease domains (ADAM-15/PM−), or the full-length mouse ADAM-12 cDNA (*solid line*) was transfected into CHO cells. These cells and mock-transfected (*thin line*) CHO cells were analyzed 48 h after transfection. Expression was analyzed by flow cytometry (excitation at 488 nm and emission at 507 nm). Transient EGFP expression was used as a marker of ADAM expression, and typically approximately 30% of transfected cells are EGFP-positive. *C*, $\alpha_9\beta_1$ and ADAM-15 or ADAM-12 mediate cell-cell interaction. CHO cells transiently expressing ADAMs were plated in wells of 96-well plastic culture plates, and grown overnight to near confluence. Fluorescence-labeled α_9-K562 or parent K562 cells were added to the wells and incubated with CHO cells in RPMI 1640 medium. After rinsing the wells to remove unbound cells, bound cells were quantified using a fluorescent plate reader at 485 nm for excitation and at 530 nm for emission. Cell-cell interaction was assayed in the absence (*closed bar*) or presence (*open bar*) of the anti-α_9 mAb, Y9A2 (10 μg/ml). Note that only approximately 30% of the transfected CHO cells is EGFP positive. Thus, binding of 15–20% of added α_9-K562 cells is substantial. The data suggest that ADAM-15 (wt and truncated) and ADAM-12 on the cell-surface specifically interact with $\alpha_9\beta_1$ on the surface of apposing cells and mediate cell-cell interaction. *D*, binding of α_9-K562 cells to CHO cells expressing ADAM-12 or -15. *A*, a monolayer of CHO cells expressing ADAM-15 before adding α_9-K562 cells; *B*, α_9-K562 cells on CHO cells expressing EGFP only; *C*, α_9-K562 cells on CHO cells expressing ADAM-15; *D*, α_9-K562 cells bound to CHO cells expressing only EGFP after rinsing the well to remove unbound cells; *E*, α_9-K562 cells bound to CHO cells expressing ADAM-15; *F*, α_9-K562 cells bound to CHO cells expressing ADAM-15 in the presence of Y9A2. Note that only K562 cells bound to CHO cells after rinsing the wells to remove unbound cells are shown in D–F.

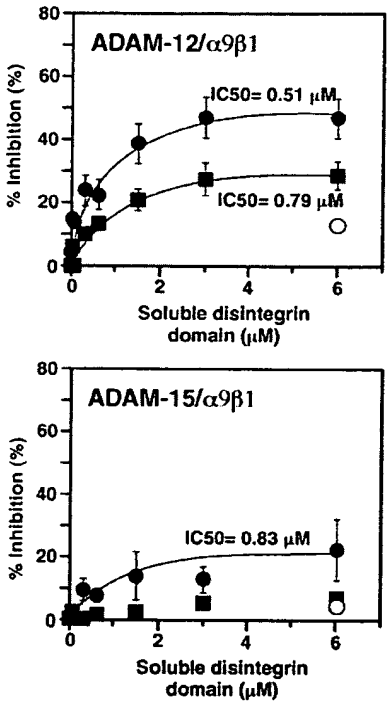

FIG. 5. **Inhibition of interaction between membrane-bound ADAM and $\alpha_9\beta_1$ by soluble disintegrin domains.** CHO cells were transiently transfected with ADAM-12 (*top*) or ADAM-15 (*bottom*) cDNA in the IRES/EGFP bicistronic expression vector, and plated in wells of 96-well plates as described under "Experimental Procedures." Labeled α_9-K562 cells were first preincubated with soluble GST-ADAM disintegrin domain fusion proteins, and then incubated with CHO cell monolayer expressing ADAMs. Data are shown as means ± S.D. of triplicate experiments. Inhibition (%) of α_9-K562 cell binding was plotted against concentrations of soluble disintegrin fusion protein used. Binding of α_9-K562 cells in the presence of Y9A2 (anti-α_9) was used as background binding, and binding in the absence of added protein was used as total binding. *Closed circle*, ADAM-15 disintegrin domain GST fusion protein; *closed square*, ADAM-12 disintegrin domain GST fusion protein; *open circle*, wild-type GST.

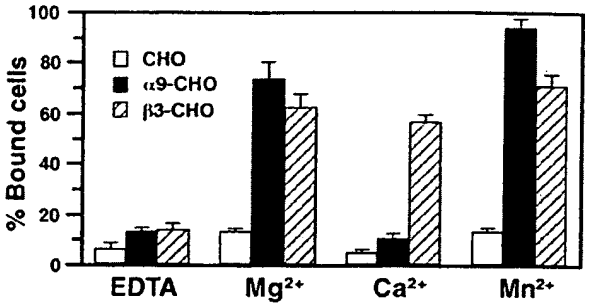

FIG. 6. **Cation requirement for adhesion of integrin $\alpha_9\beta_1$ or $\alpha_v\beta_3$ to the recombinant disintegrin-like domain of human ADAM-15.** The GST portion was removed from the GST-disintegrin domain fusion protein of human ADAM-15. Wells of 96-well microtiter plates were coated with protein (20 μg/ml). Cells homogeneously expressing different human integrins were incubated in wells at 37 °C for 1 h. Hepes-Tyrode buffer supplemented with 1 mM EDTA, 2 mM Mg^{2+}, 2 mM Ca^{2+}, or 1 mM Mn^{2+} was used. Adhesion of α_9-CHO cells (*closed column*) to human ADAM-15 disintegrin recombinant protein was promoted by Mg^{2+} or Mn^{2+} and inhibited by Ca^{2+}, whereas adhesion of β_3-CHO cells (*shaded column*) was promoted by all cations used. CHO cells (*open column*) were used as a negative control. Data are shown as means ± S.D. of triplicate experiments. The data suggest that $\alpha_9\beta_1$ adhesion to the ADAM-15 disintegrin domain has a cation requirement similar to that for known integrin-extracellular matrix interactions.

CHO cells that express EGFP but no ADAM (Fig. 4*C*). α_9-K562 cells bound to cells expressing these ADAMs at significantly higher (approximately 3 times) levels than control parent K562 cells (Fig. 4, *C* and *D*). Levels of binding of α_9-K562 cells to CHO cells expressing ADAM-12 or ADAM-15 is low (15–20% of added cells) compared with those in other adhesion studies in this study. However, this binding is substantial considering that only approximately 30% of added cells express EGFP and ADAM-12 or -15. Parent K562 cells bound to CHO cells expressing ADAM-15 or -12 at the background levels. Binding of α_9-K562 cells to CHO cells expressing ADAM-15 (full-length and truncated) or ADAM-12 was completely blocked by anti-α_9 antibody. These results suggest that this interaction is specific to $\alpha_9\beta_1$, and to ADAM-15 or ADAM-12.

We studied whether the soluble ADAM disintegrin domains affect ADAM/$\alpha_9\beta_1$-mediated cell-cell interaction. Binding of α_9-K562 cells to CHO cells transiently expressing ADAM-12 or -15 was determined in the presence of soluble ADAM-12 or -15 disintegrin domain in the assay medium (Fig. 5). The ADAM-15 and -12 disintegrin domain effectively blocked ADAM-12/$\alpha_9\beta_1$-mediated cell-cell interaction (with IC_{50} of about 0.5 and 0.8 μM, respectively). The ADAM-15 disintegrin domain blocked (with IC_{50} of about 0.5 μM), but the ADAM-12 disintegrin domain did not significantly block, ADAM-15/$\alpha_9\beta_1$-mediated cell-cell interaction. The level of maximal inhibition is much higher with the soluble ADAM-15 disintegrin domain than with the ADAM-12 disintegrin domain in both cases. These results suggest that ADAM disintegrin domains synthesized in bacteria effectively compete with those synthesized in mammalian cells for binding to $\alpha_9\beta_1$, and that, consistent with the adhesion and cell-cell interaction results, ADAM-15 disintegrin domain has a higher binding affinity to $\alpha_9\beta_1$ than the ADAM-12 disintegrin domain.

Cation Dependence of $\alpha_9\beta_1$ Interaction with ADAM-15 or ADAM-12—Chen *et al.* (4) recently reported that the cation and integrin activation states that are required for $\alpha_6\beta_1$/ADAM-2 (fertilin β) interaction are different from those required for $\alpha_6\beta_1$-extracellular matrix protein interaction. They have shown that Ca^{2+} promotes and Mn^{2+} inhibits $\alpha_6\beta_1$ binding to ADAM-2. In contrast, Ca^{2+} suppresses and Mn^{2+} stimulates $\alpha_6\beta_1$ binding to laminin (4).

We determined the cation requirement for adhesion of α_9-CHO cells to the recombinant disintegrin domain of human ADAM-15 (Fig. 6). We removed the GST portion of the fusion protein, since it generates high background binding to integrins in the presence of Mg^{2+}. We found that Mg^{2+} and Mn^{2+} stimulated, but Ca^{2+} suppressed, $\alpha_9\beta_1$ adhesion to the ADAM-15 disintegrin domain. Ca^{2+} supported $\alpha_v\beta_3$ binding to ADAM-15. We also examined the cation requirement for $\alpha_9\beta_1$/ADAM-15-mediated cell-cell interaction (Fig. 7). This interaction is higher in the presence of Mn^{2+} and Mg^{2+} than in the presence of Ca^{2+}. We obtained essentially the same results with $\alpha_9\beta_1$/ADAM-12-mediated cell-cell interaction (Fig. 7). These results suggest that the cation requirements for $\alpha_9\beta_1$ adhesion to the ADAM-15 disintegrin domain, and for $\alpha_9\beta_1$/ADAM-15- or ADAM-12-mediated cell-cell interaction, are not different from known integrin-extracellular matrix interactions, but are different from the reported ADAM-2/$\alpha_6\beta_1$-mediated cell-cell interaction (4).

Effect of Activating and Blocking Antibodies on $\alpha_9\beta_1$/ADAM-15, or ADAM-12-mediated Cell-Cell Interaction—Although the cation requirement for $\alpha_9\beta_1$-ADAM protein-mediated cell-cell interaction is not different from that for known integrin extracellular matrix interactions, it is still possible that a different activation status of $\alpha_9\beta_1$ is required for this interaction. To address this question, we studied the effect of the activating anti-β_1 antibody TS2/16, and the inhibitory anti-β_1 antibody AIIB2, on this interaction. These mAbs stimulate or block β_1

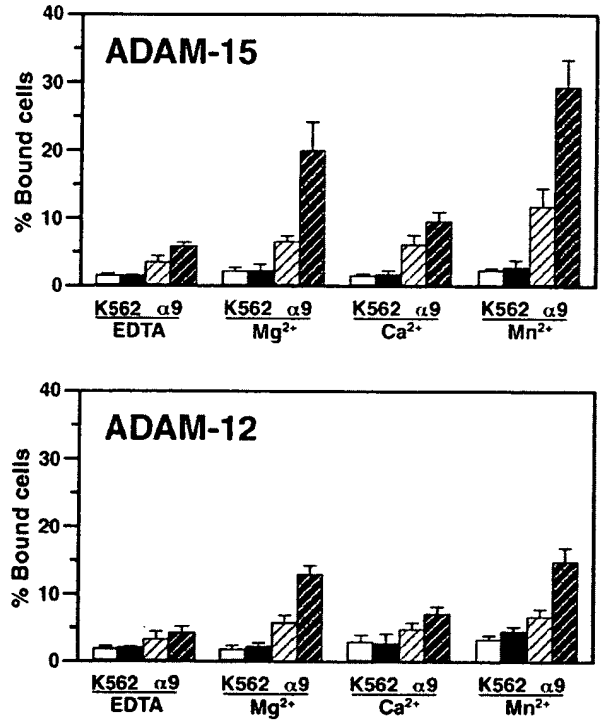

FIG. 7. **Cation dependence of cell-cell interaction between $\alpha_9\beta_1$ and ADAM-15 or ADAM-12.** CHO cells transiently expressing ADAMs were plated in wells of 96-well plastic culture plates, and grown overnight to near confluence. Fluorescence-labeled α_9-K562 (*shaded column*) or parent K562 cells were added to the wells and incubated with CHO cells in Hepes-Tyrode buffer supplemented with 1 mM EDTA, 2 mM Mg^{2+}, 2 mM Ca^{2+}, or 1 mM Mn^{2+} at 37 °C for 90 min. After rinsing the wells to remove unbound cells, K562 cells bound to CHO cells were quantified utilizing a fluorescent plate reader. EGFP alone (*open* or *shaded open column*) or EGFP containing human ADAM-15 (*closed* or *shaded closed column*) or mouse ADAM-12 (*closed* or *shaded closed column*). Data are shown as means ± S.D. of triplicate experiments. The data suggest that the cation dependence of cell-cell interaction between $\alpha_9\beta_1$ and ADAM-15 or -12 is similar to that for known integrin-extracellular matrix interactions.

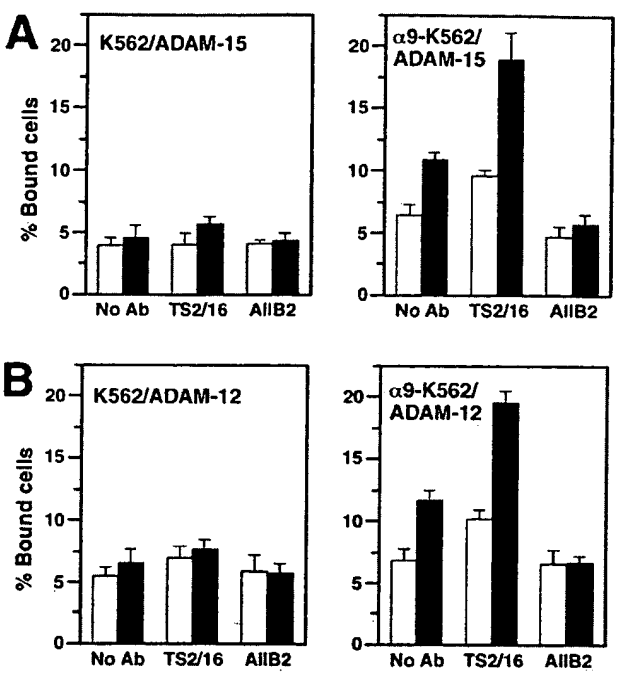

FIG. 8. **Effect of activating and blocking antibodies on $\alpha_9\beta_1$/ADAM-15-mediated (*A*) or $\alpha_9\beta_1$/ADAM-12-mediated (*B*) cell-cell interaction.** CHO cells transiently expressing ADAMs (*closed columns*) were plated in wells of 96-well plastic culture plates, and grown overnight to near confluence. Fluorescence-labeled α_9-K562 or parent K562 cells were added to the wells and incubated with CHO cells in the absence or presence of the activating anti-β_1 antibody TS2/16 at 1.0 μg/ml or the inhibiting anti-β_1 antibody AIIB2 (at 6.5μg/ml). After rinsing the wells to remove unbound cells, bound cells were quantified using a fluorescent plate reader. Data are shown as means ± S.D. of triplicate experiments. The data suggest that the activation status of $\alpha_9\beta_1$ that is required for cell-cell interaction with ADAM-15 or ADAM-12 is similar to that required for known integrin extracellular matrix interactions. *Open columns*, CHO cells expressing EGFP alone.

integrin binding to many extracellular matrix proteins (*e.g.* fibronectin) (reviewed in Ref. 33). We have previously reported that the epitopes for these antibodies overlap (residues 207–218 of β_1) (33). These mAbs probably induce high or low affinity states by binding to the non-ligand binding site of β_1, thereby changing its conformation. We found that TS2/16 significantly increased the binding of α_9-K562 cells to CHO cells expressing ADAM-15, but AIIB2 completely blocked ADAM-15-mediated cell-cell interaction (Fig. 8*A*). We obtained essentially the same results with ADAM-12 (Fig. 8*B*). Binding of α_9-K562 cells to CHO cells expressing ADAM-15 (10–20% of added cells) is substantial considering that only approximately 30% of added cells express EGFP and ADAM-15. These results again suggest that the activation status of β_1 integrin that is required for ADAM-mediated cell-cell interaction is very similar to that required for adhesion of β_1 integrins to extracellular matrix proteins.

DISCUSSION

A Novel Link between ADAMs and Integrin $\alpha_9\beta_1$—It has not been established whether most of the ADAM disintegrin domains interact with integrins, since they generally lack the RGD motif in their putative integrin binding site. The present study establishes that ADAM disintegrin domains that lack an RGD motif (mouse ADAM-15, human ADAM-15 mutants, and human and mouse ADAM-12) support cell adhesion to $\alpha_9\beta_1$ in an RGD-independent manner. Thus $\alpha_9\beta_1$ may be a major receptor for ADAMs that lack RGD motifs. The human ADAM-15 disintegrin domain, which has the RGD motif, binds to $\alpha_v\beta_3$ in an RGD-dependent manner (15), and to $\alpha_9\beta_1$ in an RGD-independent manner. However, its interaction with $\alpha_9\beta_1$ appears to be physiologically more important, since this interaction is evolutionary conserved, while the RGD motif of ADAM-15 is not conserved.

The present study for the first time demonstrated that ADAM-15 and ADAM-12 binding to $\alpha_9\beta_1$ mediates cell-cell interaction. $\alpha_9\beta_1$ is distributed in tissues including airway epithelia, the basal layer of squamous epithelia, smooth muscle, skeletal muscle, hepatocytes, neutrophils, and monocytes (34–36). $\alpha_9\beta_1$ has been reported to recognize tenascin C type III repeat (22, 37), vascular cell adhesion molecule-1 (36), and osteopontin (38) in an RGD-independent manner. It has been proposed that $\alpha_9\beta_1$-mediated binding of neutrophils to endothelial cells may be involved in chemotaxis across activated endothelial monolayers by interacting with the endothelial ligand vascular cell adhesion molecule-1 (36) during inflammation. Thus, integrin $\alpha_9\beta_1$ may have broad ligand specificity similar to integrins of the α_v family. Considering a wide distribution of ADAMs and $\alpha_9\beta_1$, ADAM/$\alpha_9\beta_1$-mediated cell-cell interaction may be involved in many developmental and pathological situations, including myoblast fusion, fertilization, and vascular and cartilage remodeling.

Human ADAM-15 potentially participates in vascular remodeling such as in atherosclerosis, since its protein level is increased in the core of atherosclerotic lesions and in intimal

cells close to the lumen, but not in normal vessel (18). In addition, the mRNA level of ADAM-15 is up-regulated in human osteoarthritic cartilage and neoplastic cartilage (chondrosarcoma), and therefore ADAM-15 has a potential role in cartilage remodeling (39). ADAM-15 has a catalytically active metalloprotease domain with a metalloprotease catalytic site consensus sequence (HEXXH)- (17). Since $\alpha_9\beta_1$ is highly and uniformly expressed in neutrophils, and weakly expressed in monocytes (34), $\alpha_9\beta_1$/ADAM-15-mediated cell-cell interaction may be critically involved in recruitment of these cells to inflammatory sites, and subsequent vessel or tissue damage (40). ADAM-15/$\alpha_9\beta_1$ and ADAM-15/$\alpha_v\beta_3$ interaction (15) may play a crucial role during atherosclerosis and cartilage remodeling.

ADAM-12 has been implicated in myoblast fusion during myogenesis (5, 6). The cysteine-rich domain of ADAM-12 has a putative fusion peptide and a short hydrophobic stretch (19, 20). The metalloprotease domain-less mouse ADAM-12, not the full-length ADAM-12, induces fusion of C2C12 myoblastic cells *in vitro* (5). The myogenic activity of the processed ADAM-12 was also demonstrated in tumor cells expressing a secreted form of human ADAM-12 that has only disintegrin and cysteine-rich domains (6). The function of the metalloprotease domain during myoblast fusion is not established, although ADAM-12 has a catalytically active metalloprotease domain. Integrin $\alpha_9\beta_1$ is highly expressed in skeletal and smooth muscle cells (34), and therefore ADAM-12/$\alpha_9\beta_1$ interaction *in vivo* through the disintegrin domain may be involved in myogenesis.

Recently Bigler *et al.* reports that GST-ADAM-2 disintegrin domain fusion protein expressed in bacteria effectively blocks sperm-egg binding and fusion (41). We have shown in the present paper that $\alpha_9\beta_1$ interacts both with GST-ADAM-12, or ADAM-15 disintegrin domain fusion protein that are expressed in bacteria and with ADAM-12 and -15 that are expressed on mammalian cells. Furthermore, we have shown that GST-ADAM disintegrin domains effectively competed with ADAMs on mammalian cells for binding to $\alpha_9\beta_1$. These results suggest that the ADAM disintegrin domains expressed in bacteria are similar in integrin binding function to those expressed in mammalian cells, although the bacterial disintegrin domains lack glycosylation. Additionally, these results suggest that the disintegrin domains primarily mediate interaction with integrins, although we do not rule out the possibility that other domains (*e.g.* Cys-rich domain) may be involved in this interaction (42).

We have shown that Ntera-2 embryonic carcinoma cells and G361 melanoma cells expressing native $\alpha_9\beta_1$ adhere to ADAM-12 and -15 in an $\alpha_9\beta_1$-dependent manner. Considering the wide distribution of ADAMs, it is possible that $\alpha_9\beta_1$/ADAM interaction may be involved in cell-cell interaction during cancer metastasis. It is also possible that this interaction mediates transduction of proliferative signals through cell-cell interaction in tumor mass. Since $\alpha_9\beta_1$ on these cells requires activation for binding to ADAM disintegrin domains, it is likely that $\alpha_9\beta_1$/ADAM interaction may be regulated by $\alpha_9\beta_1$ activation in these cells, unlike $\alpha_9\beta_1$ on CHO cells, which appears to be constitutively active.

Activation Status of Integrins during ADAM/Integrin-mediated Cell-Cell Interaction—Integrin $\alpha_6\beta_1$, on mouse eggs and on α_6-transfected cells, has been reported to interact with the disintegrin domain of the sperm surface protein ADAM-2 (fertilin β) (2). Additionally, the activation status of $\alpha_6\beta_1$ for ADAM-2 binding has been reported to be different from that for laminin (4). Thus, a major question is whether ADAM-15- or -12-mediated cell-cell interaction is different from known integrin/extracellular matrix interactions. We have shown that ADAM-15- or ADAM-12/$\alpha_9\beta_1$-mediated cell-cell interaction is similar in cation requirement to $\alpha_9\beta_1$ adhesion to ADAM-15 or ADAM-12, and to their interaction with known integrin-extracellular matrix proteins (*e.g.* fibronectin). Consistently, both ADAM-15/$\alpha_9\beta_1$ and ADAM-12/$\alpha_9\beta_1$ interactions are stimulated by the activating anti-β_1 mAb TS2/16, and blocked by the function-blocking anti-β_1 mAb AIIB2. These results establish that the β_1 integrin activation status that is required for ADAM-15 or ADAM-12 interaction with $\alpha_9\beta_1$ is similar to that required for the interaction between β_1 integrins and extracellular matrix ligands. Thus, our results do not fit in well with the reported ADAM-2/egg interaction (4). Further studies will be required to resolve this apparent discrepancy.

Very recently, Miller *et al.* (43) reported that the $\alpha_6\beta_1$ is not essential for sperm-egg fusion using eggs from α_6 null mice and proposed that β_1 integrins other than $\alpha_6\beta_1$ might be involved in this process. In our preliminary experiments, we found that $\alpha_9\beta_1$ specifically binds to the disintegrin domain of ADAM-2 synthesized in bacteria,[2] suggesting that $\alpha_9\beta_1$ is a likely candidate integrin that interacts with ADAM-2 during sperm-egg binding and fusion. This is consistent with the idea that $\alpha_9\beta_1$ is a predominant receptor for non-RGD disintegrin domains of ADAMs. Further studies will be required to establish whether $\alpha_9\beta_1$ is really involved in sperm-egg binding and fusion.

Acknowledgments—We thank Eva Engvall for critical reading of the manuscript and Amos Baruch for Ntera-2 cells.

REFERENCES

1. Wolfsberg, T., and White, J. (1996) *Dev. Biol.* **180,** 389–401
2. Almeida, E. A., Huovila, A. P., Sutherland, A. E., Stephens, L. E., Calarco, P. G., Shaw, L. M., Mercurio, A. M., Sonnenberg, A., Primakoff, P., Myles, D. G., and White, J. M. (1995) *Cell* **81,** 1095–1104
3. Evans, J. P., Schultz, R. M., and Kopf, G. S. (1995) *J. Cell Sci.* **108,** 3267–3278
4. Chen, M., Almeida, E., Huovila, A., Takahashi, Y., Shaw, L., Merurio, A., and White, J. (1999) *J. Cell Biol.* **144,** 549–561
5. Yagami-Hiromasa, T., Sato, T., Kurisaki, T., Kamijo, K., Nabeshima, Y., and Fujisawa-Sehara, A. (1995) *Nature* **377,** 652–656
6. Gilpin, B. J., Loechel, F., Mattei, M. G., Engvall, E., Albrechtsen, R., and Wewer, U. M. (1998) *J. Biol. Chem.* **273,** 157–166
7. Werb, Z., and Yan, Y. (1998) *Science* **282,** 1279–1280
8. Blobel, C. P. (1997) *Cell* **90,** 589–592
9. Pan, D., and Rubin, G. M. (1997) *Cell* **90,** 271–280
10. Qi, H., M, D. R., Wu, X., Sestan, N., Wang, W., Rakic, P., Xu, T., and Artavanis-Tsakonas, S. (1999) *Science* **283,** 91–94
11. Weskamp, G., and Blobel, C. P. (1994) *Proc. Natl. Acad. Sci. U. S. A.* **91,** 2748–2751
12. Wolfsberg, T. G., Primakoff, P., Myles, D. G., and White, J. M. (1995) *J. Cell Biol.* **131,** 275–278
13. Black, R. A., and White, J. M. (1998) *Curr. Opin. Cell. Biol.* **10,** 654–659
14. Kratzschmar, J., Lum, L., and Blobel, C. P. (1996) *J. Biol. Chem.* **271,** 4593–4596
15. Zhang, X. P., Kamata, T., Yokoyama, K., Puzon-McLaughlin, W., and Takada, Y. (1998) *J. Biol. Chem.* **273,** 7345–7350
16. Nath, D., Slocombe, P., Stephens, P., Warn A, Hutchinson, G., Yamada, K., Docherty, A., and Murphy, G. (1999) *J. Cell Sci.* **112,** 579–587
17. Lum, L., Reid, M. S., and Blobel, C. P. (1998) *J. Biol. Chem.* **273,** 26236–26247
18. Herren, B., Raines, E. W., and Ross, R. (1997) *FASEB J.* **11,** 173–180
19. Loechel, F., Gilpin, B. J., Engvall, E., Albrechtsen, R., and Wewer, U. M. (1998) *J. Biol. Chem.* **273,** 16993–16997
20. Loechel, F., Overgaard, M. T., Oxvig, C., Albrechtsen, R., and Wewer, U. M. (1999) *J. Biol. Chem.* **274,** 13427–13433
21. Kurisaki, T., Masuda, A., Osumi, N., Nabeshima, Y., and Fujisawa-Sehara, A. (1998) *Mech. Dev.* **73,** 211–215
22. Yokosaki, Y., Palmer, E., Prieto, A., Crossin, K., Bourdon, M., Pytela, R., and Sheppard, D. (1994) *J. Biol. Chem.* **269,** 26691–26696
23. Wang, A., Yokosaki, Y., Ferrando, R., Balmes, J., and Sheppard, D. (1996) *Am. J. Respir. Cell Mol. Biol.***15,** 664–672
24. Smith, D. B., and Johnson, K. S. (1988) *Gene (Amst.)* **67,** 31–40
25. Gill, S., and Von Hippel, P. (1989) *Anal. Biochem.* **182,** 319–326
26. Prater, C. A., Plotkin, J., Jaye, D., and Frazier, W. A. (1991) *J. Cell Biol.* **112,** 1031–1040
27. Takada, Y., Ylanne, J., Mandelman, D., Puzon, W., and Ginsberg, M. (1992) *J. Cell Biol.* **119,** 913–921
28. Takagi, J., Kamata, T., Meredith, J., Puzon-McLaughlin, W., and Takada, Y. (1997) *J. Biol. Chem.* **272,** 19794–19800
29. Mosser, D. D., Caron, A. W., Bourget, L., Jolicoeur, P., and Massie, B. (1997) *BioTechniques* **22,** 150–154, 156, 158–161
30. Wu, Z., Puigserver, P., Andersson, U., Zhang, C., Adelmant, G., Mootha, V., Troy, A., Cinti, S., Lowell, B., Scarpulla, R. C., and Spiegelman, B. M. (1999) *Cell* **98,** 115–124
31. Deng, W. P., and Nickoloff, J. A. (1992) *Anal. Biochem.* **200,** 81–88
32. Takahashi, H., Isobe, T., Horibe, S., Takagi, J., Yokosaki, Y., Sheppard, D., and

[2] X.-P. Zhang, K. Eto, and Y. Takada, unpublished results

Saito, Y. (2000) *J. Biol. Chem.* **275,** 23589–23595
33. Takada, Y., and Puzon, W. (1993) *J. Biol. Chem.* **268,** 17597–17601
34. Palmer, E. L., Ruegg, C., Ferrando, R., Pytela, R., and Sheppard, D. (1993) *J. Cell Biol.* **123,** 1289–1297
35. Wang, A., Patrone, L., McDonald, J. A., and Sheppard, D. (1995) *Dev. Dyn.* **204,** 421–431
36. Taooka, Y., Chen, J., Yednock, T., and Sheppard, D. (1999) *J. Cell Biol.* **145,** 413–420
37. Yokosaki, Y., Matsuura, N., Higashiyama, S., Murakami, I., Obara, M., Yamakido, M., Shigeto, N., Chen, J., and Sheppard, D. (1998) *J. Biol. Chem.* **273,** 11423–11428
38. Yokosaki, Y., Matsuura, N., Sasaki, T., Murakami, I., Schneider, H., Higashiyama, S., Saitoh, Y., Yamakido, M., Taooka, Y., and Sheppard, D. (1999) *J. Biol. Chem.* **274,** 36328–36334
39. Bohm, B. B., Aigner, T., Gehrsitz, A., Blobel, C. P., Kalden, J. R., and Burkhardt, H. (1999) *Arthritis Rheum.* **42,** 1946–1950
40. Ross, R. (1993) *Nature* **362,** 801–809
41. Bigler, D., Takahashi, Y., Chen, M. S., Almeida, E. A., Osbourne, L., and White, J. M. (2000) *J. Biol. Chem.* **275,** 11576–11584
42. Zolkiewska, A. (1999) *Exp. Cell Res.* **252,** 423–431
43. Miller, B. J., Georges-Labouesse, E., Primakoff, P., and Myles, D. G. (2000) *J. Cell Biol.* **149,** 1289–1296

Molecular Biology of the Cell
Vol. 11, 1457–1469, April 2000

ADAM 23/MDC3, a Human Disintegrin That Promotes Cell Adhesion via Interaction with the αvβ3 Integrin through an RGD-independent Mechanism

Santiago Cal,* José M.P. Freije,* José M. López,† Yoshikazu Takada,‡ and Carlos López-Otín*§

Departamentos de *Bioquímica y Biología Molecular and †Morfología y Biología Celular, Instituto Universitario de Oncología, Facultad de Medicina, Universidad de Oviedo, 33006 Oviedo, Spain; and ‡Department of Vascular Biology, The Scripps Research Institute, La Jolla, California 92037

Submitted August 4, 1999; Revised January 27, 2000; Accepted January 31, 2000
Monitoring Editor: Richard Hynes

ADAM 23 (a disintegrin and metalloproteinase domain)/MDC3 (metalloprotease, disintegrin, and cysteine-rich domain) is a member of the disintegrin family of proteins expressed in fetal and adult brain. In this work we show that the disintegrin-like domain of ADAM 23 produced in *Escherichia coli* and immobilized on culture dishes promotes attachment of different human cells of neural origin, such as neuroblastoma cells (NB100 and SH-S_y5_y) or astrocytoma cells (U373 and U87 MG). Analysis of ADAM 23 binding to integrins revealed a specific interaction with αvβ3, mediated by a short amino acid sequence present in its putative disintegrin loop. This sequence lacks any RGD motif, which is a common structural determinant supporting αvβ3-mediated interactions of diverse proteins, including other disintegrins. αvβ3 also supported adhesion of HeLa cells transfected with a full-length cDNA for ADAM 23, extending the results obtained with the recombinant protein containing the disintegrin domain of ADAM 23. On the basis of these results, we propose that ADAM 23, through its disintegrin-like domain, may function as an adhesion molecule involved in αvβ3-mediated cell interactions occurring in normal and pathological processes, including progression of malignant tumors from neural origin.

INTRODUCTION

Cell–cell and cell–extracellular matrix interactions are essential for the development and maintenance of an organism as well as for the progression of malignant tumors. Likewise, proteolysis of the extracellular matrix is of vital importance for a series of tissue-remodeling processes occurring during both normal and pathological conditions, such as tissue morphogenesis, wound healing, inflammation, and tumor cell invasion and metastasis. These events are mediated by a variety of cell surface adhesion proteins and proteases, with different structural and functional characteristics (Werb, 1997). Among them, a group of recently described proteins called ADAMs (a disintegrin and metalloproteinase domain) have raised considerable interest because of their potential ability to perform both functions, adhesion and proteolysis (Wolfsberg *et al.*, 1995; Blobel, 1997; Wolfsberg and White, 1997). These membrane proteins have a unique domain organization containing pro, metalloproteinase-like, disintegrin-like, cysteine-rich, epidermal growth factor (EGF)-like, transmembrane, and cytoplasmic domains. Some of these domains are similar to those found in a family of soluble snake venom proteins that bind with high affinity to the platelet integrin GPIIb/IIIa, inhibiting platelet aggregation and causing hemorrhage in snake bite victims (Niewiarowski *et al.*, 1994).

ADAMs, also known as cellular disintegrins or MDCs (metalloprotease, disintegrin, and cysteine-rich domains), have been found in a wide variety of mammalian tissues as well as in other eukaryotic organisms, including *Xenopus laevis* (Alfandari *et al.*, 1997; Cai *et al.*, 1998), *Drosophila melanogaster* (Rooke *et al.*, 1996), and *Caenorhabditis elegans* (Podbilewicz, 1996), but not in plants or bacteria. Members of this protein family were first associated with reproductive processes; however, over the last several years the family has widely expanded, and to date, >20 different ADAMs with diverse functions have been identified and characterized at the molecular level. Thus, in addition to a series of family

§ Corresponding author. E-mail address: clo@dwarf1.quimica.uniovi.es.

Abbreviations used: ADAM, a disintegrin and metalloproteinase domain; CHO, Chinese hamster ovary; EGF, epidermal growth factor; EST, expressed sequence tag; GST, glutathione *S*-transferase; HA, hemagglutinin; MDC, metalloprotease, disintegrin, and cysteine-rich domain; TACE, tumor necrosis factor-α-converting enzyme.

members such as fertilins or cyritestins, involved in spermatogenesis and heterotypic sperm–egg binding and fusion (Blobel *et al.*, 1992; Houliva *et al.*, 1996; Adham *et al.*, 1998), other ADAMs such as meltrin α are implicated in homotypic myoblast–myoblast fusion (Yagami-Hiromasa *et al.*, 1995; Gilpin *et al.*, 1998). Meltrin α and β have also been suggested to play a role in osteoblast differentiation and/or osteoblast activity in bone (Inoue *et al.*, 1998). Furthermore, the cellular disintegrins MS2 (ADAM 8) and decysin have been identified as monocytic and dendritic cell-specific proteins, suggesting that they may be involved in host defense mechanisms (Yoshida *et al.*, 1990; Mueller *et al.*, 1997). Similarly, ADAMTS-1, characterized by the presence of thrombospondin motifs in its amino acid sequence, has been associated with various inflammatory processes (Kuno *et al.*, 1997). Interestingly, ADAMTS-4, another member of this subfamily of disintegrins containing thrombospondin motifs, has been characterized as an aggrecanase responsible for the degradation of cartilage aggrecan in arthritic diseases (Tortorella *et al.*, 1999). Finally, other ADAMs have been found to function as proteolytic enzymes involved in the processing of relevant cellular substrates. In fact, the recently described tumor necrosis factor-α-converting enzyme (TACE) is an ADAM implicated in the release of the proinflammatory membrane-anchored cytokine tumor necrosis factor-α from the plasma membrane (Black *et al.*, 1997; Moss *et al.*, 1997). Similarly, the product of the *kuz* gene from *Drosophila* (ADAM 10) appears to be responsible for the proteolytic activation of the transmembrane protein Notch required for lateral inhibitory signaling during neurogenic differentiation (Pan and Rubin, 1997; Sotillos *et al.*, 1997), although other studies have proposed that Kuz would be required for processing of the Notch ligand Delta (Qi *et al.*, 1999). Finally, Izumi *et al.* (1998) have reported that MDC9/ADAM 9 is involved in the ectodomain shedding of membrane-anchored heparin-binding EGF-like growth factor.

In addition to this variety of physiological functions described for ADAMs, some of these family members have been suggested to play important roles in the development and progression of tumor processes. Thus, ADAM 11 was originally identified as a candidate tumor suppressor gene for human breast cancer (Emi *et al.*, 1993), whereas ADAMTS-1 has been associated with the development of cancer cachexia (Kuno *et al.*, 1997). In addition, several disintegrins have been proposed to be responsible for some pathological features of hematological malignancies such as the premature egression of leukemic cells from bone marrow into the peripheral blood or the generalized connective tissue destruction accompanying these malignant processes (Wu *et al.*, 1997). Furthermore, ADAM 10 is overexpressed in tumors of sympathoadrenal origin such as pheochromocytomas and neuroblastomas (Yavari *et al.*, 1998). Finally, other ADAM family members with proteolytic activity such as TACE have been proposed to play indirect roles in tumor processes through their participation in the proteolytic activation and release of membrane-bound cytokine or growth factor precursors of relevance in cancer (Black *et al.*, 1997; Moss *et al.*, 1997).

These recent findings have stimulated the search for new ADAMs potentially associated with some of the conditions involving cell–cell interactions or extracellular matrix degradation taking place during both normal or pathological conditions (Blobel, 1997; Werb, 1997; Wolfsberg and White, 1997). Recently, we have cloned a full-length cDNA coding for a member of this family that has been called ADAM 23 (GenBank accession number AJ005580) and whose sequence is very similar to that reported for a novel cellular disintegrin (MDC3) recently described by Sagane *et al.* (1998). ADAM 23/MDC3 exhibits the typical structure of ADAM family members and is predominantly expressed in brain, suggesting that it may function as an integrin ligand in cells of neural origin. In this work, we demonstrate that the recombinant disintegrin-like domain of ADAM 23 promotes adhesion of neuroblastoma and astrocytoma cells. We also show that this process is mediated by a specific interaction between $\alpha v\beta 3$ and a short amino acid sequence present in the putative disintegrin loop of ADAM 23. We also provide evidence that $\alpha v\beta 3$ supports adhesion of HeLa cells transfected with a full-length cDNA for ADAM 23. According to these results, we suggest that ADAM 23, through its disintegrin-like domain, may function as an adhesion molecule involved in $\alpha v\beta 3$-mediated cell interactions taking place during normal and pathological processes.

MATERIALS AND METHODS

Materials

Restriction endonucleases and other reagents used for molecular cloning were from Boehringer Mannheim (Mannheim, Germany). Double-stranded DNA probes were radiolabeled with [α-^{32}P]dCTP (3000 Ci/mmol) purchased from Amersham International (Buckinghamshire, United Kingdom) using a commercial random-priming kit from the same company. A human brain cDNA library constructed in λDR2 and Northern blots containing polyadenylated RNAs from different adult and fetal human tissues were from Clontech (Palo Alto, CA). Synthetic peptides were obtained from the Molecular Biology Facilities Unit (University of Leicester, Leicester, United Kingdom). NB100 and SH-S$_y$5$_y$ human neuroblastoma cells were kindly provided by Dr. F. Sánchez-Madrid (Hospital de la Princesa, Madrid, Spain), and Drs. F. Barros and T. Giráldez (Universidad de Oviedo). U373 and U87 MG astrocytoma cell lines were provided by Dr. A. Nakano (Hyogo College of Medicine, Hyogo, Japan) All media and supplements for cell culture were obtained from Sigma (St. Louis, MO) except for fetal calf serum, which was from Boehringer Mannheim.

Isolation of a cDNA Clone for ADAM 23 from a Human Brain cDNA Library

A search of the GenBank database of human expressed sequence tags (ESTs) for sequences with homology to members of the ADAM family led us to identify a sequence (R52569; Washington University-Merck EST Project, St. Louis, MO) derived from a brain cDNA clone and showing significant similarity to sequences of previously described ADAMs. To obtain this DNA fragment, we performed PCR amplification of a human brain cDNA (Clontech) with two specific primers, 5′-CAACAAAGCTATTTGAGCCCACGG and 5′-TTGGTGGGCACTGACCAGAGTCT, derived from the R52569 sequence. The PCR reaction was carried out in a GeneAmp 2400 PCR system from Perkin Elmer (Norwalk, CT) for 40 cycles of denaturation (94°C, 15 s), annealing (64°C, 20 s), and extension (72°C, 20 s). The 262-bp PCR product amplified from human brain cDNA was cloned into a *Sma*I-cut pBluescript II SK vector (Stratagene, La Jolla, CA), and its identity was confirmed by nucleotide sequencing. This cDNA was then excised from the vector, radiolabeled, and used to screen a human brain cDNA library according to standard procedures (Maniatis *et al.*, 1982).

Northern Blot Analysis

Northern blots containing poly(A)$^+$ RNAs from different fetal and adult human tissues were obtained from Clontech. These blots were prehybridized at 42°C for 3 h in 50% formamide, 5× SSPE, 2× Denhardt's solution, 0.1% SDS, and 100 μg/ml denatured herring sperm DNA and then hybridizated for 16 h under the same conditions with the full-length cDNA isolated for ADAM 23. Filters were washed with 0.2× SSC and 0.1% SDS for 2 h at 50°C and subjected to autoradiography. RNA integrity and equal loading were assessed by hybridization with an actin probe as indicated by Clontech.

Reverse Transcription-PCR Amplification

To assay the presence of ADAM 23 in neuroblastoma cell lines, total RNA was isolated from NB100 and SH-S_y5_y cells by guanidium thiocyanate-phenol-chloroform extraction and used for cDNA synthesis with the RNA PCR kit from Perkin Elmer. After reverse transcription using 1 μg of total RNA and random hexamers as primer according to the instructions of the manufacturer, the whole mixture was used for PCR with the two specific oligonucleotides corresponding to the disintegrin domain of ADAM 23 as described above. Negative controls were performed using all reagents with the exception of random hexamers.

Construction of an Expression Vector for ADAM 23 and Expression in Escherichia coli

A 975-bp fragment of the ADAM 23 cDNA containing the disintegrin-like domain was generated by PCR amplification with primers 5′-TAGGGATCCCAAAGCTATTTGAGCCCA and 5′-ATGAAGATTTGGTGGGCA. The PCR amplification was performed for 20 cycles of denaturation (95°C, 20 s), annealing (52°C, 20 s), and extension (68°C, 20 s), followed by 10 additional cycles of denaturation (95°C, 15 s), annealing (62°C, 15 s), and extension (68°C, 2 min) using the Expand Long PCR kit and the GeneAmp 9700 PCR system. Because of the design of the oligonucleotides, the amplified fragment could be cleaved at the 5′ end with *Hin*dIII and ligated in frame into the pGEX-3x *E. coli* expression vector (Invitrogen, San Diego, CA) previously cleaved with *Hin*dIII–*Sma*I. The expression vector was transformed into BL21(DE3)pLysS competent *E. coli* cells and grown on agar plates containing chloramphenicol and ampicillin. Single colonies were used to inoculate 2-ml cultures in 2YT medium supplemented with 33 μg/ml chloramphenicol and 50 μg/ml ampicillin. Five hundred microliters of the corresponding culture were used to inoculate 200 ml of 2YT medium containing the above antibiotics. After culture reached an OD_{600} of 0.6, expression was induced by addition of isopropyl-1-thio-β-D-galactopyranoside (0.5 mM final concentration) followed by further incubation for 3–20 h at 30°C. Cells were collected by centrifugation, washed, and resuspended in 0.05 vol of PBS, lysed by using a French press, and centrifuged at 20,000 × *g* for 20 min at 4°C. The soluble extract was incubated with glutathione-Sepharose 4B (Pharmacia, Uppsala, Sweden) and eluted with glutathione elution buffer (10 mM reduced glutathione in 50 mM Tris-HCl, pH 8.0) following the manufacturer's instructions.

Adhesion Assays

Cell adhesion assays were essentially performed as previously described by Luque *et al.* (1994). Briefly, 96-well immunoplates (MaxiSorp; Nunc, Roskilde, Denmark) were coated with 0.1 ml of PBS containing different amounts of BSA, glutathione *S*-transferase (GST), and ADAM 23/GST. After incubating for 16 h at 4°C, wells were blocked with Dulbecco's modified Eagle's medium containing 2.5% BSA for 2 h at 37°C. Then, NB100 neuroblastoma cells (~50,000 cells per well) were added in Dulbecco's modified Eagle's medium supplemented with 1% BSA and incubated at 37°C for 2 h. For experiments directed to analyze the effect of divalent cations, the cells were washed three times in PBS and resuspended in the same buffer supplemented with either 1 mM $MgCl_2$, 50 μM $MnCl_2$, and 1 mM $CaCl_2$ or 1 mM $MgCl_2$ plus 5 mM EDTA. Nonbound cells were removed by rinsing the wells with serum-free medium, whereas bound cells were fixed with methanol and stained with Giemsa. Cells were counted per unit area with the aid of an inverted light microscope, using a 20× high-power objective and an ocular grid. For inhibition studies cells were pretreated for 30 min before the addition to the coated wells of mAb LM 609 (used at 1:400 dilution of ascites) or synthetic peptides (20 or 40 μg/ml) corresponding to the disintegrin loop of ADAM 23 (AVNEDCDIT, peptide 330) or a "scrambled" peptide (DCVTNIAE, peptide 331). In all cases, experimental treatments were performed in triplicate with a minimum of three areas counted per well.

Scanning Electron Microscopy

Glass coverslips (12-mm diameter) were immersed in 60% HNO_3 for 1 h, washed with distilled water, immersed in 7% NaOH, and washed with water again. After drying, coverslips were placed in a 24-well tissue culture plate and coated with ADAM 23 or fibronectin in PBS (20 μg/ml). After overnight incubation at 4°C, coverslips were washed with PBS to remove free protein and coated with 2.5% BSA. NB100 cells were then seeded (~15,000 cells per cm^2) in the same buffer used for cell adhesion experiments and allowed to adhere for 2 h at 37°C. Unbound cells were then removed by washing with free serum medium, and adherent cells were fixed with 2.5 glutaraldehyde in 0.1 M cacodylate buffer, pH 7.5, for 3 h and then washed, osmicated, dehydrated with acetone, critical point dried, and gold coated. Cells were then viewed under a JEOL (Tokyo, Japan) JSM 6100 scanning electron microscope and photographed.

Immunofluorescence Microscopy

NB100 cells were grown on glass coverslips as described above, fixed with 3.7% paraformaldehyde in PBS for 20 min at room temperature, and permeabilized with 0.2% Triton X-100 for 10 min. Coverslips were then incubated with 10% fetal bovine serum in PBS (30 min), followed by a 1:400 dilution of a commercial anti-vinculin mAb (Sigma) for 1 h. After washing with PBS, incubation was made with a mix of a 1:500 dilution of a goat anti-rabbit immunoglobulin G FITC-conjugated antibody (Amersham). For staining of filamentous actin, 0.1 μg/ml rhodamine-phalloidine was included during incubation with the secondary antibodies. Finally, washed coverslips were mounted, and cells were examined using a Zeiss (Thornwood, NY) fluorescent microscope equipped with a charge-coupled device camera (Photometrics, Tucson, AZ).

Generation of Chinese Hamster Ovary (CHO) Cells Expressing Different Human Integrins

The development of these cell lines has been described previously (Zhang *et al.*, 1998). Briefly, cDNA constructs for different integrins were transfected into CHO cells, together with a neomycin resistance gene. After selection with G-418, cells stably expressing human integrins were cloned by sorting to obtain high expressers. The α2, α3, α4, α5, α6, and αv subunits of human integrins were expressed in combination with the β1 subunit of hamster, whereas β subunits were expressed in combination with α human subunits. The β3-CHO cells expressed human β3/hamster αv hybrid.

Construction of Eukaryotic Expression Vectors for ADAM 23-HA and Immunolocalization

A full-length cDNA encoding ADAM 23 was PCR amplified with oligonucleotides Ad23-D (5′-TATGAGCCATGAAGCCGCCCG-3′) and Ad23-R (5′-GATGGGGCCTTGCTGAGTAGG-3′) and cloned in the *Eco*RV site of a modified pcDNA3 vector containing a 24-bp linker coding for the hemagglutinin (HA) epitope of human influ-

enza virus. Thus, the resulting ADAM 23 protein was HA tagged at the COOH terminus. HeLa cells were transfected with 1 μg of plasmid pcDNA3-ADAM 23-HA or pcDNA alone using LipofectAMINE reagent (Life Technologies, Gaithersburg, MD), according to the manufacturer's instructions. Transfected cells were used for binding experiments to purified αvβ3 or to protein extracts from integrin-transfected CHO cells as above, with the exception that experiments were performed without divalent cations. For immunolocalization experiments, 48 h after transfection, cells were fixed for 10 min in cold 4% paraformaldehyde in PBS, washed in PBS, and incubated for 10 min in 0.2% Triton X-100 in PBS. Fluorescent detection was performed by incubating the slides with mAb 12CA5 (Boehringer Mannheim) against HA (diluted 1:100), followed by another incubation with goat anti-mouse fluoresceinated antibody (diluted 1:50). Antibodies were diluted in blockage solution (15% FCS in PBS). After washing in PBS, slides were mounted with Vectashield (Vector Laboratories, Burlingame, CA) and observed in a Bio-Rad (Hercules, CA) confocal laser microscope.

Site-directed Mutagenesis

The E466A mutation in the disintegrin loop of ADAM 23 was carried out by PCR-based methods. An oligonucleotide containing the mutation 5'-GTAATATCACACGCGTTCACAGCA (with G indicating a change of T to G in the original sequence) and a second oligonucleotide containing a *Bam*HI site (5'-GTGGATCCCCAAGCTATTG) were first used to PCR amplify a DNA fragment. This amplified product was then used as a "megaprimer" for a second PCR amplification with an oligonucleotide corresponding to the 3' end of the cloning site of pGEX-3X. PCR conditions were 94°C, 2 min (1 cycle), and 94°C, 0.1 s; 60°C, 0.1 s; and 68°C, 30 s (20 cycles). The PCR product of the expected size was digested with *Bam*HI and *Eco*RI and cloned in pGEX-3X. The presence of the mutation was confirmed by nucleotide sequencing. Finally, production of the recombinant mutant protein in *E. coli* was carried out as described above.

Western Blot Analysis

Purified integrins (αvβ3, α1β1, or α5β1, 0.3 μg each; Chemicon International, Temecula, CA) were incubated with Sepharose 4B beads containing 0.5 μg of disintegrin-GST, in a buffer containing 50 mM Tris-HCl, 200 mM NaCl, and 0.2 mM $MnCl_2$, pH 7.4, for 4 h at 37°C. After incubation, beads were washed six times with 200 μl of the same buffer to remove unbound protein. Beads were then resuspended in Laemmli buffer, and after boiling, solubilized proteins were loaded in a 6% SDS-PAGE gel and visualized by silver staining. Alternatively, samples were blotted to a nitrocellulose membrane, and the presence of αv or β3 integrin subunits was detected using polyclonal antibodies raised against these subunits (kindly provided by Drs. R. Lacalle and C. Martínez-A., Centro Nacional de Biotecnología, Madrid, Spain). Similarly, the putative presence of β1 integrin subunits was examined with the B3B11 mAb (mAb 2251; Chemicon). Western-blots were visualized by enhanced chemiluminescence according to the manufacturer's instructions (Amersham).

RESULTS

Cloning of a Full-Length cDNA Encoding ADAM 23/MDC3, a Member of the Cellular Disintegrin Family

To identify novel members of the ADAM family produced by human tissues, we screened the GenBank database of ESTs looking for sequences with similarities to those of previously described family members. This analysis allowed us to identify a 405-bp EST (R52569) that, when translated, exhibited significant amino acid sequence similarity to the disintegrin domain characteristic of ADAMs. A cDNA containing part of this EST was generated by PCR amplification of DNA prepared from a human brain cDNA library and used as a probe to screen this library. Sequence analysis of one of the positive clones (called 6D) revealed an open reading frame coding for a protein of 832 amino acids with a predicted molecular mass of 91.9 kDa (European Molecular Biology Laboratory accession number AJ005580). An alignment of the deduced amino acid sequence revealed that this protein possesses all characteristic domains of the ADAM family members, including propeptide, metalloproteinase-like, disintegrin-like, and cysteine-rich domains, an EGF-like repeat, a transmembrane domain, and a cytoplasmic tail (Figure 1). Further analysis of the identified amino acid sequence revealed that it was virtually identical to that derived from a brain cDNA cloned by Sagane *et al.* (1998) during preparation of this manuscript and called MDC3. Both sequences are identical in the coding region, although the cDNA isolated in this work is ~1 kb longer than that of MDC3 and shows some sequence discrepancies, which could be derived from genetic polymorphisms or sequencing errors. Following the nomenclature system for cellular disintegrins (see http://www.med.virginia.edu/~jag6n/whitelab.html), we would assign the name ADAM 23 to this enzyme. Further comparative analysis of the ADAM 23 amino acid sequence revealed a significant similarity with other human ADAMs, the maximum percentage of identities being with ADAM 11 (53%) and ADAM 22 (51%). Expression analysis of ADAM 23 in human tissues revealed a restricted pattern of expression to fetal and adult brain (Figure 2A; also see Sagane *et al.*, 1998). It is also remarkable that tumor cells from neural origin such as NB 100, SH-S_y5_y, U373, and U87 MG, also expressed this gene. In contrast, a variety of tumor cell lines from diverse sources such as HL-60 (promyelocytic leukemia), K-562 (chronic myelogenous leukemia), Raji (Burkitt's lymphoma), HeLa (cervical adenocarcinoma), SW480 (colorectal adenocarcinoma), and A549 (lung adenocarcinoma) did not show significant levels of ADAM 23 expression (Figure 2B; our unpublished observations).

Production of Recombinant ADAM 23 in Bacterial Cells and Analysis of its Cell Adhesive Properties

According to the above structural data, ADAM 23 has a number of features characteristic of ADAM family members. However, its deduced amino acid sequence lacks essential residues conserved in metalloproteinases (Figure 1), suggesting that this protein could be involved in cell adhesion processes rather than in protease-mediated events. As a preliminary step to elucidate whether ADAM 23 is active in cell–cell adhesion processes, we expressed its disintegrin-like domain in a bacterial system following the strategy described for expression of other cellular disintegrins (Zhang *et al.*, 1998). The predicted disintegrin domain of ADAM 23 was subcloned into the expression vector pGEX-3X, and the resulting plasmid, called pGEX-3X ADAM 23, as well as the original vector, were transformed into *E. coli* BL21(DE3)pLysS. Transformed bacteria were induced with isopropyl-1-thio-β-D-galactopyranoside, and protein extracts were analyzed by SDS-PAGE. According to the obtained results, extracts from bacteria transformed with the recombinant plasmid contained a fusion protein of ~40 kDa,

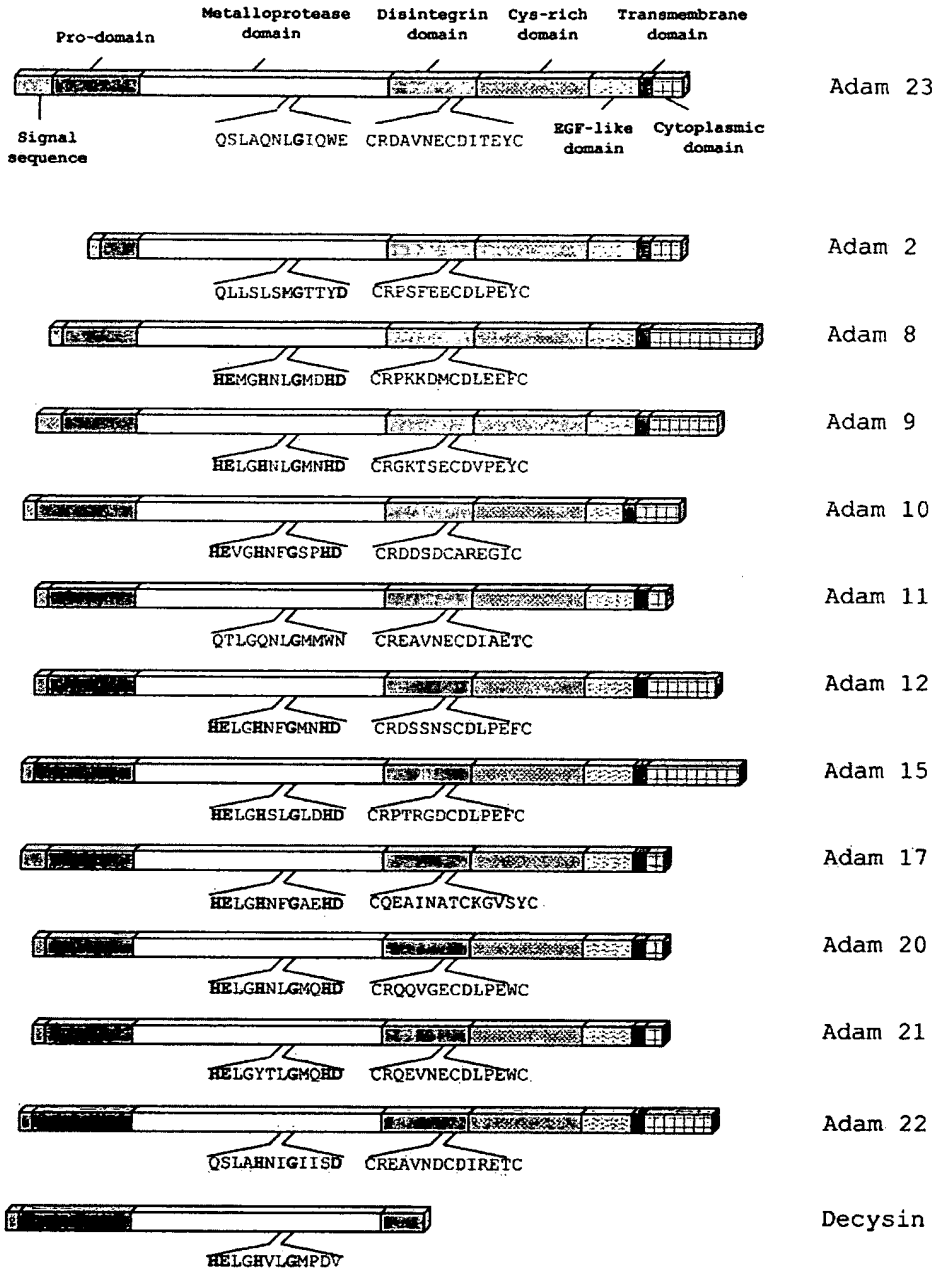

Figure 1. Comparison of the domain structure of ADAM 23 and human ADAMs. The amino acid sequences of the regions around the consensus sequence for metalloproteinases (HEXXHXXGXXH) and the putative integrin-binding loops of ADAMs are shown. Sequences for human fertilin α (ADAM 1) and cyritestin 1 (ADAM 3) are not included, because their respective genes are not functional (Jury *et al.*, 1997; Frayne and Hall, 1998). The disintegrin domain of decysin is truncated and lacks the region compared in the alignment of the remaining family members. All amino acid sequences were extracted from the SwissProt database. The modular structure of members of the recently described ADAM-TS subfamily containing thrombospondin-1 repeats is shown by Hurskainen *et al.* (1999).

which was not present in the control extracts (Figure 3). The recombinant protein was purified by affinity chromatography in a glutathione-Sepharose 4B column, which was eluted with a reduced glutathione-containing buffer. After elution and SDS-PAGE analysis of proteins present in the chromatographic eluate, a single band of the expected size was detected (Figure 3).

To examine the activity of the purified disintegrin domain of ADAM 23, wells of microtiter plates were coated with the recombinant protein and seeded with NB100 human neuroblastoma cells. After rinsing the wells to remove unbound cells, bound cells were stained and quantified. As shown in Figure 4B, ADAM 23-GST promoted cell adhesion in a manner similar to that observed when wells were coated with fibronectin (Figure 4A). By contrast, wells coated with GST, albumin, or buffer alone did not support any significant cell adhesion. Morphological studies of NB100 cells adherent to ADAM 23-GST or fibronectin by using light and scanning electron microscopy revealed differences in cell morphology that were mainly related to changes in the number and length of surface protrusions (Figure 4, C and D). We also examined

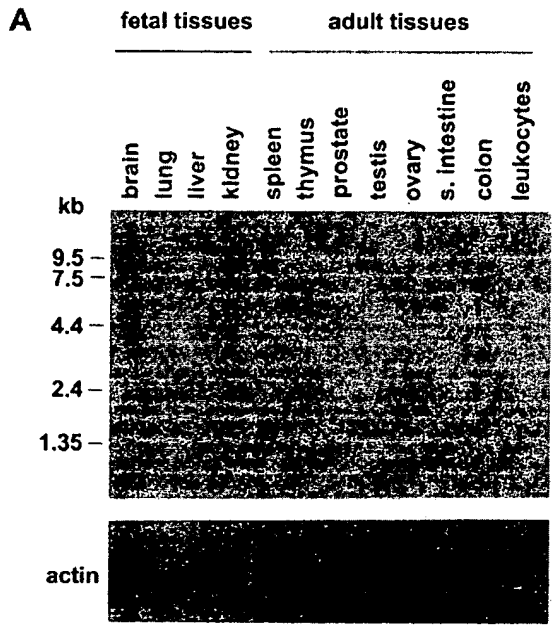

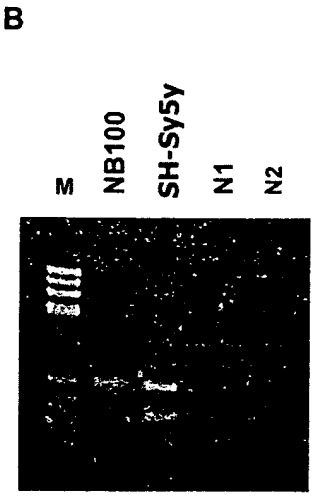

Figure 2. Analysis of ADAM 23 expression in human tissues and cell lines. (A) Approximately 2 μg of polyadenylated RNA from the indicated tissues were analyzed by hybridization with the full-length cDNA isolated for human ADAM 23. The positions of RNA size markers are shown. Filters were subsequently hybridized with a human actin probe to ascertain the differences in RNA loading among the different samples. (B) Reverse transcription-PCR analysis of ADAM 23 expression in human neuroblastoma NB100 and SH-S_y5_y cells. N1 and N2 indicate negative controls for each cell line. M, molecular size markers.

the structure of the actin cytoskeleton in NB100 cells adherent to either ADAM 23 or fibronectin (Figure 4, E–H). Neuroblastoma cells adherent to fibronectin showed a conventional F-actin distribution including relatively little F-actin in the central region of the cell and concentrated F-actin in a layer just beneath the plasma membrane (Figure 4E). Cells adherent to ADAM 23 contained actin filaments mainly located at specific cortical regions, but, compared with cells adherent to fibronectin, they tended to have decreased levels of assembled actin filaments and a lower polarized pattern (Figure 4F). In both cells adherent to ADAM 23 and cells adherent to fibronectin, phalloidine labeling was not uniform but usually was relatively dense in some areas and relatively sparse in others. Some of the dense labeling occurred in fairly distinct patches localized in close apposition to the plasma membrane. To confirm that these patches were actin–filament attachment sites in the plasma membrane and to study their distribution, staining of the same cells with antibodies to vinculin was performed. A clear relationship among the sites of vinculin localization, the actin–filament bundles, and the sites of filopodial protrusion was observed (Figure 4, G and H). Although differences in the vinculin labeling pattern between cells adherent to either ADAM 23 or fibronectin were found, such differences were restricted to the degree of aggregation, being higher in cells adherent to fibronectin (Figure 4, G and H). Nevertheless, in both cases, vinculin-positive patches were heterogeneously distributed, being concentrated at specific cortical regions, which presumably corresponded to the leading edge of the cells.

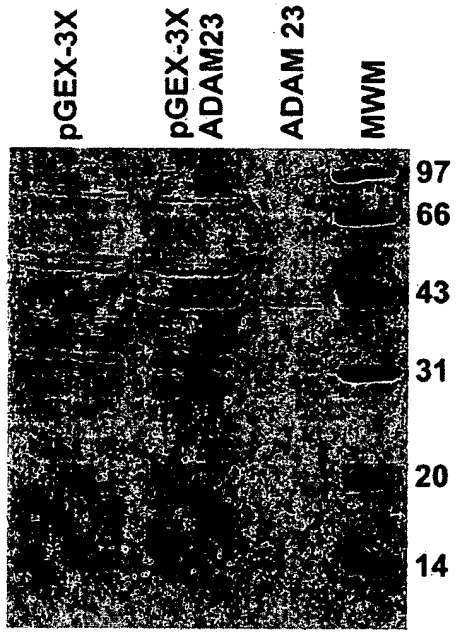

Figure 3. SDS-PAGE analysis of purified recombinant ADAM 23 produced in *E. coli*. Five-microliter aliquots of bacterial extracts (pGEX-3X and pGEX-3X ADAM 23) as well as 1 μl of purified ADAM 23 were analyzed by SDS-PAGE. The sizes in kilodaltons of the molecular size markers (MWM) are indicated at the right.

Further analysis of the ADAM 23-promoted cell adhesiveness revealed that this effect was dose dependent (Figure 5). In addition, the attachment of NB 100 neuroblastoma cells was stimulated in the presence of divalent cations such as Mn^{2+} and Mg^{2+} (Figure 5). Similar results were obtained when these experiments were performed with other cells from neural origin such as SH-S_y5_y, U373, and U87 MG. In contrast, when similar experiments were performed with other cell lines from different sources,

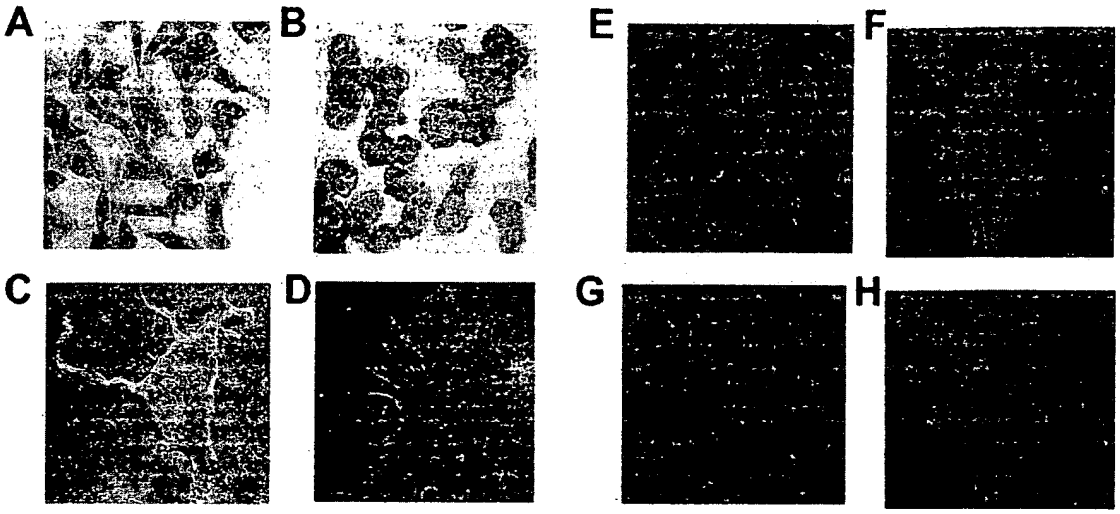

Figure 4. Analysis of the role of ADAM 23 in neuroblastoma cell adhesion. Adhesion of NB 100 cells to dishes coated with 10 μg/ml fibronectin (A) or with 10 μg/ml recombinant ADAM 23 (B) is shown. Several differences in cell morphology are found at the light microscopic level. Scanning electron microscopy proved that differences in cell morphology between NB 100 cells adherent to fibronectin (C) and those adherent to ADAM 23 (D) are mainly due to variations in the number and length of surface protrusions. Cells adherent to fibronectin (C) have a relatively low number of long asymmetric filopodial extensions, whereas those attached to ADAM 23 are devoid of long surface extensions but show many short protrusions resembling microspikes, most of which appeared to be firmly attached to the glass coverslip. The effect of ADAM 23 on F-actin and vinculin distribution is shown in E–H. Confocal optical sections of NB100 cells adherent to fibronectin (E and G) and ADAM 23 (F and H) were double labeled for F-actin (rhodamine-phalloidine; red) and vinculin (anti-vinculin, visualized with FITC-labeled goat anti-rabbit; green). Neuroblastoma cells adherent to fibronectin (E) show relatively little F-actin in the central region of the cell and numerous parallel bundles at the axis of the filopodial protrusions. In cells adherent to ADAM 23 (F), the assembly of actin filaments is lower, but they are mainly located at specific cortical regions and display a moderate polarization. Vinculin in neuroblastoma cells adherent to fibronectin (G) is mainly located at the sites of filopodial protrusion. Vinculin-positive patches in cells adherent to ADAM 23 (H) show a lower degree of aggregation, but they are also concentrated at specific cortical regions.

including HT1080, HeLa, and T47D cells, no significant ADAM 23-mediated adhesion was observed (our unpublished observations). These results suggest that the effect of this cellular disintegrin on cell adhesion may be dependent on the presence of specific integrins in the adherent cells.

ADAM 23 Promotes Cell Adhesion via Interaction with αvβ3 Integrin

To evaluate the possibility that ADAM 23 mediates cell adhesion through interaction with specific integrins, we used a panel of CHO cells expressing different recombinant integrins. According to previous data (Takada *et al.*, 1992; Takagi *et al.*, 1997), parent CHO cells express α5β1 as a major integrin but do not express significant amounts of β2 or β3 integrins. However, when wells of microtiter plates were coated with the disintegrin domain of ADAM 23 (10 μg/ml) and seeded with these parent CHO cells, no significant cell adhesion-promoting effect was observed (Figure 6A). Similar results were obtained with CHO cells expressing a variety of exogenous integrins, including α2β1, α3β1, α4β1, α6β1, and αvβ1. In contrast, the recombinant ADAM 23 promoted adhesion of β3-CHO cells that express functional αvβ3 (Figure 6A). These results are consistent with the proposal that ADAM 23 mediates cell adhesion through interactions with αvβ3. To provide further evidence on this question, we examined the effect of a function-blocking anti-αvβ3 mAb (LM 609) on the cell adhesion properties supported by ADAM 23. As shown in Figure 6B, adhesion of ADAM 23 to β3-CHO cells was substantially diminished in the presence of LM 609. Similarly, this anti-αvβ3 antibody was able to reduce the ADAM 23-mediated adhesion of NB100 neuroblastoma cells, whereas a β1-blocking antibody (LIA 1/2) did not show any significant effect on this activity (Figure 6B). The specificities of function-blocking antibodies LM 609 and LIA 1/2 have been described previously (Cheresh and Spiro, 1987; Luque *et al.*, 1994).

To further examine αvβ3–ADAM 23 interaction, Sepharose beads containing the ADAM 23 disintegrin domain fused to GST were incubated with purified αvβ3 integrin. After extensive washing to remove the unbound integrin, the presence of bound αvβ3 was examined by SDS-PAGE of proteins solubilized in an SDS-containing buffer. As shown in Figure 7A, two bands corresponding to αv (145 kDa) and β3 (95 kDa) were detected in extracts from beads containing ADAM 23-GST but not in those derived from beads containing GST alone. The identity of these bands as αv and β3 was confirmed by Western blot analysis with antibodies raised against each integrin subunit (Figure 7B). It is remarkable that similar experiments performed with protein extracts from other integrin-transfected CHO cells or with other purified integrins such as α1β1 and α5β1 did not reveal any

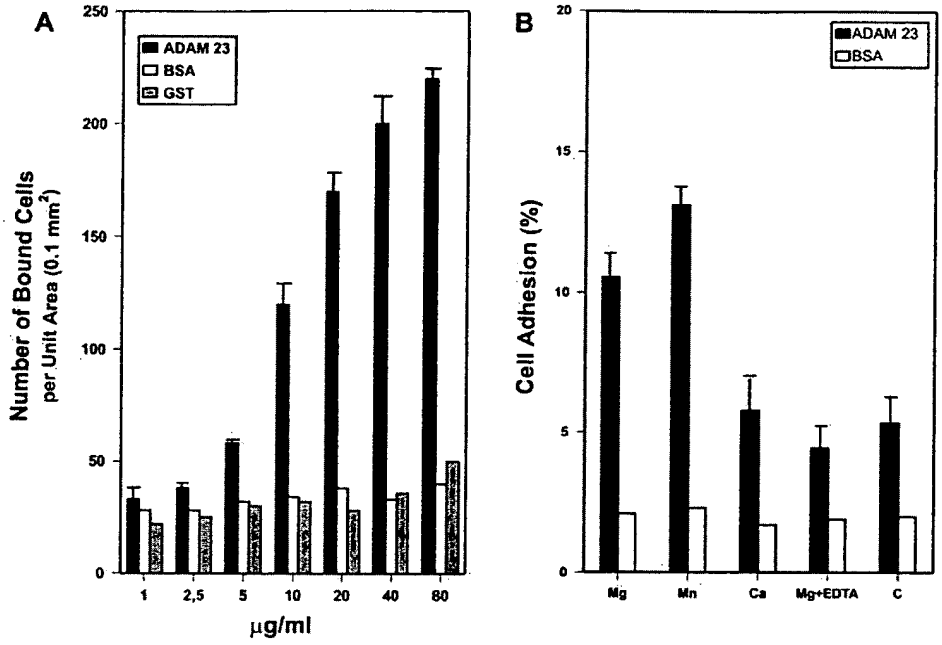

Figure 5. Dose- and cation-dependent analysis of the effect of ADAM 23 on NB100 adhesion. (A) Culture dishes were coated with the indicated concentrations of ADAM 23, BSA, and GST and blocked for nonspecific binding with BSA (2.5%). Cells were allowed to adhere for 2 h at 37°C. Nonbound cells were removed by washing, and adhesion was determined by counting bound cells per unit area using a 20× high-power objective and an ocular grid. (B) Analysis of the effect of divalent cations on NB100 adhesion mediated by ADAM 23. The experiments were performed as above with the exception that cells were washed three times in PBS and resuspended in the same buffer supplemented either with 1 mM $MgCl_2$, 50 μM $MnCl_2$, and 1 mM $CaCl_2$ or 1 mM $MgCl_2$ plus 5 mM EDTA. C, control cells, corresponding to NB100 cells plated on wells coated with BSA in the absence of divalent cations. The results presented are the mean of three independent experiments.

evidence of interaction with the recombinant ADAM 23 (Figure 7B). This result provides additional evidence of the specificity of the interaction between $\alpha v\beta 3$ integrin and the ADAM 23 disintegrin domain.

Finally, we performed an additional series of experiments directed to analyze the interaction between $\alpha v\beta 3$ and ADAM 23 in the context of the full-length ADAM 23 protein. To this purpose, the full-length cDNA for ADAM 23, containing a linker encoding the HA epitope at its 3′-end, was cloned into the eukaryotic expression vector pcDNA3. The resulting plasmid (pcDNA3-ADAM 23-HA) was transfected into HeLa cells, and then the ability of transfected cells to bind $\alpha v\beta 3$ was examined. As shown in Figure 8A, wells of microtiter plates coated with this integrin strongly supported cell adhesion of HeLa cells transfected with the ADAM 23 expression vector. In contrast, HeLa cells transfected with pcDNA3 alone did not support any significant cell adhesion (Figure 8A). To provide additional evidence that ADAM 23 was located at the cell surface, a prerequisite for mediating the observed cell adhesion effect, HeLa cells transfected with pcDNA3-ADAM 23-HA were analyzed by immunofluorescence with an mAb against the HA viral epitope. As shown in Figure 8B, a clear fluorescent pattern surrounding transfected cells was visualized in a serial op-

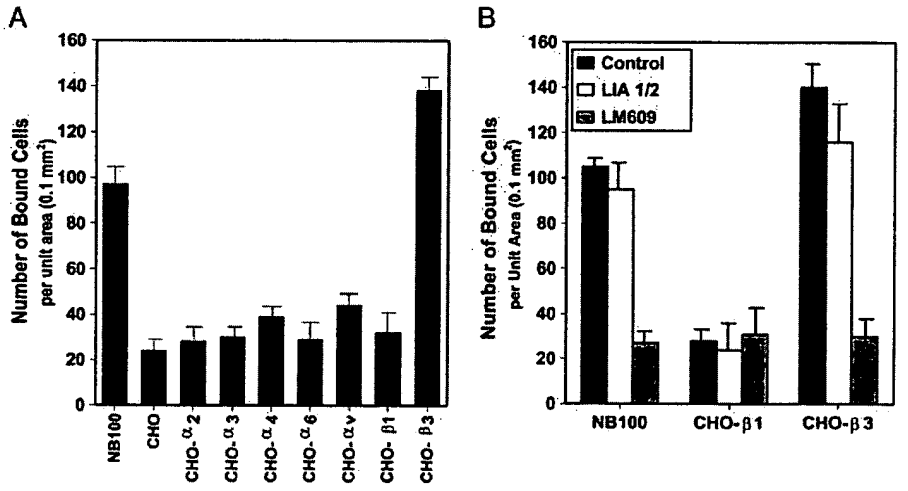

Figure 6. Analysis of ADAM 23 interaction with cell lines expressing specific integrins. (A) Microtiter plates were coated with ADAM 23-GST (10 μg/ml) and seeded with parental CHO cells or with CHO cells transfected with the indicated integrins. (B) Effect of a function-blocking anti-$\alpha v\beta 3$ antibody (LM 609) on $\beta 3$-CHO and NB100 neuroblastoma cell adhesion mediated by ADAM 23. Control, control sample (without addition of antibody); LIA 1/2, samples analyzed with this blocking anti-$\beta 1$ antibody.

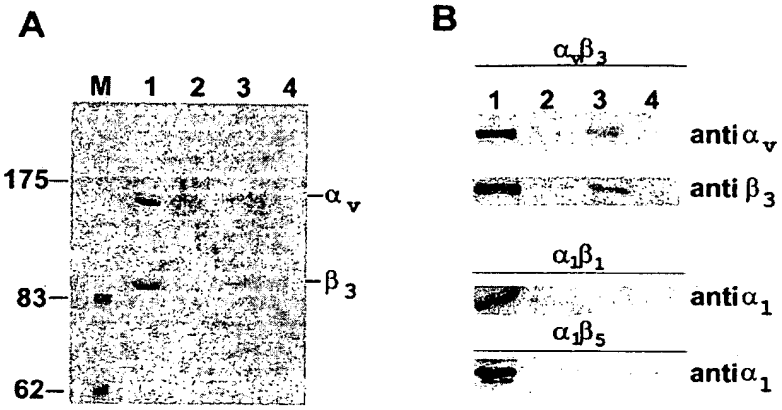

Figure 7. Interaction between human αvβ3 and the disintegrin domain of ADAM 23. (A) Purified αvβ3 integrin and Sepharose beads containing recombinant ADAM 23-GST were incubated in a Mn-containing buffer. After repeated washings, the presence of bound αvβ3 was analyzed by SDS-PAGE of proteins solubilized from Sepharose beads after treatment with Laemmli denaturing buffer. Staining was carried out with silver nitrate. (B) Western blot analysis of the solubilized material from Sepharose beads using antibodies anti-αv, anti-β3, and anti-β1. M, molecular weight markers (indicated at the left). Lane 1, 300 ng of αvβ3, α1β1, or α5β1; lane 2, beads incubated with the indicated integrins; lane 3, beads containing recombinant ADAM 23-GST (500 ng) incubated with the integrins; lane 4, beads containing GST incubated with the indicated integrins.

tical section obtained by the confocal microscope. In contrast, untransfected HeLa cells did not show any evidence of immunofluorescence signal at the cell surface. Taken together, these results are consistent with the proposal that ADAM 23 located at the cell surface is able to promote αvβ3-mediated cell adhesion.

Interaction between ADAM 23 and αvβ3 is Mediated by a Short Amino Acid Sequence Present in the Disintegrin-like Domain of ADAM 23

Analysis of the amino acid sequence of ADAM 23 shows the absence of any RGD motif (Figure 1; European Molecular Biology Laboratory accession number AJ005580). This sequence has been found to be the major structural determinant supporting αvβ3-mediated interactions in different systems, including those involving metargidin, the only cellular disintegrin described to date containing an RGD motif (Krätzschmar *et al.*, 1996; Herren *et al.*, 1997; Zhang *et al.*, 1998). A comparison of the amino acid sequence of different human disintegrins around the putative region involved in integrin binding allowed us to select a short motif (AVNECDIT) as a candidate to mediate the above-observed effect of ADAM 23 on cell adhesion (Figure 1). To determine whether this sequence is actually involved in the adhesive effect, we first mutated the Glu residue of the central position to Ala. The disintegrin-like domain of the mutant protein, designated mutADAM 23, was expressed as a fusion protein with GST following the same strategy described above for the wild-type disintegrin domain of ADAM 23. After affinity chromatography purification (Figure 9A, inset), the recombinant mutant protein was used for cell adhesion assays. As shown in Figure 9A, the mutant ADAM 23 showed a significantly lower adhesion-promoting activity of NB100 cells than the effect observed when the wild-type ADAM 23 protein was used. Similarly, when wells of microtiter

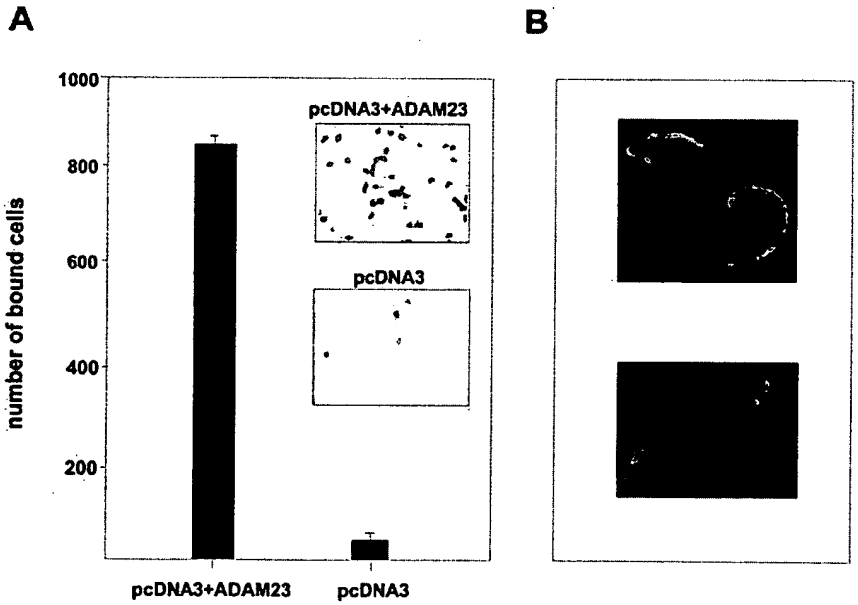

Figure 8. Interaction between human αvβ3 and HeLa cells transfected with full-length cDNA for ADAM 23. (A) HeLa cells were transfected with the expression vector pcDNA3-ADAM 23-HA containing the full-length cDNA for ADAM 23 linked to a 24-bp oligonucleotide coding for the HA epitope. Transfected cells were added to microtiter plates coated with 10 μg/ml purified αvβ3. Cells were allowed to adhere for 2 h at 37°C. Nonbound cells were removed by washing, and adhesion was observed at the light microscopic level using a 20× high-power objective. (B) Immunofluorescence analysis of HeLa cells transfected with plasmid pcDNA3-ADAM 23-HA. Top, transfected cells were incubated with a monoclonal anti-HA antibody (12CA5) diluted 1:2500 followed by another incubation with goat anti-mouse fluoresceinated antibody (diluted 1:50). Fluorescence was observed under a confocal laser microscope and localized to the surface of the ADAM 23-HA transfected cells. Bottom, negative control showing HeLa cells transfected with pcDNA3.

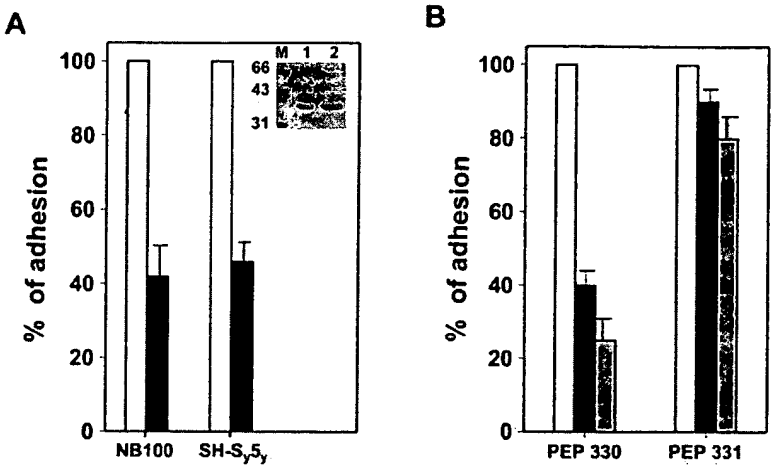

Figure 9. Delineation of the ADAM 23 region mediating the interaction with $\alpha v\beta 3$. (A) Effect of a point mutation (E→A) in the sequence of ADAM 23 on its adhesive-promoting properties represented as percentage of adhesion using neuroblastoma cell lines. ADAM 23 wild-type and experiments using mutant ADAM 23 are shown as white and black bars, respectively. Inset, SDS-PAGE gel with both ADAM 23 wild-type (lane 1) and E→A mutant (lane 2). M, molecular weight markers. (B) Effect of a synthetic peptide (AVNECDIT, pep 330) on the adhesion of NB100 cells. Pep 331 indicates the assay carried out with a scrambled peptide (DCVTNIAE). Two different concentrations of peptides were used: 20 μg/ml (black bars) and 40 μg/ml (gray bars). White bars indicate control using NB100 cells grown on ADAM 23.

plates were coated with the mutant ADAM 23 and seeded with SH-S$_y$5$_y$ neuroblastoma cells, the observed cell adhesion-promoting effect was ~40% compared with that obtained with the wild-type protein (Figure 9A).

To further examine the role of the sequence motif AVNECDIT in mediating the cell adhesion-promoting properties of ADAM 23, we next prepared a synthetic peptide enclosing this region (pep330) and a scrambled peptide, DCVTNIAE (pep 331), with the same amino acid composition. NB100 cells were incubated separately with both peptides before being seeded on plates containing ADAM 23. As shown in Figure 9B, a significant loss of adherent cells was detected with samples incubated with pep 330 (~75%). In contrast, this effect could not be observed in samples incubated with the scrambled peptide derived from the same protein region (Figure 9B). These results indicate that human ADAM 23 specifically interacts with $\alpha v\beta 3$ through a protein region whose amino acid sequence is AVNECDIT and, therefore, in an RGD-independent manner.

DISCUSSION

Over the last few years the ADAM family of cellular disintegrins has grown considerably after the finding of a series of new members identified by using a variety of homology-cloning strategies. These cloning efforts have been largely stimulated by the putative dual functions of ADAMs as proteolytic enzymes and cell adhesion molecules. Recent studies have allowed characterization of the enzymatic properties and substrate specificity of several cellular disintegrins acting as proteinases, including TACE, MDC9, kuz/ADAM 10, ADAMTS-1, and ADAMTS-4 (Black *et al.*, 1997; Moss *et al.*, 1997; Kuno *et al.*, 1997; Pan and Rubin, 1997; Izumi *et al.*, 1998; Qi *et al.*, 1999; Roghani *et al.*, 1999; Tortorella *et al.*, 1999). However, their function as cell adhesion molecules is unclear in most cases. This is the case of ADAM 23 (MDC3), a recently described disintegrin whose expression in human tissues appears to be restricted to the brain (Sagane *et al.*, 1998). Structural analysis of the ADAM 23 amino acid sequence shows the presence of all protein domains characteristic of ADAMs, including metalloproteinase-like and disintegrin-like regions. However, the metalloproteinase-like domain of ADAM 23 lacks the three histidine residues as well as the glutamic acid residue forming part of the Zn-binding site characteristic of metalloproteinases (HEXXHXXGXXH) (Rawlings and Barrett, 1995). Therefore, it was tempting to speculate that ADAM 23 could be exclusively involved in cell adhesion processes rather than in protease-mediated events (Blobel, 1997; Wolfsberg and White, 1997). Consistent with this proposal, in this work we have provided evidence that the disintegrin-like domain of ADAM 23 strongly promotes neuroblastoma cell adhesion in a dose-dependent manner. Maximal adhesion was detected in the presence of divalent cations such as Mg^{2+} or Mn^{2+} at physiological concentrations, but not Ca^{2+}. This finding agrees well with results from a number of studies of regulation of integrin activity by divalent cations, demonstrating that the activity of several integrins is stimulated by Mg^{2+} or Mn^{2+} (Elices *et al.*, 1991; Luque *et al.*, 1994; Garratt and Humphries, 1995; Camper *et al.*, 1997). On the basis of these data, it was likely that the cell adhesion-promoting effects of ADAM 23 were mediated through interaction with some integrin receptor. In fact, by using a panel of CHO cells expressing different recombinant integrins, we have found that ADAM 23 specifically interacts with $\alpha v\beta 3$. In addition, the observed binding was inhibited by a function-blocking anti-$\alpha v\beta 3$ mAb but not by antibodies specific for other integrins. The specificity of the interaction between ADAM 23 and $\alpha v\beta 3$ was further confirmed by direct binding assays using purified proteins. Finally, we provide evidence that $\alpha v\beta 3$ promotes adhesion of HeLa cells transfected with an expression vector for full-length ADAM 23, thus extending the above observations performed with a recombinant protein exclusively containing the disintegrin-like domain of ADAM 23.

The finding that ADAM 23 is a ligand for $\alpha v\beta 3$ and promotes cell adhesion indicates that these properties are not exclusive of typical extracellular matrix adhesive proteins, being also shared by a variety of molecules with diverse biological functions, including thrombin (Bar-Shavit *et al.*, 1991), perlecan (Hayashi *et al.*, 1992), matrix metalloproteinase 2 (Brooks *et al.*, 1996), and basic fibroblast growth factor (Rusnati *et al.*, 1997). In this regard, it is also remark-

able that cells adherent to ADAM 23 exhibit differences in morphology when compared with those attached to characteristic extracellular matrix proteins such as fibronectin. These differences include the presence of numerous short protrusions resembling microspikes in cells grown on ADAM 23 as well as a distinct organization of actin filaments.

In this work, we have also tried to identify the molecular determinants mediating the observed interaction between ADAM 23 and αvβ3. At present, the best characterized disintegrin domains are those derived from snake venom proteins, which contain an RGD sequence at the tip of a flexible loop joining two strands of β-sheet protruding from the protein core (Adler *et al.*, 1993). This tripeptide interacts with platelet integrins inhibiting blood clot formation and favoring the generation of hemorrhages (Niewiarowski *et al.*, 1994). However, with the exception of metargidin (ADAM 15) (Krätzschmar *et al.*, 1996), all the other human ADAMs, including ADAM 23, lack this tripeptide motif in their disintegrin-like domains, which has led to the suggestion that they may promote rather than disrupt cell–cell interactions (Blobel, 1997; Wolfsberg and White, 1997). In fact, the disintegrin domain of different ADAMs has been proven to be essential in processes involving cell–cell interactions such as sperm–egg adhesion and muscle cell fusion (Blobel *et al.*, 1992; Almeida *et al.*, 1995; Yagami-Hiromasa *et al.*, 1995; Evans *et al.*, 1997; Yuan *et al.*, 1997; Inoue *et al.*, 1998). The results reported here for ADAM 23 and neuroblastoma cells are also consistent with this proposal. Thus, a peptide analogue of the ADAM 23 disintegrin loop specifically inhibited cell adhesion, whereas a scrambled ADAM 23 disintegrin loop peptide analogue did not. In addition, a mutant protein with a single alteration in a conserved residue present in the predicted binding loop of ADAM 23 had a significantly diminished ability to support neuroblastoma cell adhesion. Collectively, these results indicate that the receptor recognition and subsequent binding of ADAM 23 is mediated, at least in part, by the disintegrin loop present in this protein. In addition, the observation that the disintegrin-like domain of ADAM 23 produced in bacteria is enough to exert cell adhesive activity indicates that this protein does not require the remaining domains or the effective glycosylation of the disintegrin domain for performing this activity. Furthermore, the fact that ADAM 23 interaction with αvβ3 is independent of an RGD sequence distinguishes this cellular disintegrin from human metargidin (ADAM 15), which has also been reported to interact with αvβ3, albeit in an RGD-dependent manner (Zhang *et al.*, 1998; Nath *et al.*, 1999). It is also remarkable that the binding specificity of other disintegrins lacking RGD motifs is distinct from that determined herein for ADAM 23. Thus, the sperm surface protein ADAM 2 (fertilin β) interacts with the integrin α6β1 on mouse eggs and α6-transfected somatic cells (Almeida *et al.*, 1995; Yuan *et al.*, 1997, Chen *et al.*, 1999). Finally, the observation that αvβ3 integrins can bind to non-RGD sequences is not unprecedented, because such an interaction has been reported for other proteins, including matrix metalloproteinase 2, and basic fibroblast growth factor (Brooks *et al.*, 1996; Rusnati *et al.*, 1997), although in all cases the molecular basis of the observed interactions with αvβ3 remains unclear.

The interaction of ADAM 23 with αvβ3 may be related to the biological and/or pathological functions of this disintegrin. On the basis of data reported in this work demonstrating that ADAM 23 may promote adhesion of cells of neural origin, together with the predominant expression of ADAM 23 in the human brain in both fetal and adult stages, it is tempting to speculate that this protein could play some specialized role in the development and/or maintenance of neural functions. It is well known that development of the nervous system involves an orderly set of connections between the different parts of the system through the outgrowth of cellular protusions to create a functional network that is extremely complex. Axons and dendrites extend from the cell bodies by means of growth cones, which travel along precisely specified paths to connect with a concrete target cell with which they are going to synapse. Neurons of different functional classes show distinctive surface characteristics that determine specific contact interactions with other cell surfaces, especially from glial cells, and with components of the extracellular matrix. Such interactions are of major importance for leading neuronal growth cones toward their targets along precisely specified routes (Reichardt and Tomaselli, 1991; Tessier-Lavigne and Goodman, 1996; Shibata *et al.*, 1998; Davenport *et al.*, 1999). ADAM 23 could modulate some of these interactions through its ability to interact with αvβ3 in a manner similar to that found in the in vitro studies with neuroblastoma cells described in this work. Consistent with this, αvβ3 is abundantly expressed in the radial glial cells during mouse development and has been proposed to play an important role in the facilitation of neuronal migration within the central nervous system (Hirsch *et al.*, 1994).

In addition to potential roles of ADAM 23 in normal processes, the results here reported for ADAM 23 and neuroblastoma cells also suggest that this cellular disintegrin can favor tumor progression through the facilitation of integrin-mediated cell–cell interactions (Varner and Cheresh, 1996; Ruoslahti, 1997). Consistent with this, αvβ3 has been shown to be involved in the progression of melanoma and the induction of neovascularization by tumor cells (Seftor *et al.*, 1992; Brooks *et al.*, 1994). Similarly, the expression of integrin αvβ3 in undifferentiated neuroblastoma cells in vivo has been proposed to contribute to the rapid growth of these tumors and their tendency to metastasize (Gladson *et al.*, 1996). Finally, preliminary analysis of the nature of the signaling cascades initiated upon ADAM 23 binding to αvβ3 appear to indicate that this interaction results in the induction of active matrix metalloproteinases (S. Cal and C. López-Otín, unpublished results). As previously reported in other systems (Werb *et al.*, 1989; Riikonen *et al.*, 1995; Pilcher *et al.*, 1997; Lochter *et al.*, 1999) these proteolytic enzymes could act as effector molecules modifying the surrounding of the involved cells and facilitating further migration of tumor cells. The availability of recombinant ADAM 23 will open future studies directed to clarify its role in the context of other proteins involved in cell–cell or cell–matrix interaction processes taking place during the development and maintenance of neural functions, as well as in the alterations occurring in the metastatic events of tumor cells.

ACKNOWLEDGMENTS

We thank Drs. I. Santamaría, G. Velasco, M. Balbín, and A.M. Pendás for helpful comments, Dr. A. Pérez and O. Conejero for advice in electron microscopy studies, Drs. D. Cheresh, A. Nakano, F. Sánchez-Madrid, M. Yáñez, C. Martínez-A., R. Lacalle, F. Barros, and T. Giráldez for providing cells and reagents, and S. Alvarez and F. Rodríguez

for excellent technical assistance. This work was supported by grants from Comisión Interministerial de Ciencia y Tecnología-Spain (SAF97-0258), FEDER-Spain, European Union-BIOMED II (BMH4-CT96-0017), and National Institutes of Health (GM-47157 and GM-49899 to Y.T.). S.C. is a recipient of a research contract from Ministerio de Educación y Ciencia, Spain. The Instituto Universitario de Oncología is supported by a grant from Obra Social Cajastur.

REFERENCES

Adham, I.M., Kim, Y., Shamsadin, R., Heinlein, U.A.O., Von Beust, G., Mattei, M.G., and Engel, W. (1998). Molecular cloning, chromosomal localization, and expression analysis of CYRN1 and CYRN2, two human genes coding for cyritestin, a sperm protein involved in gamete interaction. DNA Cell Biol. *17*, 161–168.

Adler, M., Carter, P., Lazarus, R.A., and Wagner, G. (1993). Cysteine pairing in the glycoprotein IIbIIIa antagonist kistrin using NMR, chemical analysis, and structure calculations. Biochemistry *32*, 282–289.

Alfandari, D., Wolfsberg, T.G., White, J.M., and DeSimone, D.W. (1997). ADAM 13: a novel ADAM expressed in somitic mesoderm and neural crest cells during *Xenopus laevis* development. Dev. Biol. *182*, 314–330.

Almeida, E.A.C., *et al.* (1995). Mouse egg integrin $\alpha 6\beta 1$ functions as a sperm receptor. Cell *81*, 1095–1104.

Bar-Shavit, R., Sabbah, V., Lampugnani, M.G., Marchisio, P.C., Fenton, J.W., Vlodawsky, I., and Dejana, E. (1991). An Arg-Gly-Asp sequence within thrombin promotes endothelial cell adhesion. J. Cell Biol. *112*, 335–344.

Black, R.A., *et al.* (1997). A metalloproteinase disintegrin that releases tumor-necrosis factor-α from cells. Nature *385*, 729–733.

Blobel, C.P. (1997). Metalloprotease-disintegrins: links to cell adhesion and cleavage of TNF-α and Notch. Cell *90*, 589–592.

Blobel, C.P., Wolfsberg, T.G., Turck, C.W., Myles, D.G., Primakoff, P., and White, J.M. (1992). A potential fusion peptide and an integrin ligand domain in a protein active in sperm-egg fusion. Nature *356*, 248–252.

Brooks, P.C., Montgomery, A.M., Rosenfeld, R.A., Hu, T., Klier, G., and Cheresh, D.A. (1994). Integrin $\alpha v\beta 3$ antagonists promote tumor regression by inducing apoptosis of angiogenic blood vessels. Cell *79*, 1157–1164.

Brooks, P.C., Strombald, S., Sanders, L.C., von Schalscha, T.L., Aimes, R.T., Stetler-Stevenson, W.G., Quigley, J.D., and Cheresh, D.A. (1996). Localization of matrix metalloproteinase MMP-2 to the surface of invasive cells by interaction with integrin $\alpha v\beta 3$. Cell *85*, 683–693.

Cai, H., Krätzschmar, J., Alfandari, D., Hunnicutt, G., and Blobel, C.P. (1998). Neural crest-specific and general expression of distinct metalloprotease-disintegrins in early *Xenopus laevis* development. Dev. Biol. *204*, 508–524.

Camper, L., Heinegard, D., and Lundgren-Akerlund, E. (1997). Integrin $\alpha 2\beta 1$ is a receptor for the cartilage matrix protein chondroadherin. J. Cell Biol. *138*, 1159–1167.

Chen, M.S., Almeida, E.A., Houvila, A.P., Takahashi, Y., Shaw, L.M., Mercurio, A.M., and White, J.M. (1999). Evidence that distinct states of the integrin $\alpha 6\beta 1$ interact with laminin and an ADAM. J. Cell Biol. *144*, 549–561.

Cheresh, D.A., and Spiro, R.C. (1987). Biosynthesis and functional properties of Arg-Gly-Asp directed receptor involved in human melanoma cell attachment to vitronectin, fibrinogen, and von Willebrand factor. Proc. Natl. Acad. Sci. USA *84*, 6471–6475.

Davenport, R.W., Thies, E., and Cohen, M.L. (1999). Neuronal growth cone collapse triggers lateral extensions along trailing axons. Nat. Neurosci. *2*, 254–259.

Elices, M.J., Urry, L.A., and Hemler, M.E. (1991). Receptor functions for the integrin VLA-3: fibronectin, collagen, and laminin binding are differentially influenced by Arg-Gly-Asp peptide and by divalent cations. J. Cell Biol. *112*, 169–181.

Emi, M., Katagiri, T., Harada, Y., Saito, H., Inazawa, J., Ito, I., Kasumi, F., and Nakamura, Y. (1993). A novel metalloprotease/disintegrin-like gene at 17q21.3 is somatically rearranged in two primary breast cancers. Nat. Genet. *5*, 151–157.

Evans, J.P., Kopf, G.S., and Schultz, R.M. (1997). Characterization of the binding of recombinant mouse sperm fertilin β subunit to mouse eggs: evidence for adhesive activity via an egg $\beta 1$ integrin-mediated interaction. Dev. Biol. *187*, 79–93.

Frayne, J., and Hall, L. (1998). The gene for the human tMDC I sperm surface protein is non-functional: implications for its proposed role in mammalian sperm-egg recognition. Biochem. J. *334*, 171–176.

Garratt, A.N., and Humphries, M.J. (1995). Recent insights into ligand binding, activation and signaling by integrin adhesion receptors. Acta Anat. *154*, 34–45.

Gilpin, B.J., Loeche, F., Mattei, M.G., Engvall, E., Alberchtsen, R., and Wewer, U.M. (1998). A novel, secreted form of human ADAM 12 (meltrin α) provokes myogenesis in vivo. J. Biol. Chem. *273*, 157–166.

Gladson, C.L., Hancock, S., Arnold, M.M., Faye-Petersen, O.M., Castleberry, R.P., and Kelly, D.R. (1996). Stage-specific expression of integrin $\alpha v\beta 3$ in neuroblastic tumors. Am. J Pathol. *148*, 1423–1434.

Hayashi, K., Madri, J.A., and Yurchenco, P.D. (1992). Endothelial cells interact with the core protein of basement membrane perlecan through $\beta 1$ and $\beta 3$ integrins: an adhesion modulated by glycosaminoglycan. J. Cell Biol. *119*, 945–959.

Herren, B., Raines, E.W., and Ross, R. (1997). Expression of a disintegrin-like protein in cultured human vascular cells and in vivo. FASEB J. *11*, 173–180.

Hirsch, E., Gullberg, D., Balzac, F., Altruda, F., Silengo, L., and Tarone, G. (1994). αv integrin subunit is predominantly located in nervous tissue and skeletal muscle during mouse development. Dev. Dyn. *201*, 108–120.

Houliva, A.-P.J., Almeida, E.A.C., and White, J.M. (1996). ADAMs and cell fusion. Curr. Opin. Cell. Biol. *8*, 692–699.

Hurskainen, T.L., Hirohata, S., Seldin, M.F., and Apte, S.S. (1999). ADAM-TS5, ADAM-TS6, and ADAM-TS7, novel members of a new family of zinc metalloproteases. J. Biol. Chem. *274*, 2555–25563.

Inoue, D., Reid, M., Lum, L., Krätzschmar, J., Weskamp, G., Myung, Y.M., Baron, R., and Blobel, C.P. (1998). Cloning and initial characterization of mouse meltrin β and analysis of the expression of four metalloprotease-disintegrins in bone cells. J. Biol. Chem. *273*, 4180–4187.

Izumi, Y., *et al.* (1998). A metalloprotease-disintegrin, MDC9/meltrin-gamma/ADAM9 and PKCdelta are involved in TPA-induced ectodomain shedding of membrane-anchored heparin-binding EGF-like growth factor. EMBO J. *17*, 7260–7272.

Jury, J.A., Frayne, J., and Hall, L. (1997). The human fertilin α gene is non-functional: implications for its proposed role in fertilization. Biochem. J. *32*, 577–581.

Krätzschmar, J., Lum, L., and Blobel, C.P. (1996). Metargidin, a membrane-anchored metalloprotease-disintegrin protein with an RGD integrin binding sequence. J. Biol. Chem. *271*, 4593–4598.

Kuno, K., Kanada, N., Nakashima, E., Fujiki, F., Ichimura, F., and Matsushima, K. (1997). Molecular cloning of a gene encoding a new type of metalloproteinase-disintegrin family protein with thrombospondin motifs as an inflammation associated gene. J. Biol. Chem. *272*, 556–562.

Lochter, A., Navre, M., Werb, Z., and Bissell, M.J. (1999). $\alpha 1$ and $\alpha 2$ integrins mediate invasive activity of mouse mammary carcinoma cells

through regulation of stromelysin-1 expression. Mol. Biol. Cell *10*, 271–282.

Luque, A., Sánchez-Madrid, F., and Cabañas, C. (1994). Functional regulation of the human integrin VLA-1 (CD49a/CD29) by divalent cations and stimulatory $\beta 1$ antibodies. FEBS Lett. *346*, 278–284.

Maniatis, T., Fritsch, E.F., and Sambrook, J. (1982). Molecular Cloning: A Laboratory Manual, Cold Spring Harbor, NY: Cold Spring Harbor Laboratory Press.

Moss, M.L., *et al.* (1997). Cloning of a disintegrin metalloproteinase that processes precursor tumor-necrosis factor-α. Nature *385*, 733–736.

Mueller, C.G., Rissoan, M.C., Salinas, B., Ait-Yahia, S., Ravel, O., Bridon, J.M., Briere, F., Lebecque, S., and Liu, Y.J. (1997). Polymerase chain reaction selects a novel disintegrin proteinase from CD40-activated germinal center dendritic cells. J. Exp. Med. *189*, 655–663.

Nath, D., Slocombe, P.M., Stephens, P.E., Warn, A., Hutchinson, G.R., Yamada, K.M., Docherty, A.J., and Murphy, G. (1999). Interaction of metargidin (ADAM-15) with αvb3 and $\alpha 5\beta 1$ integrins on different hemopoietic cells. J. Cell Sci. *112*, 579–587.

Niewiarowski, S., McLane, M.A., Kloczewiak, M., and Stewart, G.J. (1994). Disintegrins and other naturally occurring antagonists of platelet fibrinogen receptors. Semin. Hematol. *31*, 289–300.

Pan, D., and Rubin, G.M. (1997). Kuzbanian controls proteolytic processing of Notch and mediates lateral inhibition during *Drosophila* and vertebrate neurogenesis. Cell *90*, 271–280.

Pilcher, B.K., Dumin, J.A., Sudbeck, B.D., Krane, S.M., Welgus, H.G., and Parks, W.C. (1997). The activity of collagenase-1 is required for keratinocyte migration on a type I collagen matrix. J. Cell Biol. *137*, 1445–1457.

Podbilewicz, B. (1996). ADM-1, a protein with metalloprotease- and disintegrin-like domains, is expressed in syncytial organs, sperm, and sheath cells of sensory organs in *Caenorhabditis elegans*. Mol. Biol. Cell *7*, 1877–1893.

Qi, H., Rand, M.D., Wu, X., Sestan, N., Wang, W., Rakic, P., Xu, T., and Artavanis-Tsakonas, S. (1999). Processing of the notch ligand delta by the metalloprotease Kuzbanian. Science *283*, 91–94.

Rawlings, N.D., and Barrett, A.J. (1995). Evolutionary families of metallopeptidases. Methods Enzymol. *248*, 183–228.

Reichardt, L.F., and Tomaselli, K.J. (1991). Extracellular matrix molecules and their receptors: functions in neural development. Annu. Rev. Neurosci. *14*, 531–570.

Riikonen, T., Westermarck, J., Koivisto, L., Broberg, A., Kahari, V.M., and Heino, J. (1995). Integrin $\alpha 2\beta 1$ is a positive regulator of collagenase (MMP-1) and collagen $\alpha 1$(I) gene expression. J. Biol. Chem. *270*, 13528–13552.

Roghani, M., Becherer, J.D., Moss, M.L., Atherton, R.E., Erdjument-Bromage, H., Arribas, J., Blackburn, R.K., Weskamp, G., Tempst, P., and Blobel, C.P. (1999). Metalloprotease-disintegrin MDC9: intracellular maturation and catalytic activity. J. Biol. Chem. *274*, 3531–3540.

Rooke, J., Pan, D., Xu, T., and Rubin, G.M. (1996). KUZ, a conserved metalloprotease-disintegrin protein with two roles in *Drosophila* neurogenesis. Nature *273*, 1227–1231.

Ruoslahti, E. (1997). Integrins as signaling molecules and targets for tumor therapy. Kidney Int. *51*, 1413–1417.

Rusnati, M., Tanghetti, E., Dell'Eva, P., Gualandris, A., and Presta, M. (1997). $\alpha v\beta 3$ integrin mediates the cell-adhesive capacity and biological activity of basic fibroblast growth factor (FGF-2) in cultured endothelial cells. Mol. Biol. Cell *8*, 2449–2461.

Sagane, K., Ohya, Y., Hasegawa, Y., and Tanaka, I. (1998). Metalloproteinase-like, disintegrin-like, cysteine-rich proteins MDC2 and MDC3: novel human cellular disintegrins highly expressed in the brain. Biochem. J. *334*, 93–98.

Seftor, R.E., Seftor, E.A., Gehlsen, K.R., Stetler-Stevenson, W.G., Brown, P.D., Ruoslahti, E., and Hendrix, M.J. (1992). Role of the $\alpha v\beta 3$ integrin in human melanoma cell invasion. Proc. Natl. Acad. Sci. USA *89*, 1557–1561.

Shibata, A., Wright, M.V., David, S., McKerracher, L., Braun, P.E., and Kater, S.B. (1998). Unique responses of differentiating neuronal growth cones to inhibitory cues presented by oligodendrocytes. J. Cell Biol. *142*, 191–202.

Sotillos, S., Roch, F., and Campuzano, S. (1997). The metalloproteas disintegrin Kuzbanian participates in Notch activation during growth and patterning of *Drosophila* imaginal discs. Development *124*, 4769–4779.

Takada, Y., Ylanne, J., Mandelman, D., Puzon, W., and Ginsberg, M.H. (1992). A point mutation of integrin $\beta 1$ subunit blocks binding of $\alpha 5\beta 1$ to fibronectin and invasion but not recruitment to adhesion plaques. J. Cell Biol. *119*, 913–921.

Takagi, J., Kamata, T., Meredith, J., Puzon-McLaughlin, W., and Takada, Y. (1997). Changing ligand specificities of $\alpha v\beta 1$ and v3 integrins by swapping a short diverse sequence of the β subunit. J. Biol. Chem. *272*, 19794–19800.

Tessier-Lavigne, M., and Goodman, C.S. (1996). The molecular biology of axon guidance. Science *274*, 1123–1132.

Tortorella, M.D., *et al.* (1999). Purification and cloning of aggrecanase-1: a member of the ADAMTS family of proteins. Science *284*, 1664–1666.

Varner, J.A., and Cheresh, D.A. (1996). Integrins and cancer. Curr. Opin. Cell. Biol. *8*, 724–730.

Werb, Z. (1997). ECM and cell surface proteolysis: regulating cellular ecology. Cell *91*, 439–442.

Werb, Z., Tremble, P.M., Behrendtsen, O., Crowley, E., and Damsky, C.H. (1989). Signal transduction through the fibronectin receptor induces collagenase and stromelysin gene expression. J. Cell Biol. *109*, 877–889.

Wolfsberg, T.G., Primakoff, P., Myles, D.G., and White, J.M. (1995). ADAM, a novel family of membrane proteins containing a disintegrin and metalloprotease domain: multipotential functions in cell-cell and cell-matrix interactions. J. Cell Biol. *131*, 275–278.

Wolfsberg, T.G., and White, J.M. (1997). ADAMs in fertilization and development. Dev. Biol. *180*, 389–401.

Wu, E.P.I., Croucher, N., and McKie, N. (1997). Expression of members of the novel membrane linked metalloproteinase family ADAM in cells derived from a range of hematological malignancies. Biochem. Biophys. Res. Commun. *235*, 437–442.

Yagami-Hiromasa, T., Sato, T., Kurisaki, T., Kamijo, K., Nabeshima, Y., and Fujisawa-Sehara, A. (1995). A metalloprotease-disintegrin participating in myoblast fusion. Nature *377*, 652–656.

Yavari, R., Adida, C., Bray-Ward, P., Brines, M., and Xu, T. (1998). Human metalloprotease-disintegrin kuzbanian regulates sympathoadrenal cell fate in development and neoplasia. Hum. Mol. Genet. *7*, 1161–1167.

Yoshida, S., Setoguchi, M., Higuchi, Y., Akizuki, S., and Yamamoto, S. (1990). Molecular cloning of cDNA encoding MS2 antigen, a novel cell surface antigen strongly expressed in murine monocytic lineage. Int. Inmunol. *2*, 585–591.

Yuan, R., Primakoff, P., and Myles, D.G. (1997). A role for the disintegrin domain of cyritestin, a sperm surface protein belonging to the ADAM family, in mouse sperm-egg plasma membrane adhesion and fusion. J. Cell Biol. *137*, 105–112.

Zhang, X.-P., Kamata, T., Yokoyama, K., Puzon-McLaughlin, W., and Takada, Y. (1998). Specific interaction of the recombinant disintegrin-like domain of MDC-15 (metargidin, ADAM-15) with integrin $\alpha v\beta 3$. J. Biol. Chem. *273*, 7345–7350.